

**Synthesis of Novel Neutral and Cationic Diamine-bis(ether-
phosphine)ruthenium(II) Complexes in Homogeneous and Heterogeneous States
as Tools for Parallel Catalyst Screening**

**Synthese neuartiger neutraler und kationischer Diamin-bis(ether-
phosphan)ruthenium(II)-Komplexe in homogener und heterogener Phase als
Werkzeug für paralleles Katalysator-Screening**

Dissertation

der Fakultät für Chemie und Pharmazie
der Eberhard-Karls-Universität Tübingen

zur Erlangung des Grades eines Doktors
der Naturwissenschaften

2002

Samer Ibrahim Abed-Rabbo Al-Gharabli

**Im Namen Allahs, des Sich Erbarmenden, des
Barmherzigen**



**In the Name of Allah, the Most Beneficent, the
Most Merciful**

Tag der mündlichen Prüfung:

26 . 04. 2002

Dekan:

Prof. Dr. H. Probst

1. Berichterstatter:

Prof. Dr. E. Lindner

2. Berichterstatter:

Prof. Dr. H. A. Mayer

*To my Parents
Sisters and Brothers
To my Wife and Daughter*

Die vorliegende Arbeit wurde am
Institut für Anorganische Chemie
der Eberhard-Karls-Universität
Tübingen unter der Leitung von
Herrn Professor Dr. rer. nat.
Ekkehard Lindner angefertigt.

Meinem Doktorvater,
Herrn Prof. Dr. Ekkehard
Lindner danke ich herzlich für
die Themenstellung, für die
Bereitstellung ausgezeichneter
Arbeitsbedingungen, die wert-
vollen Anregungen und
Diskussionen sowie sein stetes
Interesse an dieser Arbeit

Ich danke ganz herzlich:

Herrn Prof. Dr. H. A. Mayer für die vielen fachlichen Gespräche und die Diskussionen der NMR Spektren,

Herrn Dr. Klaus Eichele und Herrn Manfred Steimann für stete Hilfsbereitschaft und zahlreiche fruchtbare Diskussionen,

Frau Barbara Saller für die Durchführung zahlreicher IR Messungen und viele Hilfestellungen,

Herrn Dipl.-Chem. Michael Henes für seine Hilfestellungen bei technischen und Computerproblemen,

Herrn Dipl.-Chem. Stefan Steinbrecher, Institut für Angewandte Physik der Universität Tübingen, für die SEM- und EDX-Messungen und deren Auswertung sowie Herrn-Dipl. Chem. Michael Seiler, Institut für Physikalische Chemie der Universität Stuttgart, für die EXAFS-Messungen.

Frau Heike Dorn, Frau Angelika Ehmman, Herrn Dipl.-Chem. Ulf. Kehrer für die Aufnahme zahlreicher NMR-Spektren und die große und spontane Hilfsbereitschaft,

Herrn Dr. Frank Höhn, möchte ich für die Hilfe bei meinen zahlreichen Computerproblemen,

Den ehemaligen 'Labormitinsassen' Herrn Dr. Markus Schmid, Herrn Dr. Frank Höhn, Herrn Dr. Monther Khanfar, Herrn M.Sc. Mahmoud Sunjuk, Herrn M.Sc. Ismail Warad, Herrn Dr. Zhong-Lin Lu, Frau Dr. Elisabeth Holder, Herrn Dr. Wolfram Wielandt, Frau Dr. Monika Förster, Herrn Dr. Wolfgang Wischert, Herrn Dipl.-Chem. Christoph Ayasse, Herrn M.Sc. Ruifa Zong und Frau Elli Oster für ein ausgezeichnetes Arbeitsklima, wertvolle Diskussionen am Abzug und viele Glasgeräte,

Herrn Dr. Monther Khanfar, Herrn Dr. Raid Abdel-Jalil, Herrn Dr. Rakez Kayed, Herrn M.Sc. Hani Mohammed, Herrn M.Sc. Mahmoud Sunjuk, Herrn M.Sc. Adnan Al-Labadi, Herrn M.Sc. Ahmad Alsheik und Herrn M.Sc. Ahmad Aburayyan danke ich für viele entspannende Stunden der Freizeit.

Herrn Dr. Monther Khanfar für seine Ermutigung am Beginn meines Bleibens in Deutschland

Herrn Dr. R. Müller und Herrn H. Bartholomä für die geduldige und freundliche Durchführung zahlreicher Massenspektren,

Herrn W. Bock für seine ständigen Bemühungen um gute Elementaranalysen,

Herrn Dr. Hans-Dieter Ebert und Frau Roswitha Conrad für die Beseitigung bürokratischer Probleme,

Herrn Dipl.-Phys. Walter Schaal, sowie allen technischen Angestellten, Praktikanten und Kollegen, die zum Gelingen dieser Arbeit beigetragen haben.

Schließlich meinen Kollegen in der 8. Ebene, Herrn Dr. Ulf. Kehrer, Herrn Dr. Stefan Brugger, Herrn Dr. Andreas Baumann, Herrn Dipl.-Chem. Michael Henes, Herrn Dr. Frank Höhn, Herrn Dr. Markus Schmid, Herrn Dr. Monther Khanfar, Herrn M.Sc. Mahmoud Sunjuk, Herrn Dr. Joachim Wald, Herrn Dr. Robert Veigel, Herrn Dr. Thomas Salesch, Frau Dr. Elisabeth Holder sowie Kolleginnen und Kollegen der Arbeitskreise Kuhn, Lindner, Mayer und Nagel für das gute Klima in der Anorganischen Chemie II und die ständige Diskussionsbereitschaft im Kaffeeraum.

Mein ganz besonderer Dank gilt meiner Frau

Introduction	1
General Section	4
1. Structural Studies of an Array of Mixed Diamine Phosphine Ruthenium(II) Complexes	4
1.1 General Consideration	4
1.2 Synthesis and Characterization of the RuCl₂P₂(diamine) Complexes 3a – g	6
1.3 Crystal Structures of 3a and 3e	7
1.4 Syntheses and Characterization of the Cations [RuCl(P~O)(P^O)(N^N)]X (4a – d, f) and [Ru(P^O)₂(N^N)]X₂ (5a – c, e – g)	8
1.5 Crystal Structures of 4b and 5a	10
1.6 Conclusion	14
2. T-Silyl Functionalized Diaminediphosphineruthenium(II) Precursor Complexes	15
2.1 General Consideration	15
2.2 Synthesis and Characterization of the Ligand 9(T⁰)	15
2.3 Synthesis and Characterization of the Cl₂Ru(P~O)₂(diamine) Complexes 11a(T⁰) – g(T⁰)	16
2.4 Synthesis and Characterization of the Mono- and Dicationic Ruthenium(II) Complexes 12a(T⁰) – g(T⁰) and 13a(T⁰), respectively	19
2.5 Conclusion	21
3. Heterogenization of a Matrix of Neutral and Monocationic Diaminediphosphineruthenium(II) Complexes by the Sol-Gel Process	22
3.1 General Consideration	22
3.2 Concept of the Interphases	22

3.2.1 Definition of the Interphase	22
3.2.2 Sol-Gel Process	25
3.3 Synthesis and Characterization of the Polymeric Materials	26
3.3.1 Sol-Gel Processing of the Precursor Complexes 11a(T°) – g(T°) and 12a(T°) – g(T°)	26
3.3.2 Solid-State NMR Spectroscopic Investigations	27
3.3.2.1 ²⁹ Si CP/MAS NMR Spectroscopy	27
3.3.2.2 ¹³ C and ³¹ P CP/MAS NMR Spectroscopy	27
3.3.3 EXAFS Spectroscopy	31
3.3.4 SEM, EDX, and BET Measurements	35
3.4 Conclusion	39
Experimental Part	40
1.1 General Comments	40
1.2 Preparation of the Complexes 3a – g, 4a – g, 5a – g	42
1.2.1 General Procedure for the Preparation of the Neutral Complexes 3a – g	42
1.2.2 General Procedure for the Preparation of the Mono-cationic Complexes 4a – g	43
1.2.3 General Procedure for the Preparation of the Dicationic Complexes 5a – c, e – g	44
1.3 Preparation of the T-Silyl Functionalized Complexes 10(T°), 11a(T°) – g, 12a(T°) – g, and 13a(T°)	45
1.3.1 Preparation of the T-Silyl Functionalized Ether-Phosphine Ligand 9(T°)	45
1.3.1.1 Preparation of Compound 6	45
1.3.1.2 Preparation of Compound 7	45
1.3.1.3 Preparation of Compound 8	46

<i>1.3.1.4 Preparation of the Ligand 9(T^o)</i>	46
1.3.2 Preparation of the Complex 10(T^o)	47
1.3.3 General Procedure for the Preparation of the Neutral Complexes 11a(T^o) – g(T^o)	48
<i>1.3.3.1 Preparation of 11a(T^o)</i>	48
<i>1.3.3.2 Preparation of 11b(T^o)</i>	49
<i>1.3.3.3 Preparation of 11c(T^o)</i>	49
<i>1.3.3.4 Preparation of 11d(T^o)</i>	50
<i>1.3.3.5 Preparation of 11e(T^o)</i>	50
<i>1.3.3.6 Preparation of 11f(T^o)</i>	51
<i>1.3.3.7 Preparation of 11g(T^o)</i>	51
1.3.4 General Procedure for the Preparation of the Cationic Complexes 12a(T^o) – g(T^o)	52
<i>1.3.4.1 Preparation of 12a(T^o)</i>	53
<i>1.3.4.2 Preparation of 12b(T^o)</i>	53
<i>1.3.4.3 Preparation of 12c(T^o)</i>	53
<i>1.3.4.4 Preparation of 12d(T^o)</i>	54
<i>1.3.4.5 Preparation of 12e(T^o)</i>	54
<i>1.3.4.6 Preparation of 12f(T^o)</i>	55
<i>1.3.4.7 Preparation of 12g(T^o)</i>	55
1.3.5 Preparation of the Dicationic Complex 13a(T^o)	56
1.4 Preparation of the Heterogenized Complexes X14a – g, X15a – g, X16a – g, and X17a – g	57
1.4.1 General Procedure for Sol–Gel Processing	57
<i>1.4.1.1 Preparation of X14a</i>	57
<i>1.4.1.2 Preparation of X14b</i>	57
<i>1.4.1.3 Preparation of X14c</i>	58

<i>1.4.1.4 Preparation of X15a</i>	58
<i>1.4.1.5 Preparation of X15b</i>	59
<i>1.4.1.6 Preparation of X15c</i>	59
<i>1.4.1.7 Preparation of X15d</i>	59
<i>1.4.1.8 Preparation of X15e</i>	60
<i>1.4.1.9 Preparation of X15f</i>	60
<i>1.4.1.10 Preparation of X15g</i>	60
<i>1.4.1.11 Preparation of X16a</i>	61
<i>1.4.1.12 Preparation of X16b</i>	61
<i>1.4.1.13 Preparation of X16c</i>	61
<i>1.4.1.14 Preparation of X16d</i>	62
<i>1.4.1.15 Preparation of X16e</i>	62
<i>1.4.1.16 Preparation of X16f</i>	62
<i>1.4.1.17 Preparation of X16g</i>	63
<i>1.4.1.18 Preparation of X17a</i>	63
<i>1.4.1.19 Preparation of X17b</i>	63
<i>1.4.1.20 Preparation of X17c</i>	64
<i>1.4.1.21 Preparation of X17d</i>	64
<i>1.4.1.22 Preparation of X17e</i>	65
<i>1.4.1.23 Preparation of X17f</i>	65
<i>1.4.1.24 Preparation of X17g</i>	65
References	67
Summary	73

Introduction

The basic principle of combinatorial chemistry¹⁻⁵ is to prepare a large number of different compounds at the same time, instead of synthesizing compounds in a conventional one-at-a-time manner, and then to identify the most promising compound for further development by high-throughput screening.⁶⁻⁹ The combinatorial approach as well as screening methods have become increasingly important in many areas of chemistry. Besides the enormous gain in time in the development of new drugs and catalysts, a further driving force is the saving of expensive and environmentally encumbering chemicals. While in drug design there have already been a number of successful applications of these new techniques,¹⁰⁻¹⁴ in catalysis research these new methods have been introduced only gradually.¹⁵⁻¹⁹ An intermediate step between combinatorial chemistry and traditional synthesis is parallel synthesis²⁰⁻²³ with commonly one compound per well,²⁴⁻²⁶ coupled to automated screens.²⁷⁻³⁰ Recently this technique was transferred to homogeneous and heterogeneous catalysis.³⁰⁻⁴⁰

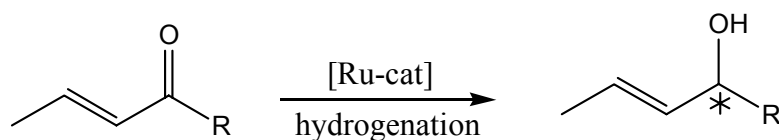
Highly selective catalysts require transition-metal complexes with well-designed structural, electronic, and stereochemical features. Small differences in the coordination sphere of the transition metal commonly lead to dramatic changes in the selectivity and activity of the catalytic conversion.⁴¹ Thus, the relation between the structure of the ligands and the physicochemical properties of the corresponding metal complexes has been the subject of many investigations in order to understand the selectivity in catalysis.

In the **first part** of this work, a synthetic route to an array of neutral and cationic diamine-bis(ether-phosphine)ruthenium(II) complexes and their complete structural characterization had to be achieved.⁴² Compounds of this type are potential candidates for the application of parallel methods. Thus, diamines which are easily accessible in various forms were introduced as coligands to modify the (ether-phosphine)ruthenium(II) complexes in

order to create a large array of structurally different compounds. Diaminediphosphineruthenium(II) complexes⁴³⁻⁵² with classical phosphine ligands were already successfully employed in the catalytic hydrogenation of unsaturated ketones with high diastereo- and enantioselectivity⁵³⁻⁶⁰ (Scheme 1). A prospective objective for future investigations is the combination of parallel synthesis and interphase chemistry.⁶¹⁻⁶⁴ An imperative prerequisite to meet these conditions is the generation of a novel phosphine which is provided with an adequate spacer carrying a triethoxysilyl group (T-silyl) at the periphery of the ligand system. Meanwhile interphase catalysts have attained a remarkable importance since they are able to combine the advantages of homogeneous and heterogeneous catalysis with a considerable reduction of notorious drawbacks like leaching and limited catalytic activity^{61, 65} of the reactive centers. Interphases are systems in which a stationary phase (e.g. a reaction center linked to a matrix via a spacer) and a mobile component (e.g. a gaseous, liquid, or dissolved reactant) penetrate each other on a molecular scale without forming a homogeneous phase. If such interphases are provided with a swellable polymer, they are able to imitate homogeneous conditions, because the active centers become highly mobile simulating the properties of a solution and hence they are accessible for substrates.

In the **second part** of this study, the ether-phosphine ligand $\text{Ph}_2\text{P}(\text{CH}_2)_2\text{OCH}_3$ was functionalized with T-silyl subgroups at the end of a spacer unit.⁶⁶ The modified ligand was used in the synthesis of a matrix of T-silyl functionalized ruthenium(II) complexes. To increase the catalytic activity by producing vacant coordination sites also cationic forms of the mentioned complexes were made accessible. The ether moieties incorporated into the phosphine ligands play a significant role,^{67,68} because they are able to protect vacant coordination sites at the metal centers and hence the stability of these complexes is increased.⁸¹ This matrix of complexes was subjected in a **third part** to a sol-gel^{69,70} process in the presence of appropriate co-condensation agents [$\text{CH}_3\text{Si}(\text{OMe})_3$ (**Me-T°**) and $(\text{MeO})_2\text{SiMe}-(\text{CH}_2)_6-\text{MeSi}(\text{OMe})_2$ (**D°-C₆-D°**)] in different amounts. In a recent paper it

was demonstrated that a variation of the T:D ratios leads to an optimization of the mobility of polymeric materials which is accompanied by an improvement of the catalytic activity of the polymeric catalysts.⁷¹ On the other hand from fluorescence spectroscopic investigations it was deduced that **Me-Tⁿ** hybrid polymers reveal a high mobility in the swollen state.⁷² For this reason the above-mentioned co-condensation agents were selected. The resulting hybrid polymers represent a new array of complexes with variable mobilities. An indispensable technique to characterize these polymeric materials is solid-state NMR spectroscopy. Some of the hybrid catalysts were also exemplarily probed by EXAFS, EDX, SEM, and BET measurements. These new stationary phases represent valuable examples for further studies regarding a parallel testing of the catalytic activity in the selective hydrogenation of unsaturated ketones. These studies will serve as benchmarks for parallel synthesized libraries of these types of complexes.



Scheme 1. Hydrogenation of unsaturated ketones

General Section

1. Structural Studies of an Array of Mixed Diamine Phosphine

Ruthenium(II) Complexes

1.1 General Consideration

In this part of the work the neutral diamine–bis(ether–phosphine)ruthenium(II) complexes **3a – g** were synthesized by treatment of the precursor complex $\text{RuCl}_2(\eta^2\text{-Ph}_2\text{PCH}_2\text{CH}_2\text{OCH}_3)_2$ (**2**) with various chelating diamines **a – g** (Scheme 2). Advantage was taken of the hemilabile character of the ether-phosphine ligand $\text{Ph}_2\text{PCH}_2\text{CH}_2\text{OCH}_3$. This route was found to be the most straightforward and efficient way to generate these complexes. Moreover, this method is generally applicable to numerous comparable examples and thus is promising for later use in parallel synthesis. The corresponding monocationic (**4a – g**) and dicationic (**5a – g**) compounds were prepared by reacting the neutral complexes **3a – g** with one of the chloride scavengers (AgSbF_6 , AgBF_4 , or TIPF_6). The resulting compounds were fully characterized by X-ray structural analyses and spectroscopic methods.

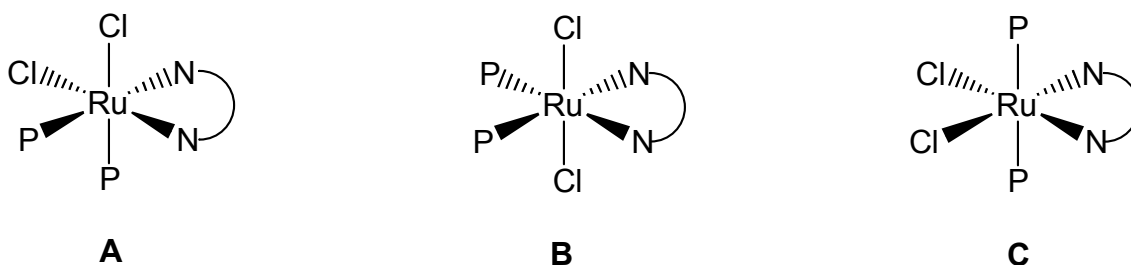
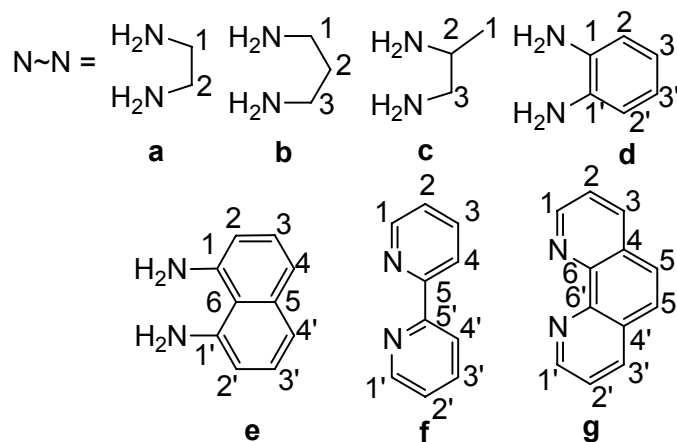
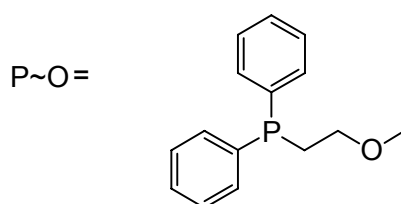
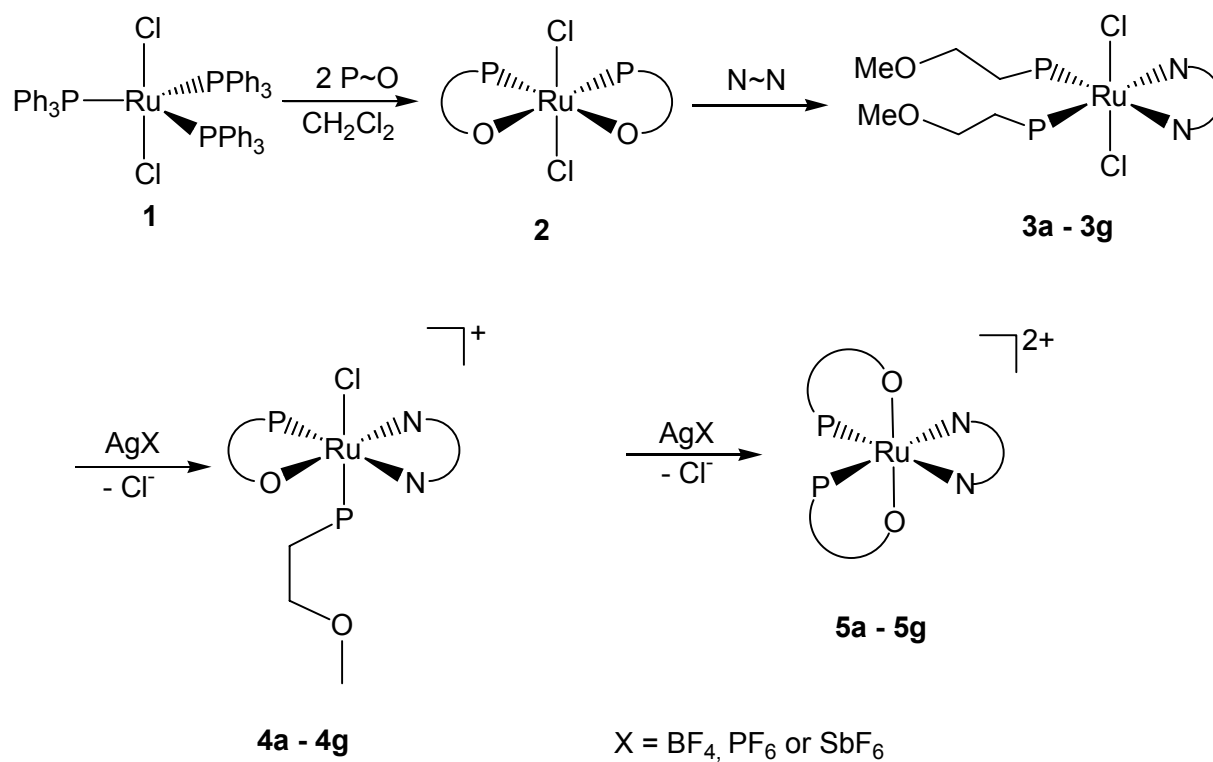


Chart 1. Three possible structural isomers of $\text{Cl}_2\text{Ru}(\text{P}\sim\text{O})_2(\text{N}\wedge\text{N})$.

Scheme 2. Synthesis of the complexes **3a – g**, **4a – g**, and **5a – g**.

1.2 Synthesis and Characterization of the RuCl₂P₂(diamine) Complexes **3a – g**

The bis(ether-phosphine)ruthenium(II) complex **2** has two weak ruthenium-oxygen interactions which were easily cleaved by the stronger nitrogen donors of bidentate diamine ligands. Thus, mixing the bischelate **2** with a slight excess of the diamines **a – g** in dichloromethane gave the ruthenium(II) species RuCl₂P₂(diamine) (**3a – g**) in good to very good yields (Scheme 2). The yellow (**3a – d**), brown (**3e,f**), and red (**3g**) solids are soluble in organic solvents. For octahedral structures of the general formula RuCl₂P₂(diamine) there are three possible coordination geometries. NMR spectroscopy allows to distinguish between the isomers which are displayed in Chart 1. In the ¹H NMR spectra of RuCl₂P₂(diamine) (**3a – g**), characteristic sets of signals are observed which can be assigned to the phosphine as well as to the diamine ligands. In all cases the broad and featureless peaks prevent a detailed analysis; however, the integration of the proton resonances indicates that the phosphine to diamine ratio is in agreement with the composition of **3a – g**. Furthermore, the chemical shifts of the singlets due to the protons of the methoxy functions agree well with the η¹-P~O unit. The singlets in the ³¹P{¹H} NMR spectra of **3a,b** and **3d – g** indicate that the phosphine groups are chemically equivalent, which is only the case if the structure of the RuCl₂P₂(diamine) isomers has C_{2v} symmetry, as in **B** or **C** (Chart 1). The nonsymmetrical diamine in **3c** causes the loss of the C₂ axis, which results in the splitting of the phosphorus resonances into an AB pattern. For compounds **3d,f**, additional AX multiplets are observed in the ³¹P{¹H} NMR spectra. These signals are generated from minor amounts of the C₁-symmetrical *cis,cis,cis*-RuCl₂P₂(diamine) isomers (structure **A**), which were also formed during the reaction. The phosphorus chemical shifts of **3a – g** and the phosphorus-phosphorus coupling constants of **3c** suggest that the ether-phosphines are η¹-(P)-coordinated and are positioned *cis* to one another. Given also the presence of the diamine chelate, the chlorines have to be in a mutually *trans* arrangement. This supports structure **B** as the most favored geometry in solution. The

$^{13}\text{C}\{^1\text{H}\}$ NMR spectra are consistent with these findings. Characteristic signals are found due to the η^1 -(P)-ether-phosphines as well as due to the aliphatic (**3a – c**) and aromatic diamines (**3d – g**). In the $^{13}\text{C}\{^1\text{H}\}$ NMR spectra of complexes **3a,b,d – g** the AXX' splitting patterns which are observed for the carbon atoms attached to phosphorus are caused by the interaction of the magnetically inequivalent phosphorus atoms with the ^{13}C nuclei. They are also compatible with structure **B** (Chart 1).

While geometry **B** is preferred in solution, all three structures **A – C** (Chart 1) are found in the solid state. This was confirmed by single-crystal X-ray diffraction studies of the complexes **3a - c, e, and g**. Examples for structure **A** (**3a**) and **B** (**3e**) are shown in Figure 1. and selected bond distances and angles are summarized in Table 1. The 1,3-diaminopropane (**3b**), 1,2-diamino-propane (**3c**), and 1,8-diaminonaphthaline (**3e**) (Figure 1) derivatives crystallize in the coordination geometry **B**, which represents the most commonly found structure for mixed-ligand ruthenium complexes of this type. Rarely observed is the *cis,cis,cis* form **A**, which is favored by the 1,2-diaminoethane complex **3a** (Figure 1), and the geometry **C**, where the phosphines are located mutually *trans* to each other as in the 1,10-phenanthroline complex **3g**. Unfortunately, the quality of the crystal of **3g** was so poor that, besides the arrangements of the ligands around ruthenium, no further information can be given with respect to bond lengths and angles.

1.3 Crystal Structures of **3a** and **3e**

In **3a**, the *all-cis* isomer **A** (Chart 1), the octahedral coordination of ruthenium is slightly distorted, the equatorial plane consisting of the atoms Cl(2), P(1), N(1), and N(2) being displaced toward the sterically less demanding Cl(1) such that Ru(1) is shifted out of this plane toward P(2) by almost 0.2 Å (Figure 1). This is also reflected in the fact that most of the angles formed by Cl(1) with ligands in *cis* positions are significantly smaller than 90°, with the Cl(1)-Ru(1)-Cl(2) angle of 92.86(6)° being the exception. In contrast, the Cl(1)-

Ru(1)-P(2) angle between the axial ligands, $174.49(6)^\circ$, deviates moderately from a linear arrangement. The different *trans* influences of the ligands at ruthenium affect the Ru-P distances only marginally, with Ru(1)-P(1) ($2.296(2)$ Å, *trans* to nitrogen) slightly longer than Ru(1)-P(2) ($2.244(2)$ Å, *trans* to chlorine). The methoxyethyl chains of both phosphine ligands implement *all-trans* conformations, with torsional angles being in the range of 171 - 176° . The 1,2-diaminoethane chelate adopts a twist conformation, with C(10) and C(11) twisted out of the plane formed by Ru(1), N(1), and N(2) by 0.4 and -0.2 Å.

In **3e**, the more common isomer **B** (Chart 1), the atoms Ru(1), P(1), P(2), N(1), and N(2) deviate by less than 0.08 Å from the equatorial least-squares plane. However, the chlorine atoms are pushed from their axial positions toward the diamine by the phosphine ligands, forming an angle of $167.56(2)^\circ$. The plane of the diamine ligand is tilted from the equatorial plane by a dihedral angle of $42.8(1)^\circ$. In comparison to **3a**, the Ru-Cl distances are slightly shorter and the Ru-N bonds slightly longer. In the methoxyethyl chains of the phosphines, the P-C bonds deviate from an *all-trans* arrangement and, with P-C-C-O torsional angles of 151 and 144° , are almost partially eclipsed (anticlinal).

1.4 Syntheses and Characterization of the Cations $[\text{RuCl}(\text{P}\sim\text{O})(\text{P}\wedge\text{O})(\text{N}\wedge\text{N})]\text{X}$ (**4a – d, f**) and $[\text{Ru}(\text{P}\wedge\text{O})_2(\text{N}\wedge\text{N})]\text{X}_2$ (**5a – c, e – g**)

Complexes **3a – g** react with different chloride scavengers such as AgSbF_6 , AgBF_4 , and TIPF_6 in dichloromethane to give solutions from which the mono- and dicationic salts **4a – d, f**, and **5a – c, e – g** are isolated (Scheme 2). Depending on the amount of silver and thallium salt used, one or two chloride ions are abstracted by simultaneously closing one or two rings via ether coordination. In the case of **3d**, the conversion into **5d** remained incomplete, even after a prolonged reaction time and the presence of a large excess of silver salt. Only traces of **5d** are observed in addition to the main product **4d**. In these reaction steps,

the advantage of the ether-phosphines becomes obvious, as they protect the vacant coordination sites and circumvent the need for further weakly coordinating ligands such as acetonitrile, THF, and acetone. The mono- and dicationic species **4a – d, f**, and **5a – c, e – g** are obtained as colored powders. In the solid state they are relatively insensitive, while in solution they are rather sensitive toward air. They readily decompose in the presence of water. Due to their polar composition they dissolve in moderately polar solvents such as dichloromethane.

The formation of only one $\eta^2\text{-P}^{\wedge}\text{O}$ chelate ring generates two sets of resonances in the ^1H , $^{13}\text{C}\{^1\text{H}\}$, and $^{31}\text{P}\{^1\text{H}\}$ NMR spectra of the monocationic complexes **4a – d, f**. In all cases, the signals caused by the ether-phosphine chelate are shifted downfield compared to the $\eta^1\text{-P}\sim\text{O}$ unit. This holds especially for the nuclei belonging to groups which are directly bound to the ruthenium-coordinated oxygen. Thus, chemical shift differences of 3-6 ppm in the $^{13}\text{C}\{^1\text{H}\}$ and of 0.1-0.5 ppm in the ^1H NMR spectra are observed for the CH_2OCH_3 fragments. The $^{31}\text{P}\{^1\text{H}\}$ NMR spectra contain AX patterns with $^2J_{\text{PP}}$ coupling constants typically found for *cis*-arranged phosphines.

The loss of symmetry which is caused by the twofold ring closure in **5a – c, e – g** results in two chemically inequivalent phosphine groups. As they are located in similar structural environments, their $^{31}\text{P}\{^1\text{H}\}$ NMR spectra display the typical splitting patterns of AB spectra. The small coupling constants ($^2J_{\text{PP}} = 35$ Hz) confirm the *cis* arrangement of both phosphine groups in the complexes **5a – c, e – g**. The chiral carbon center in the diamine ligand of **5c** generates a pair of diastereomeric complexes, which give rise to two AB multiplets in the $^{31}\text{P}\{^1\text{H}\}$ NMR spectrum. The additional low-field shifts of the ^{31}P resonances in the spectra of **5a – c, e – g** compared to those of **3a – g** are indicative of the formation of five-membered rings.⁷³ This is supported by the $^{13}\text{C}\{^1\text{H}\}$ NMR spectra. Due to the coordination of the ether oxygen, the ^{13}C signals of the carbon atoms of the methyl and methylene groups bound to the oxygen are shifted to lower field by approximately 10 ppm. In

agreement with the $^{31}\text{P}\{^1\text{H}\}$ NMR spectra, two sets of signals are observed in the $^{13}\text{C}\{^1\text{H}\}$ NMR spectra of **5a – c**, **e – g** for the phosphine ligands. The spectra are completed by the characteristic ^{13}C resonances of the diamines in the alkane (**5a – c**) and aromatic (**5e – f**) regions, respectively.

1.5 Crystal Structures of **4b** and **5a**

The cationic complex **4b** shares some structural features with the isomer **A** of complex **3a**, insofar as one phosphine ligand is located in the equatorial plane defined by the chelating diamine ligand, while the other phosphine ligand resides in an axial position (Figure 2). Consequently, the ruthenium is displaced from the equatorial plane toward P(2) by 0.17 Å and the angles involving O(1) and *cis* ligands are significantly smaller than 90°. The diaminopropane chelate adopts a chair conformation, where the tip involving ruthenium is flattened (torsional angles about the Ru-N bonds are 19-22°) but C(11) is pushed more strongly out of plane (torsional angles about the C(11)-C(10) and C(11)-C(12) bonds in the range 71-74°). The five-membered chelate created by the η^2 -phosphine forms a regular twisted ring. The two Ru-P distances differ from each other more than in the neutral compounds **3a,e**. The methoxyethyl chain of the η^1 -phosphine is in an *all-trans* conformation, except for the P-C bond that adopts a *gauche* position with respect to the chain, with a P-C-C-O torsional angle of 71°.

In the dicationic complex **5a**, the phosphorus atoms differ also with respect to the equatorial plane defined by the chelating 1,2-diaminoethane. However, the out-of-plane displacement of ruthenium toward P(2) is not as strong (0.12 Å). Similar to **4b**, the η^2 -phosphine chelate involving P(1) adopts a twist conformation, as does the ethylenediamine ring. In contrast, the η^2 -phosphine involving P(2) adopts an envelope conformation, with C(6) forming the flap.

Table 1. Selected bond lengths (Å) and bond angles (deg) for **3a**, **e**, **4b**, and **5a**

	3a	3e	4b	5a
Ru(1)-Cl(1)	2.488(2)	2.420(1)	2.412(1)	
Ru(1)-Cl(2)	2.436(2)	2.416(1)		
Ru(1)-P(1)	2.296(2)	2.275(1)	2.307(1)	2.304(2)
Ru(1)-P(2)	2.244(2)	2.272(1)	2.248(1)	2.234(2)
Ru(1)-N(1)	2.147(5)	2.211(2)	2.178(3)	2.184(7)
Ru(1)-N(2)	2.134(5)	2.208(2)	2.148(3)	2.122(7)
Ru(1)-O(1)			2.309(2)	2.283(7)
Ru(1)-O(2)				2.182(6)
Cl(1)-Ru(1)-Cl(2)	92.86(6)	167.56(2)		
Cl(1)-Ru(1)-N(1)	80.02(15)	81.81(6)	79.97(8)	
Cl(1)-Ru(1)-N(2)	80.05(15)	82.44(6)	165.67(8)	
Cl(1)-Ru(1)-P(1)	86.73(6)	90.80(3)	98.86(3)	
Cl(1)-Ru(1)-P(2)	174.49(6)	97.39(3)	93.45(3)	
P(1)-Ru(1)-P(2)	97.61(6)	92.50(3)	98.63(4)	95.45(8)
N(1)-Ru(1)-N(2)	80.2(2)	75.4(1)	90.1(1)	80.3(3)
O(1)-Ru(1)-N(1)			88.5(1)	90.7(3)
O(1)-Ru(1)-N(2)			80.7(1)	86.7(3)
P(1)-Ru(1)-O(1)			81.08(7)	81.00(18)
P(2)-Ru(1)-O(1)			177.89(7)	171.5(2)
O(2)-Ru(1)-N(1)				90.1(3)
O(2)-Ru(1)-N(2)				169.7(3)
P(1)-Ru(1)-O(2)				88.97(18)
P(2)-Ru(1)-O(2)				82.43(18)
O(1)-Ru(1)-O(2)				89.7(3)

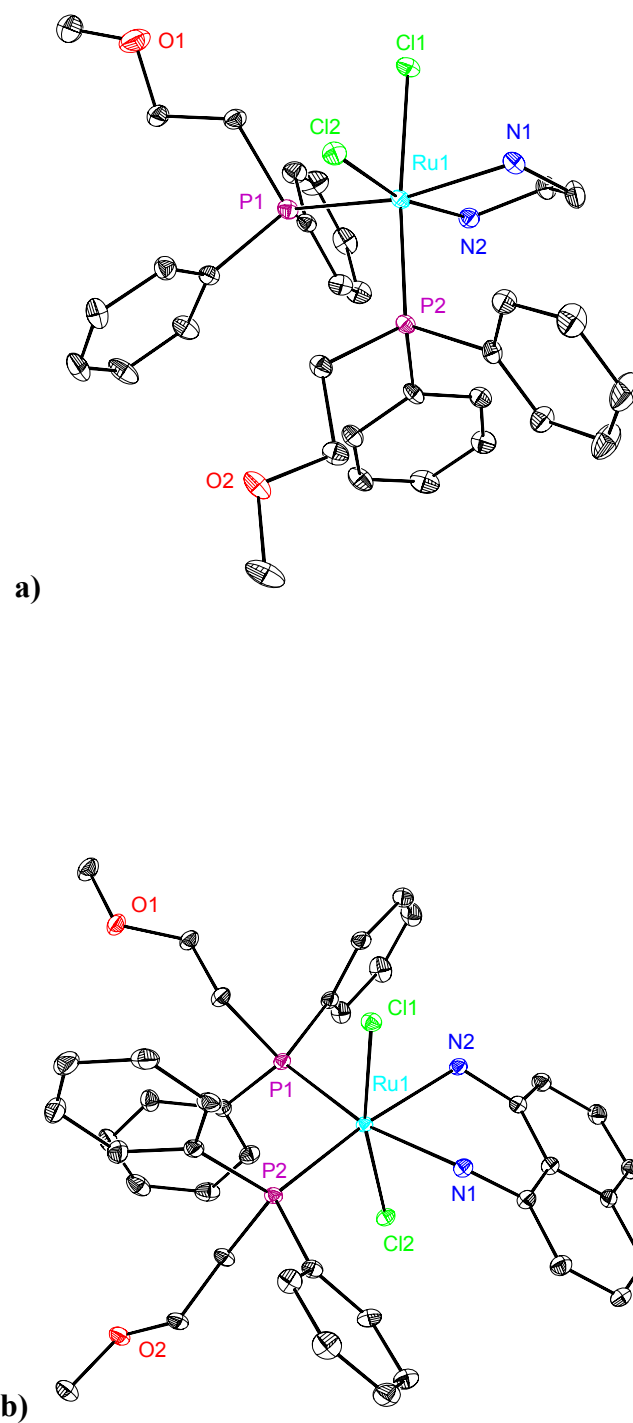


Figure 1. ORTEP plots of **3a** (a) and **3e** (b) shown at the 50% probability level. Hydrogen atoms are omitted for clarity.

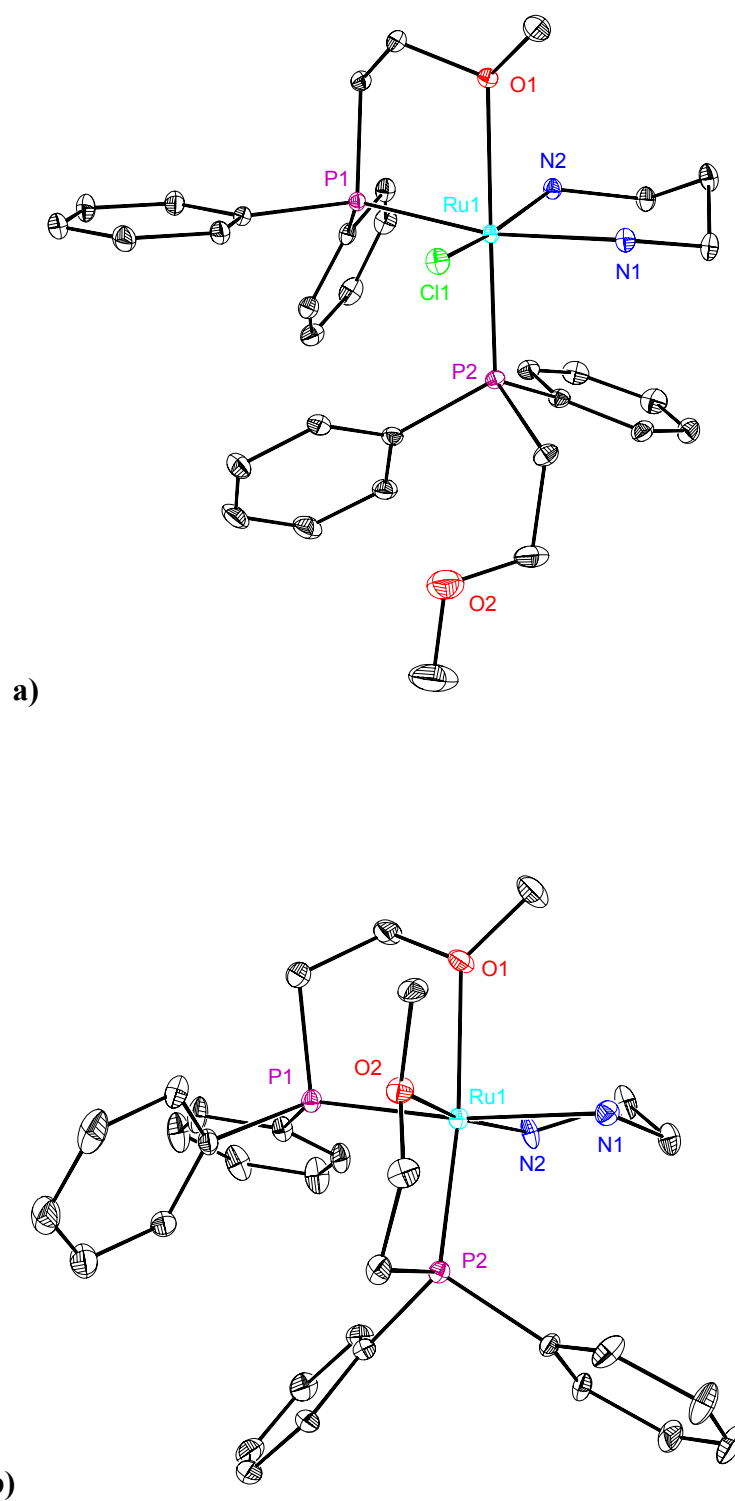


Figure 2. ORTEP plots of **4b** (a) and **5a** (b) shown at the 50% probability level. Hydrogen atoms are omitted for clarity.

1.6 Conclusion

An efficient method to produce a large variety of neutral and cationic diamine(ether-phosphine)ruthenium(II) complexes was established. The geometry of these complexes is controlled via the *cis* diamines and the ether-phosphine ligands. Of importance is the exclusive *cis* arrangement of the weak Ru-O bonds in the complexes **5a – c**, **e – g**, since many of the transition-metal-catalyzed conversions require two available coordination sites *cis* to one another. Interestingly, in the case of the neutral complexes **3a – g** without Ru-O contacts, a sensitive interplay between the stereochemistry of the diamine ligand and electronic factors decide the geometry of the complex. Therefore, all three possible isomers are found in the solid state by X-ray analysis of the complexes **3a – g**. However, as catalysis is performed in solution or under solution-like conditions, this should have no impact on the selectivity and activity of the potential catalyst precursors **3a – g**, since in solution geometry **B** is exclusively formed.

2. T-Silyl Functionalized Diaminediphosphineruthenium(II) Precursor

Complexes

2.1 General Consideration

In this section a small library of neutral and cationic diamine(ether-phosphine)ruthenium(II) complexes is described. The complexes are provided with T-silyl functions at the periphery of a novel phosphine ligand system. By this means, they can later be subjected to a sol-gel process to create new stationary phases for chemistry in interphases.

2.2 Synthesis and Characterization of the Ligand **9(T⁰)**

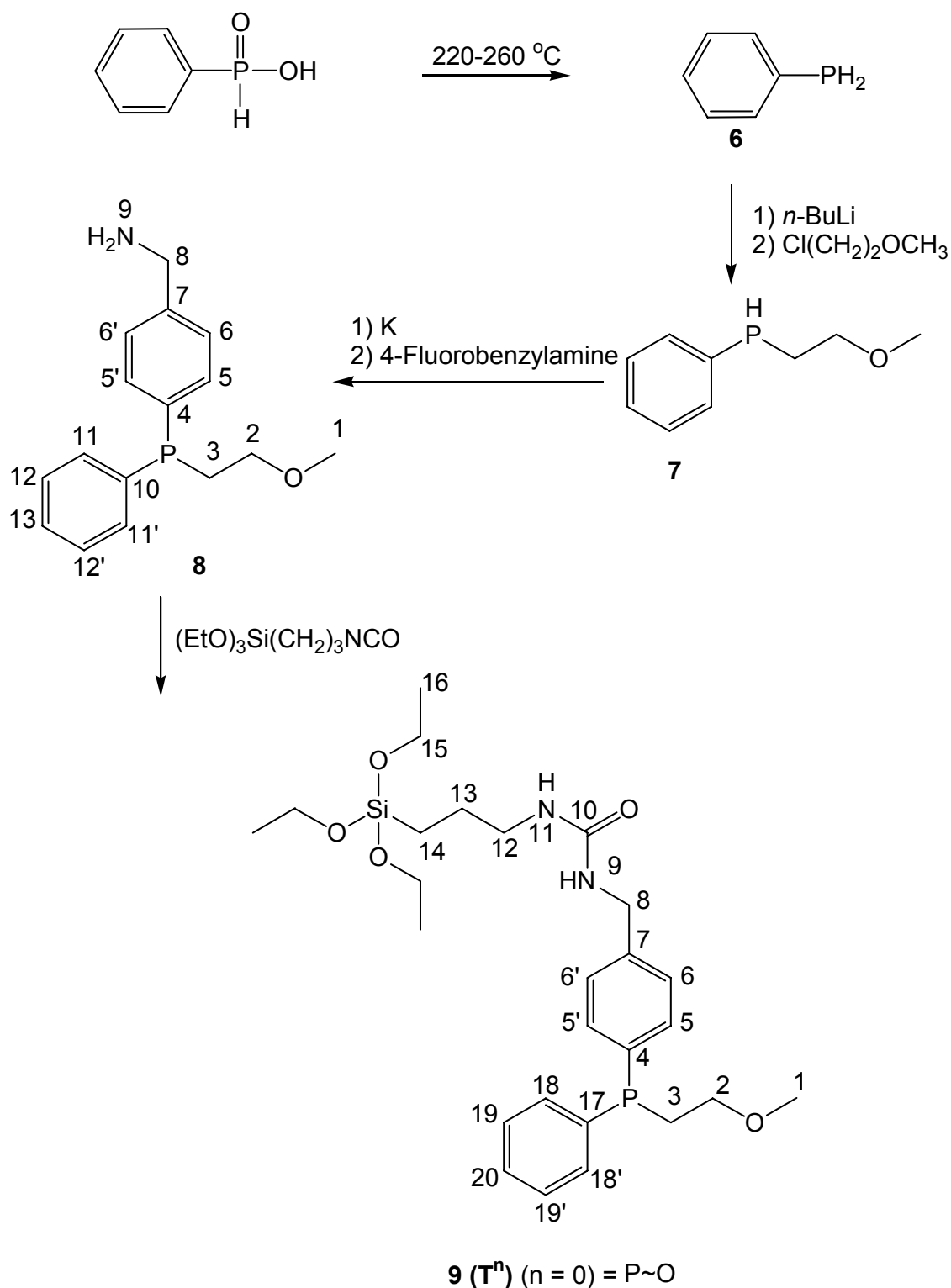
Starting compound is the phenylphosphine **6** which is easily obtained by thermolysis of phenylphosphinic acid⁷⁴ (Scheme 3). With some modifications the synthesis of the ether-phosphine **7** was carried out according to a known procedure.⁷⁵ Reaction of **7** with potassium in diethoxyethane affords the corresponding phosphide which in the presence of 4-fluorobenzylamine is transformed to the ether-phosphine ligand **8**. Slow addition of the intermediate potassium phosphide to 4-fluorobenzylamine at 50 °C reduces the formation of by-products. The fluorine atom in the *para*-position of the benzylamine enhances the nucleophilic substitution at the aromatic ring.⁷⁶ Compound **8** is obtained as a colorless air-sensitive liquid in high yields. The amine group provides an excellent substituent to introduce a spacer unit with a terminal T-silyl function. This step is realized if the ether-phosphine **8** is treated with 3-(triethoxysilyl)propylisocyanate in dichloromethane. The modified phosphine **9(T⁰)** is isolated as colorless solid which readily dissolves in medium polar organic solvents and is sensitive to air and moisture.

Both the intermediate **8** and the ligand **9(T⁰)** were completely characterized by NMR, IR, and mass spectroscopy. In the ³¹P{¹H} NMR spectra a singlet each at $\delta = -22.2$ and -22.1

is observed. This indicates that the *para*-positioned spacer function exerts nearly no influence on the ^{31}P chemical shift. In the ^1H NMR spectrum of **8** a characteristic peak at $\delta = 1.26$ is assigned to the amino group. It disappears in the case of **9(T⁰)** and because of $^3J_{\text{HH}}$ coupling two new triplets at $\delta = 4.9$ and 5.1 occur which correspond to the NH functions of the urea linkage. The $^{13}\text{C} \{^1\text{H}\}$ NMR spectrum of **9(T⁰)** reveals a singlet at $\delta = 159.0$ which is attributed to the carbonyl group of the spacer unit. For a complete assignment of the ^1H and ^{13}C signals 2D ^1H -COSY, $^{13}\text{C} \{^1\text{H}\}$ -DEPT, and $^1\text{H}, ^{13}\text{C} \{^1\text{H}\}$ HMQC NMR spectra were recorded (see Experimental part). A characteristic absorption at 3378 cm^{-1} in the IR spectrum of **8** is assigned to the NH_2 substituent. Concerning the ligand **9(T⁰)** two bands at 3329 and 1624 cm^{-1} are assigned to the NH and C=O stretching vibrations, respectively. The composition of the T-silyl functionalized ligand **9(T⁰)** was corroborated by its EI mass spectrum, showing the molecular peak at $m/z = 520.2$.

2.3 Synthesis and Characterization of the $\text{Cl}_2\text{Ru}(\text{P}\sim\text{O})_2(\text{diamine})$ Complexes **11a(T⁰)**–**g(T⁰)**

According to Scheme 4 the chelated bis(ether-phosphine)ruthenium(II) complex **10(T⁰)** is synthesized by addition of the ligand **9(T⁰)** to $\text{Cl}_2\text{Ru}(\text{PPh}_3)_3$ in CH_2Cl_2 . The red air-sensitive solid **10(T⁰)** was obtained after precipitation and separation of PPh_3 . It is soluble in most organic media, but not in diethyl ether. A FAB mass spectrum of **10(T⁰)** shows the isotopic distribution of the molecular ion which is in agreement with the calculated spectrum. The $^{31}\text{P} \{^1\text{H}\}$ NMR spectrum of **10(T⁰)** in CH_2Cl_2 displays a singlet at $\delta = 68.6$ which is markedly downfield shifted compared to that of the ligand **9(T⁰)**. Such a behavior is typical for a phosphorus atom which is incorporated into a five-membered ring.⁷⁷ For the same reason the ^1H ($\delta = 3.7$ ppm) and ^{13}C ($\delta = 72.6$) resonance of the OCH_3 group in the ^1H and $^{13}\text{C} \{^1\text{H}\}$ NMR spectrum, respectively, is also shifted to lower field.



T = T type of silicon atom (three oxygen neighbors)
 n = 0 - 3 (number of Si-O-Si bonds)

Scheme 3. Synthesis of the T-sily functionalized ligand.

Complex **10**(T^0) is provided with two weak ruthenium–oxygen bonds which are easily cleaved by the strong nitrogen donors of the bidentate diamine ligands. If the

bis(chelate)ruthenium(II) complex **10(T⁰)** is treated with a slight excess of the corresponding diamine **a – g** the η^1 -P coordinated mixed ligand complexes **11a(T⁰) – g(T⁰)** are formed (Scheme 3). The yellow **11a(T⁰) – c(T⁰)**, brown **11d(T⁰) – f(T⁰)**, and red **11g(T⁰)** solids show similar solubility as **10(T⁰)**. Electron spray mass spectra were carried out and they give evidence of the molecular composition. Expectedly the ³¹P singlets in the ³¹P{¹H} NMR spectra of **11d(T⁰) – g(T⁰)** are high field shifted compared to **10(T⁰)** indicating that the phosphines are monodentately coordinated via the P atoms. These singlet peaks indicate that the phosphine groups are chemically equivalent. In principle three different structural isomers **A – C** are possible (Chart 1). From the NMR data presented here and the literature it is concluded that only structure **B** is realized in solution.^{42,43} Since the spacer unit exerts nearly no influence on the ³¹P chemical shift, the ³¹P{¹H} NMR spectra of **11a(T⁰) – g(T⁰)** are comparable with those of the corresponding complexes without this spacer group. In the ¹H NMR spectra of **11a(T⁰) – g(T⁰)** characteristic sets of signals occur which are assigned to the aliphatic and aromatic protons of the phosphine and diamine ligands, respectively (Experimental part). Furthermore the ¹H signals of the methoxy protons experience a considerable high field shift compared to **10(T⁰)** which is in agreement with an η^1 -P~O coordination. The ¹³C{¹H} NMR spectra are consistent with these findings. As a typical example the ¹³C resonance of the OCH₃ substituent is also high field shifted compared to **10(T⁰)**. Altogether it is emphasized that all NMR data are in close agreement with the analogous complexes for the homogeneous phase.

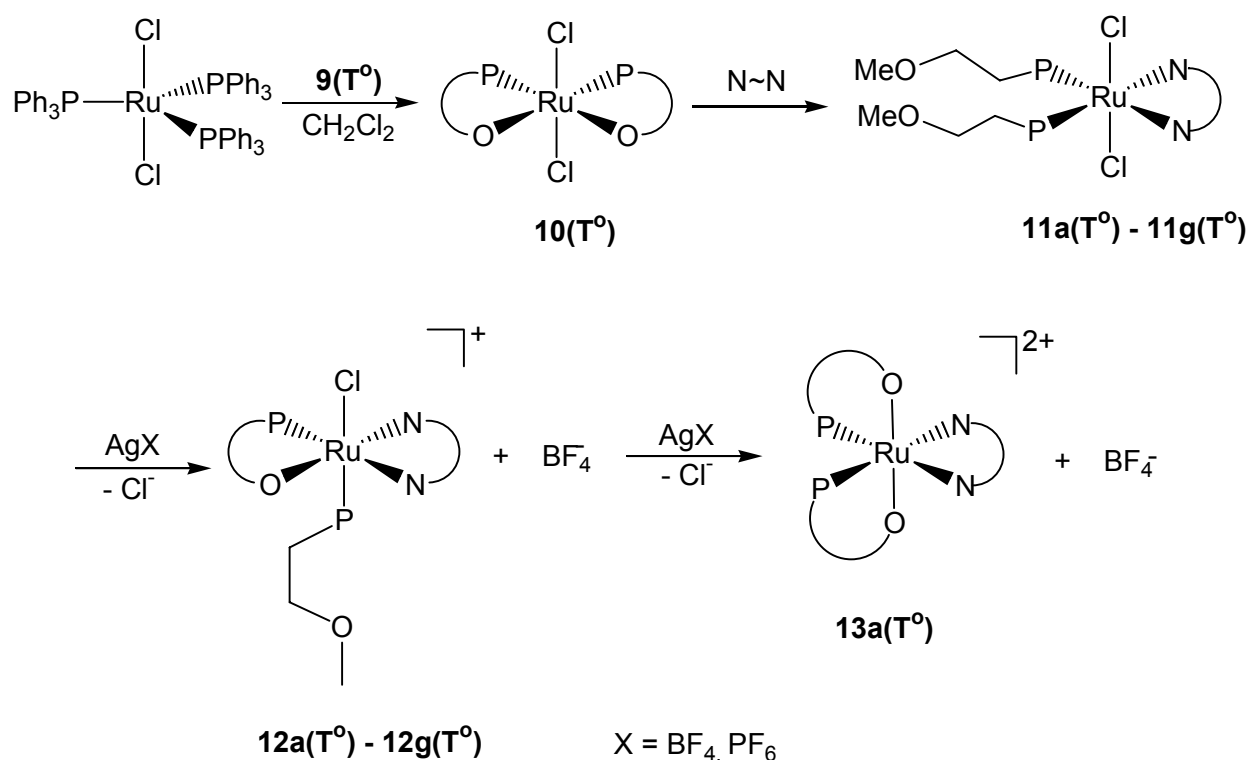
2.4 Synthesis and Characterization of the Mono- and Dicationic Ruthenium(II) Complexes **12a(T⁰) – g(T⁰)** and **13a(T⁰)**, respectively

Complexes **11a(T⁰) – g(T⁰)** react in dichloromethane with different chloride scavengers such as AgBF₄ or TlPF₆ to give solutions from which the mono- and dicationic complexes **12a(T⁰) – g(T⁰)** and **13a(T⁰)** can be isolated (Scheme 4). One chloride is abstracted with the simultaneous formation of a five-membered ring via ether coordination ($\eta^2\text{-P}^{\wedge}\text{O}$ coordination) by using an equivalent amount of one of the scavengers. Only in the case of **11a(T⁰)** it was possible to abstract both chlorides in the presence of a large excess of TlPF₆ at 40 °C in CH₂Cl₂. But the reaction did not proceed quantitatively and the yield of **13a(T⁰)** was low. It was not possible to transfer these reaction conditions to the other complexes **11b(T⁰) – g(T⁰)** due to the instability of the dicationic species. Electron spray mass spectra were recorded for **12a(T⁰) – g(T⁰)** which are in agreement with the expected values. In the transformation of compounds **11a(T⁰) – g(T⁰)** to **12a(T⁰) – g(T⁰)** the advantage of ether-phosphines becomes obvious since they protect the vacant coordination site. Hence further weakly coordinating ligands like acetonitrile, THF, or acetone are not necessary. In the solid state the cationic complexes **12a(T⁰) – g(T⁰)** are relatively insensitive while in solution they decompose in the presence of air and moisture. Due to their polar character they readily dissolve in solvents of medium polarity like dichloromethane.

Due to the existence of three chiral centers resulting from the two different phosphorus atoms and the metal center, eight isomers are to be expected. However, up to three diastereomers can be distinguished in the ³¹P{¹H} NMR spectra. In all cases the resonances caused by the chelated ether-phosphine are downfield shifted compared to those of the $\eta^1\text{-P}\sim\text{O}$ bonded ligand. In particular this is the case for nuclei belonging to groups which are in direct vicinity of the ruthenium coordinated oxygen. Thus two sets of resonances are observed in the ¹H and ¹³C{¹H} NMR spectra of **12a(T⁰) – g(T⁰)** which are caused by the CH₂OCH₃

moieties. Each diastereomer give rise to an AX pattern in the $^{31}\text{P}\{^1\text{H}\}$ NMR spectrum. The signals at lower field are attributed to the phosphorus atom which is incorporated into the five-membered ring.⁷³ The size of the $^2J_{\text{PP}}$ coupling (35 Hz) indicates a *cis*-arrangement of the phosphine groups.⁷⁸

Both of the ^{31}P resonances for the two different phosphorus atoms in **13a(T⁰)** are shifted to lower field compared to **12a(T⁰)**. Again each diastereomer is characterized by an AX spin system with a $^2J_{\text{PP}}$ coupling constant of 35 Hz which is typical for *cis*-phosphines. These spectral data are consistent for two $\eta^2\text{-P}^{\wedge}\text{O}$ bonded ligands. The molecular ion of the dicationic complex **13a(T⁰)** was detected by electron spray mass spectroscopy and gives evidence for the molecular composition.



N~N = diamines as mentioned in Scheme 3

Scheme 4. Synthesis of the complexes **11a(T⁰) – g(T⁰)**, **12a(T⁰) – g(T⁰)**, and **13a(T⁰)**.

2.5 Conclusion

A small library of neutral and cationic diamine(ether-phosphine)ruthenium(II) complexes was obtained. The complexes are provided with T-silyl functions at the periphery of a novel phosphine ligand system. By this means they can later be subjected to a sol-gel process to create new stationary phases for chemistry in interphases. Complexes of this type represent potential catalysts for the hydrogenation of conjugated ketones. Due to the reasonable effect of the co-ligand on the catalytic activity of such complexes, a series of different aliphatic and aromatic amines was selected to vary the electronic and steric character of the metal center and the complex, respectively. By the employment of ether-phosphines the introduction of amines is kinetically controlled and the formation of by-products is avoided. The weak ruthenium-oxygen bonds are easily cleaved during the reaction with the amines.

3. Heterogenization of a Matrix of Neutral and Monocationic Diaminediphosphineruthenium(II) Complexes by the Sol-Gel Process

3.1 General Consideration

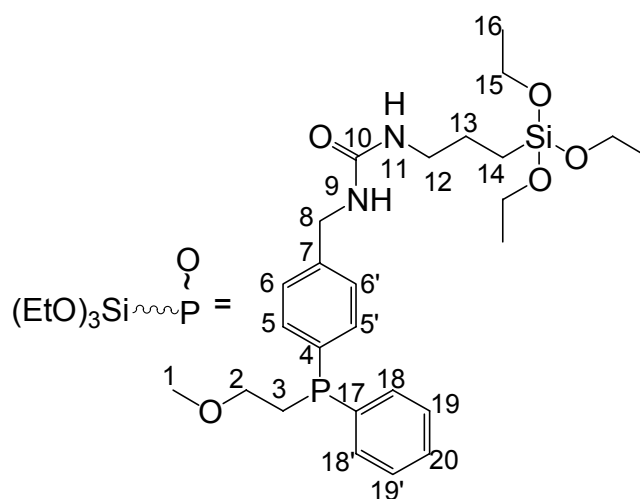
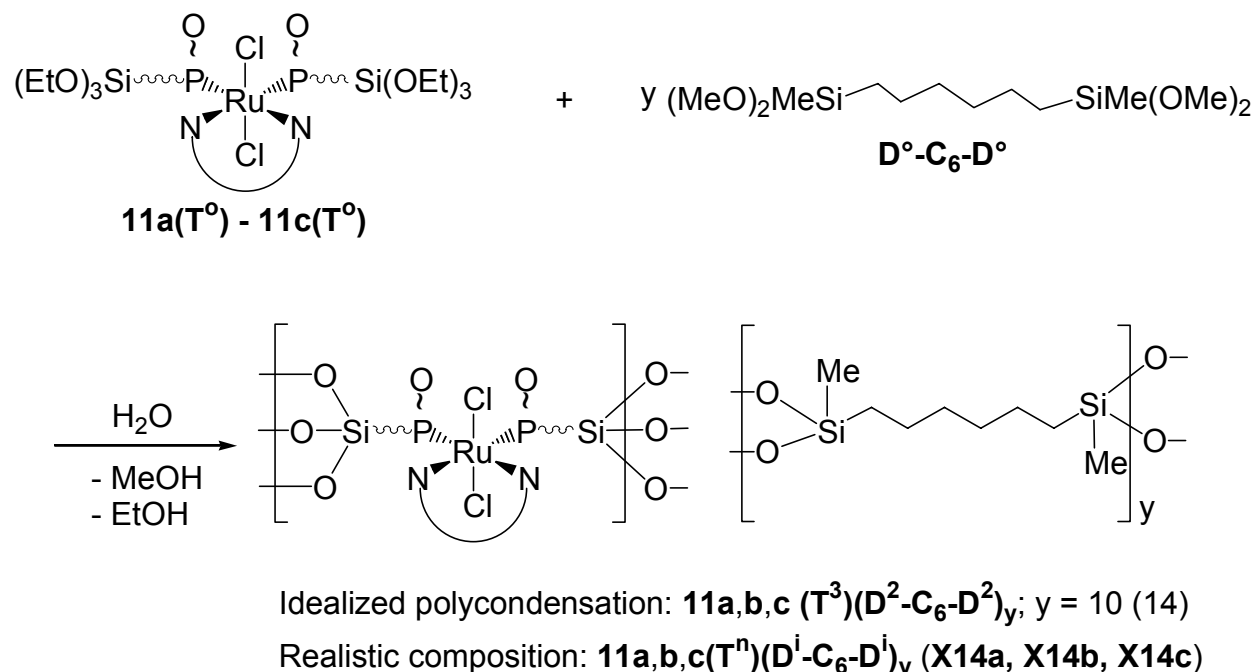
The T-silyl functionalized diamine-bis(ether-phosphine)ruthenium(II) complexes **11a(T^o) – 11g(T^o)** (Scheme 4) were sol-gel processed in the presence of different amounts of the co-condensation agents $\text{CH}_3\text{Si}(\text{OMe})_3$ (**Me-T^o**) and $(\text{MeO})_2\text{SiMe}-(\text{CH}_2)_6-\text{MeSi}(\text{OMe})_2$ (**D^o-C₆-D^o**) to produce a library of heterogenized neutral (**X14a – c**, **X15a – g**, and **X16a – g**) and cationic (**X17a – g**) catalysts (Scheme 5 and 6). These stationary phases are transformed to interphases when they are swollen in a solvent.

3.2 Concept of the Interphases

3.2.1 Definition of the Interphase

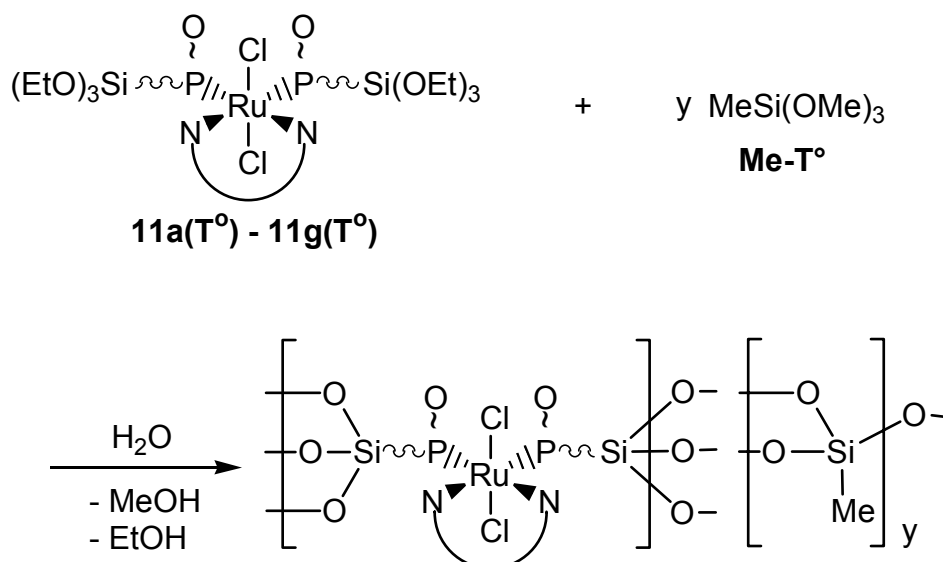
Optimal results in the performance of heterogenized homogeneous catalysts should be obtained if the reactive center is in a state which is able to simulate homogeneous reaction conditions. Interphases are systems in which a stationary phase (e.g. a reaction center linked to a matrix via a spacer) and a mobile component (e.g. a gaseous, liquid, or dissolved reactant) penetrate each other on a molecular scale without forming a homogeneous phase (see Figure 3). The inorganic-organic hybrid materials are comprised of a highly swellable stationary phase consisting of chemically and thermally inert carrier matrices (e.g. TiO_2 , polysiloxane, organic polymer), a spacer unit (PEG, alkyl chains, combined alkyl phenyl systems), and the reactive center (ligand or transition metal complex). These materials have the advantages of nearly unlimited modifiability, reduced leaching of functional groups, and controlling the density of the reaction centers.⁷¹ The proper selection⁷⁹⁻⁸² of the co-condensation agents concerning flexibility and dimension of the copolycondensate coupled

with particular design of the catalytic active centers produce ideal interphases. This affords a solution-like state (Figure 3), in which the reactive centers are nearly homogeneously dispersed and similarly accessible like in homogeneous phase.



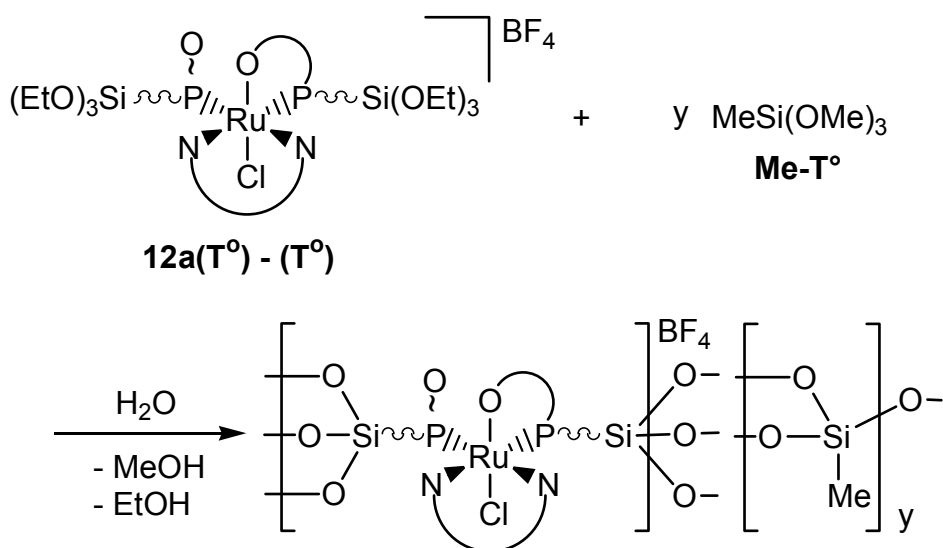
T = T type of silicon atom (three oxygen neighbours)
 D = D type of silicon atom (two oxygen neighbours)
 i, n = numbers of Si-O-Si bonds (i = 0-2; n = 0-3)

Scheme 5. Structures, idealized, and realistic compositions of the xerogels **X14a – c**.



Idealized polycondensation: **11a - g(T³)(Me-T³)_y**; y = 10 (15), 20 (16)

Realistic composition: **11a - g(Tⁿ)(Me-Tⁿ)_y (X15a - g, X16a - g)**



Idealized polycondensation: **12a - g(T³)(Me-T³)_y**; y = 20

Realistic composition: **12a - g(Tⁿ)(Me-Tⁿ)_y (X17a - g)**

T = T type of silicon atom (three oxygen neighbours)

D = D type of silicon atom (two oxygen neighbours)

i, n = numbers of Si-O-Si bonds (i = 0-2; n = 0-3)

Scheme 6. Structures, idealized, and realistic compositions of the xerogels **X15a - g**, **X16a - g**, and **X17a - g**.

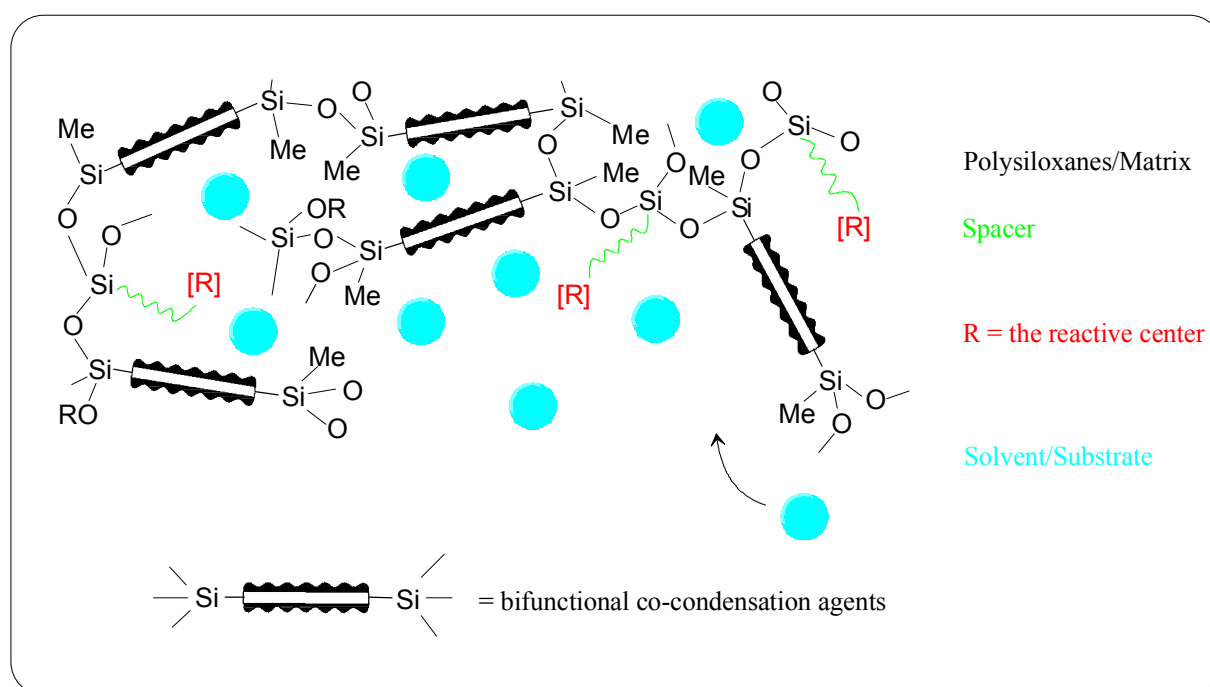
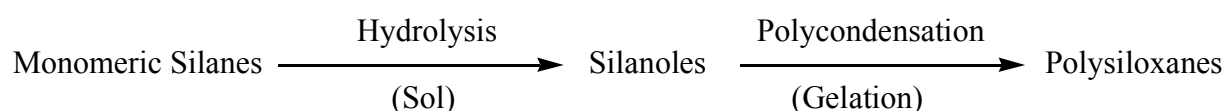


Figure 3. Schematic description of an interphase.

3.2.2 Sol-Gel Process

The sol-gel process^{69,70} is a method where the supporting matrix is generated via controlled hydrolysis and condensation of suitable precursor molecules.



The simultaneous co-condensation of functionalized trialkoxysilyl groups (**F-T**) (**F** denotes for the reactive group and the spacer, respectively) with other co-condensation agents e.g. Q, T, D, and D-C_n-D alkoxy silanes [Q = Si(OR)₄, T = RSi(OR')₃, D = R₂Si(OR')₂, D-C_n-D = (OR')₂RSi(CH₂)_nSiR(OR')₂; R, R' = Me, Et] offers the possibility to modify the resulting matrices. The obtained two- and three-dimensional networks represent stationary phases, in which the amount of the catalyst, the polarity of the matrix, and the mobility of the reactive

center can be varied in a wide range. Furthermore the leaching of the reactive centers is strongly reduced by the high degree of condensation.

3.3 Synthesis and Characterization of the Polymeric Materials

3.3.1 Sol-Gel Processing of the Precursor Complexes $11a(T^\circ) - g(T^\circ)$ and $12a(T^\circ) - g(T^\circ)$

For the access of reproducible polymeric materials uniform reaction conditions have to be maintained. The properties of the sol-gel processed products strongly depend on reaction conditions like type of solvent, kind of catalyst, concentration of the monomers, reaction time, and temperature⁶⁹. All polycondensations were performed in a mixture of THF/MeOH with an excess of water and $(n\text{-Bu})_2\text{Sn}(\text{OAc})_2$ as catalyst. The alcohol is necessary to homogenize the reaction mixture. Sol-gel processes were carried out at ambient temperature in the presence of the two different co-condensation agents $(\text{MeO})_2\text{SiMe}(\text{CH}_2)_6\text{MeSi}(\text{OMe})_2$ ($\text{D}^\circ\text{-C}_6\text{-D}^\circ$) and $\text{MeSi}(\text{OMe})_3$ (Me-T°).

Three kinds of stationary phases were obtained (Table 2): (i) xerogels **X14a – c** were synthesized by co-condensation of $11a(T^\circ) - c(T^\circ)$ with $\text{D}^\circ\text{-C}_6\text{-D}^\circ$ (Scheme 5); (ii) xerogels **X15a – g** and **X16a – g** were formed by co-condensation of $11a(T^\circ) - 11g(T^\circ)$ with two different amounts of Me-T° ($T : T' = 1 : 5$ and $1 : 10$, respectively), and (iii) the cationic polymers **X17a – X17g** could be generated by sol-gel processing of $12a(T^\circ) - g(T^\circ)$ with Me-T° in a $1 : 10$ ratio (Scheme 6).

Table 2. Labeling of the compounds

Ruthenium complex ^{a)}	Co-condensation agent	Ideal T:D or T:T' ratio ^{b)}	Compound	Xerogel
$11a(T^\circ) - c(T^\circ)$	$\text{D}^\circ\text{-C}_6\text{-D}^\circ$	1:10	$11^\circ, \text{b}, \text{c}(T^n)(\text{D}^i\text{-C}_6\text{-D}^i)_{10}$	X14a–c
$11a(T^\circ) - g(T^\circ)$	Me-T°	1:5	$11a\text{-}g(T^n)(\text{Me-T}^i)_{10}$	X15a–g
$11a(T^\circ) - g(T^\circ)$	Me-T°	1:10	$11a\text{-}g(T^n)(\text{Me-T}^i)_{20}$	X16a–g
$12a(T^\circ) - g(T^\circ)$	Me-T°	1:10	$12a\text{-}g(T^n)(\text{Me-T}^i)_{20}$	X17a–g

^{a)}See Scheme 4. ^{b)}T and T' refer to the complex and co-condensation agent, respectively.

3.3.2 Solid-State NMR Spectroscopic Investigations

Due to cross-linking effects the solubility of the polymeric materials **X14a**, **X14b**, **X14c**, **X15a – g**, **X16a – g**, and **X17a – g** is rather limited. Therefore solid-state NMR spectroscopy was used as a powerful technique for their characterization.

3.3.2.1 ^{29}Si CP/MAS NMR Spectroscopy

As it is demonstrated in Figure 4, the ^{29}Si CP/MAS NMR spectra of the different materials show signals for substructures corresponding to D^{i} and T^{n} functions. The average chemical shifts for D° ($\delta = -2.2$), D^1 ($\delta = -13.4$), D^2 ($\delta = -22.5$), T^2 ($\delta = -58.0$), and T^3 ($\delta = -65.3$) species are not significantly changed by the incorporation of different amounts of the co-condensation agents $\text{D}^{\text{i}}\text{-C}_6\text{-D}^{\text{i}}$ and Me-T^{n} and are in agreement with values reported in the literature for comparable systems⁸³. Since all silicon atoms are in direct proximity of protons the Hartmann–Hahn⁸⁴ match could efficiently be achieved. This allows the cross polarization method to be adapted for ^{29}Si solid-state NMR spectroscopic investigations.

The employment of $\text{D}^{\circ}\text{-C}_6\text{-D}^{\circ}$ in the sol-gel process leads to a high degree of condensation for all D-type polymers. Overlapping ^{29}Si resonances of the T-subgroups in the spectra of **X15a – g**, **X16a – g**, and **X17a – g** prevent the calculation of the degree of condensation. T^1 and T^2 signals represent very low intensity indicating also a high degree of cross-linking.

3.3.2.2 ^{13}C and ^{31}P CP/MAS NMR Spectroscopy

In the ^{13}C CP/MAS NMR spectra of the supported complexes **X14a – X14c**, **X15a – g**, **X16a – g**, and **X17a – g** a characteristic peak at approximately $\delta = -0.3$ and -3.8 is assigned to the carbon atom of the silicon adjacent methyl group in the Si–O–Si substructure of the copolycondensates $\text{D}^{\text{i}}\text{-C}_6\text{-D}^{\text{i}}$ and Me-T^{n} , respectively (Figure 5). As a consequence of the sol-gel process, resulting in the formation of hybrid polymers, the carbon nuclei of the silicon

neighboring methylene functions are shifted to lower field of about 5 ppm compared to the monomeric starting compounds. Only weak or even no ^{13}C signals were detected in the spectra of the above-mentioned materials indicating Si-OR functionalities pointing to a high degree of hydrolysis during the polycondensation process. Regarding the ether-phosphine moiety both the methyl and methylene groups vicinal to the ether oxygen atom are sensitive as to whether the oxygen atom coordinates to the metal center or not. Within the polymers the complexes **X17a – g** contain O, P ligands with a $\eta^1\text{-P}$ and $\eta^2\text{-P}\text{O}$ binding mode. In some cases mainly for CH_2O groups this situation is confirmed by the occurrence of two sets of ^{13}C signals for the respective carbon atoms, the chemical shifts of which are in good agreement with those of the monomeric congeners.^{42,66}

All ^{31}P resonances in the ^{31}P CP/MAS NMR spectra of **X14a – c**, **X15a – g**, and **X16a – g** are found in the expected ranges and are broadened due to the chemical shift dispersion (Figure 6). In the case of **X17a – g** diastereomers are present exerting an additional influence on the line width of the ^{31}P resonances. Therefore the expected AX pattern for the $\eta^1\text{-P}$ and $\eta^2\text{-P}\text{O}$ bonded phosphine ligands was not resolved.

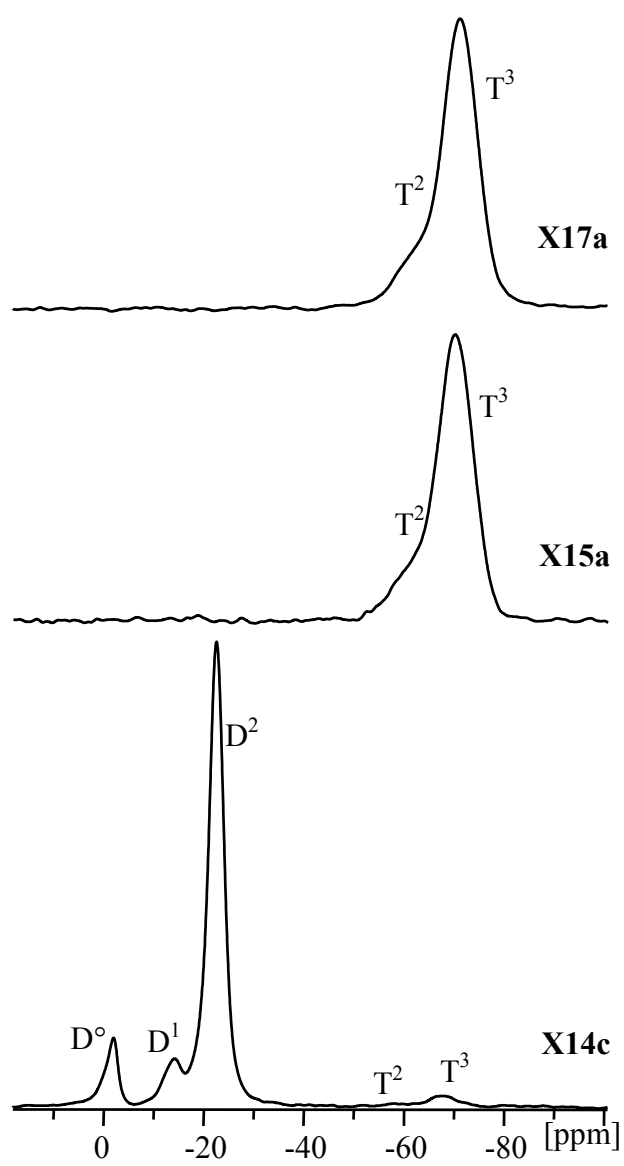


Figure 4. ^{29}Si CP/MAS NMR spectra of the polymeric materials **X14c**, **X15a**, and **X17a** (selected).

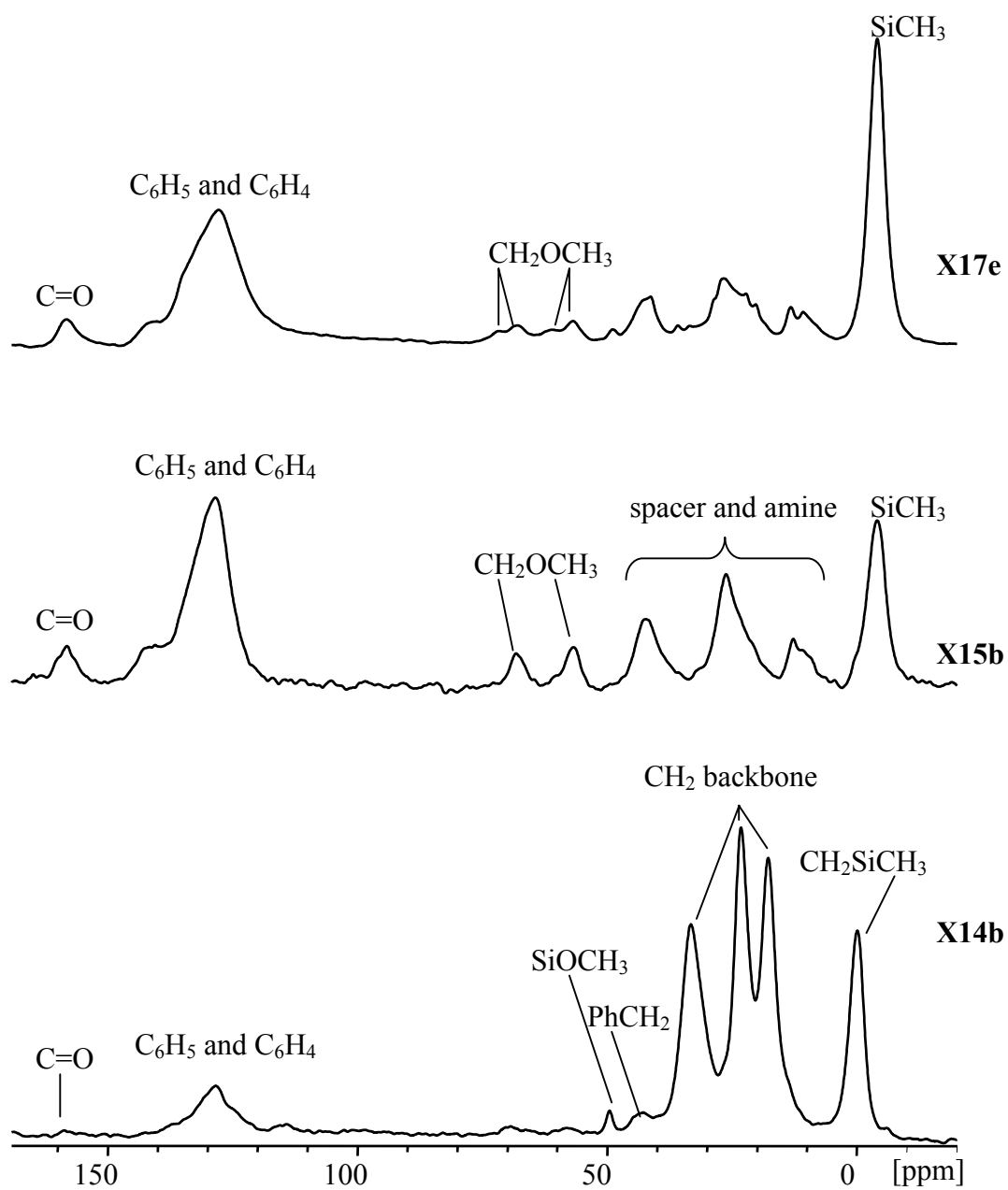


Figure 5. ^{13}C CP/MAS NMR spectra of the polymeric materials **X14b**, **X15b**, and **X17e** (selected).

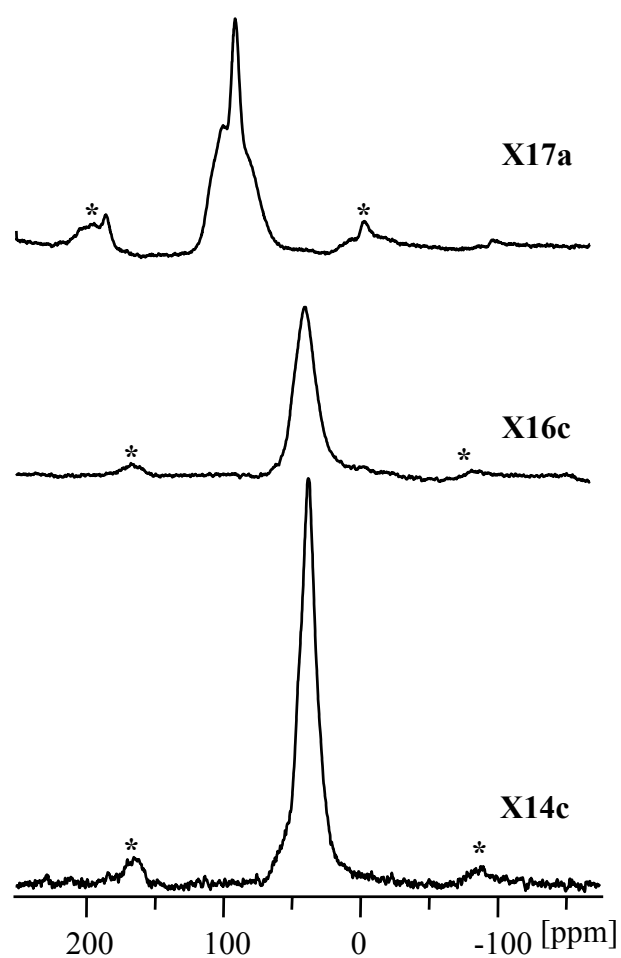


Figure 6. ^{31}P CP/MAS NMR spectra of the polymeric materials **X14c**, **X16c**, and **X17a** (selected). Asterisks denote the spinning side bands.

3.3.3 EXAFS Spectroscopy

Due to the amorphous character of the polymeric materials it is impossible to attain any structural information using the conventional X-ray diffraction method. However, **EXAFS** (*Extended X-ray Absorption Fine Structure*) spectroscopy offers the possibility to investigate the coordination sphere of the reactive centers, without any limitation of the internal structure. An EXAFS analysis provides information on bond distances, coordination

numbers, “Debye-Waller” factors, and the nature of the scattering atoms surrounding an excited atom.^{85,86}

EXAFS measurements were carried out exemplarily on the hybrid materials **X16a** and **X16f** in the solid and suspended state (in toluene). Expectedly the experimental functions for the structural investigations of the hybrid materials in both states are quite similar. Therefore Figure 7 (EXAFS function of **X16a** in suspended state) is offered as a representative example for both complexes in the same state. The EXAFS functions of the mentioned polymeric materials in both states (Figures 8 and 9) can be described by three different atom shells for both complexes. Upon assuming two equivalent Ru–P and Ru–N bond distances, respectively, a good agreement between the calculated and experimental functions of all probed complexes is found. An additional contribution around the central ruthenium atom was established consisting of two equivalent Ru–Cl atomic distances. Structural parameters of **X16a** obtained by EXAFS (Table 3) can directly be compared with X-ray structural data of the monomeric congener.^{42,66} Only small differences were observed concerning the ruthenium–ligand bond distances. Whereas the Ru–P bond lengths are nearly equal (2.26 vs. 2.27 Å), the Ru–N and Ru–Cl distances differ slightly (2.19 vs. 2.14 Å and 2.38 vs. 2.45 Å, respectively). In contrast to the Ru–N bond length in **X16f** (2.08), all other distances (Ru–P and Ru–Cl) do not deviate much from **X16a** (Table 3). The differences of the bond distances of **X16a** and **X16f** in the stationary phase and in the interphase are only marginally.

EXAFS measurements were also done on the charged polymeric material **X17b** and **X17f** (Table 3). Unfortunately, the expected $\eta^2\text{-P}^{\ominus}\text{O}$ chelating behavior was not observed although the deficiency of one chloride ligand was established. This could be due to decomposition of the air sensitive material during the handling and measuring time.

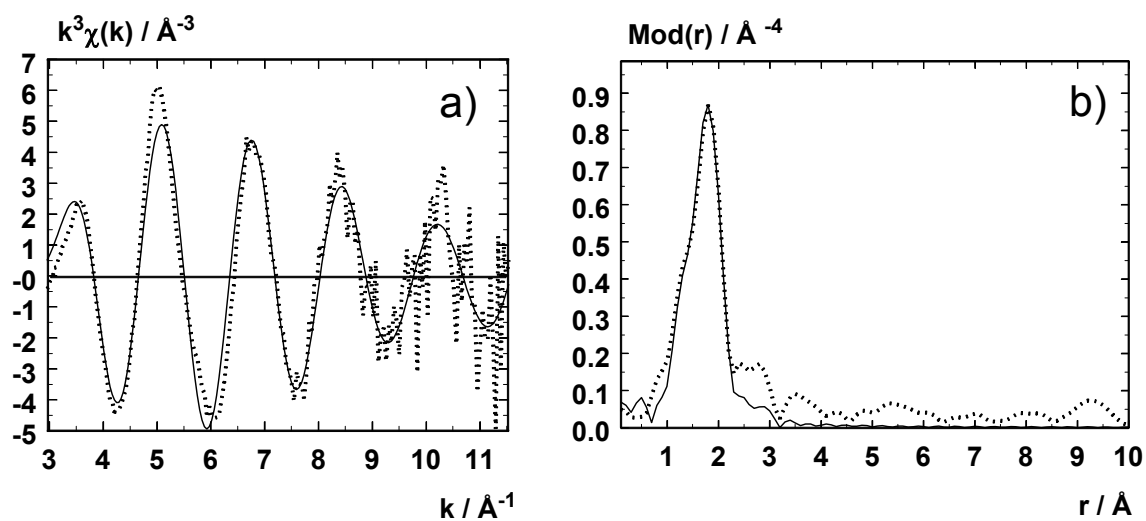


Figure 7. Experimental (dotted line) and calculated (solid line) $k^3 \chi(k)$ functions (a) (k range: 3.29 – 14.90 \AA^{-1}) and their Fourier transforms (b) for **X16a** in suspension with toluene (Ru-K-edge) (see Table 3 for fit parameter).

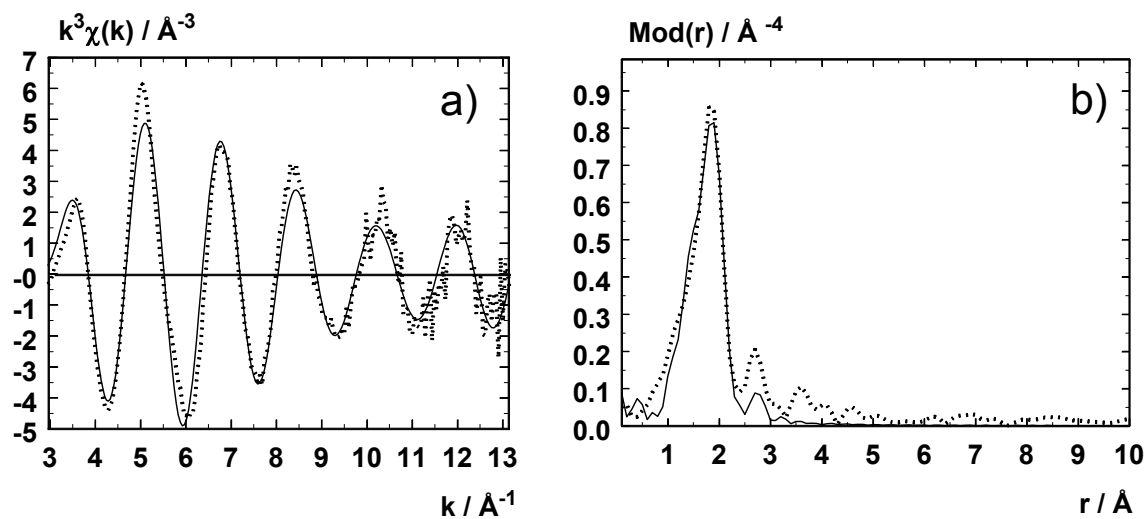


Figure 8. Experimental (dotted line) and calculated (solid line) $k^3 \chi(k)$ functions (a) (k range: 3.40 – 13.30 \AA^{-1}) and their Fourier transforms (b) for **X16a** (Ru-K-edge) (see Table 3 for fit parameter).

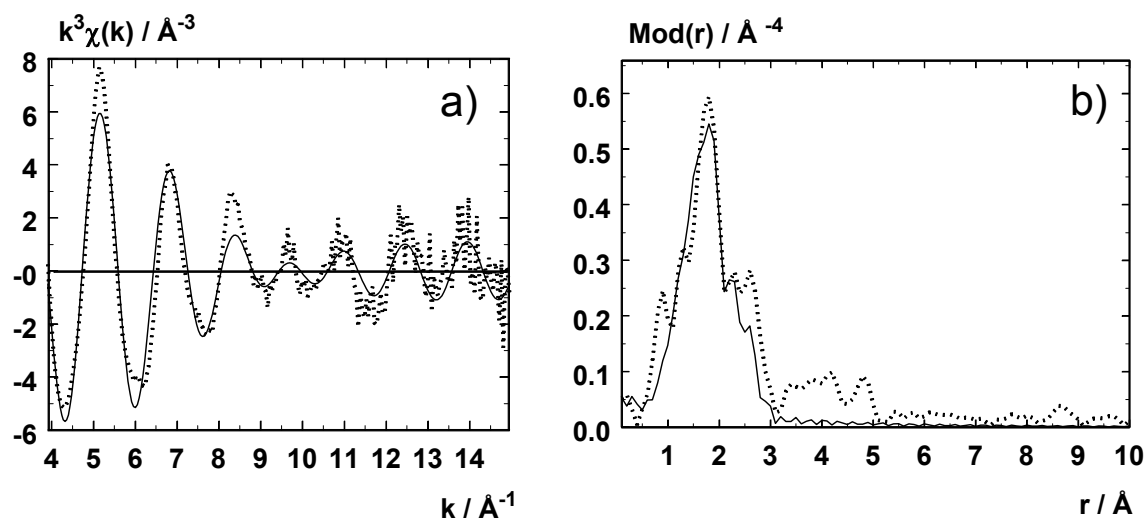


Figure 9. Experimental (dotted line) and calculated (solid line) $k^3 \chi(k)$ functions (a) (k range: 3.29 – 15.00 \AA^{-1}) and their Fourier transforms (b) for **X16f** (Ru-K-edge) (see Table 3 for fit parameter).

Table 3. EXAFS spectroscopically determined structural data of **X16a**, **X16f**, **X17b**, and **X17f** in solid and suspension state (in toluene)^{a)}

		X16a			X16f		
		N	r [\AA]	σ [\AA]	N	r [\AA]	σ [\AA]
Ru–N	solid	2	2.19 ± 0.02	0.050 ± 0.008	2	2.08 ± 0.02	0.100 ± 0.015
Ru–N	suspension	2	2.15 ± 0.02	0.050 ± 0.008	2	2.08 ± 0.02	0.102 ± 0.015
Ru–P	solid	2	2.26 ± 0.02	0.050 ± 0.008	2	2.26 ± 0.02	0.122 ± 0.018
Ru–P	suspension	2	2.22 ± 0.02	0.059 ± 0.009	2	2.26 ± 0.02	0.071 ± 0.018
Ru–Cl	solid	2	2.38 ± 0.02	0.063 ± 0.016	2	2.39 ± 0.02	0.063 ± 0.016
Ru–Cl	suspension	2	2.36 ± 0.02	0.067 ± 0.017	2	2.38 ± 0.03	0.059 ± 0.015

^{a)}Absorber-backscatterer distance r , coordination number N , Debye-Waller factor σ with calculated standard deviations.

3.3.4 SEM, EDX, and BET Measurements

Figure 10 displays the SEM images of **X14b** and **X15a**. Due to the high amount of the co-condensation agent **D^o-C₆-D^o X1b** has a rather smooth surface structure. In contrast to these findings the employment of the co-condensation agent **Me-T^o** leads to an uneven surface in the case of **X15a**. From BET measurements low surface areas between 2.3 and 5.94 m²/g for **X14b – X16b** are derived.

A typical EDX (*Energy Dispersive X-ray analysis*⁸⁷) spectrum of compound **X15f** is displayed in Figure 11. The K_α lines of carbon, oxygen, silicon, phosphorus, and chlorine and the L line series of ruthenium and tin are visible. An overlap occurs between the L lines of ruthenium and the K lines of chlorine. This phenomenon is corrected by peak deconvolution. Due to its high fluorescence yield, the Au M_α line also appears under the K_β emission of phosphorus. However, the gold coating can be neglected with respect to quantification as owing to its thickness of only 20 nm additional absorption effects are not introduced. Quantification of EDX spectra was carried out using the ZAF correction procedure. This correction model is valid only for flat and homogeneous specimens. As the xerogels exhibit a pronounced morphology (see Figure 10), special care was taken to find a locally flat specimen area larger than the expected electron range which is certainly below 10 μm under the present conditions. However, several analyses of stationary phases generated by sol-gel processing have shown that this problem can be handled successfully.⁸⁸

As X-rays are strongly attenuated by the detector entrance window, EDX is not very sensitive towards the detection and quantification of light elements embedded to a matrix of higher Z material. Uncertainties in fundamental parameters and spectrometer calibration in the soft X-ray regime are an important source of error in the quantification of light elements, for which a relative error of up to 10 % has to be taken into account. In this respect, nitrogen, which is a minor constituent in all samples under investigation, is below the detection threshold and therefore has to be omitted from quantification.

Despite the numerous sources of error EDX is the only method to provide a simultaneous quantification of all present elements, including oxygen in the presence of silicon, which is usually not possible with chemical methods due to the formation of silicon carbide during the combustion process. The elemental analyses of stationary phases **X15a**, **X15b**, **X15c**, **X15f**, **X16a**, **X16e**, and **X16f** by EDX are summarized in Table 4 and compared to data obtained from the stoichiometry of the educts. These have been renormalized excluding nitrogen and hydrogen, which is a single-electron atom and thus does not emit characteristic X-rays. Finally it has to be noted that an average amount of 4 mass-% tin is observed in the materials.

Table 4. Elemental analysis of compounds **X15a – c**, **X15f**, **X16a**, **X16e**, and **X16f** by EDX

Xerogel	Reference data ^{a)}						EDX ^{b)}					
	Composition [%]						Composition [%]					
	C	O	P	Si	Cl	Ru	C	O	P	Si	Cl	Ru
X15a	40.4	22.8	4.0	21.7	4.6	6.5	40.7	21.2	4.8	23.2	3.0	7.1
X15b	40.8	22.6	4.0	21.6	4.5	6.5	39.4	19.0	5.6	24.3	3.5	8.2
X15c	40.8	22.6	4.0	21.6	4.5	6.5	34.8	16.7	6.3	28.7	4.4	9.1
X15f	45.0	21.0	3.7	20.1	4.2	6.0	41.9	11.4	5.3	27.1	4.1	10.2
X16a	34.1	27.1	2.8	28.2	3.2	4.6	44.3	21.5	4.1	23.5	2.0	4.6
X16e	36.9	25.9	2.7	27.0	3.1	4.4	36.0	24.0	3.7	28.8	2.3	5.2
X16f	37.1	25.8	2.7	26.9	3.1	4.4	40.4	18.2	4.4	27.3	3.0	6.7

^{a)}Derived from the stoichiometry of the educts, excluding hydrogen and nitrogen (see text for explanation). ^{b)}Quantified by the ZAF correction procedure.

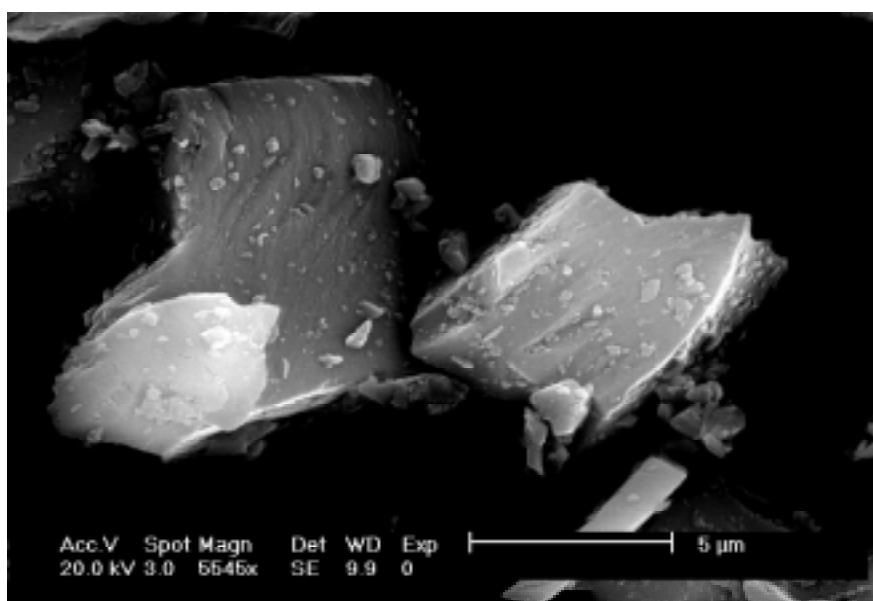
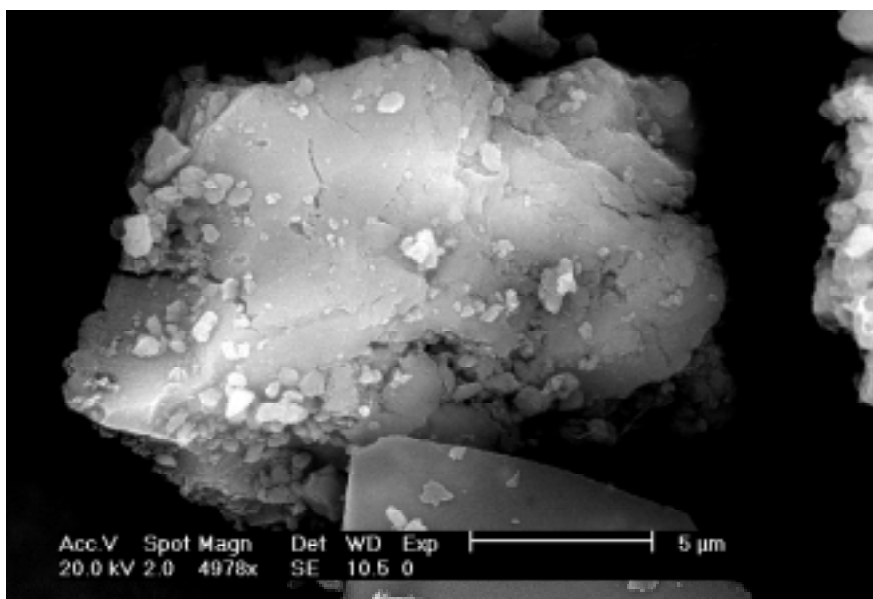


Figure 10. Scanning electron micrographs of **X15a** (top) and **X14b** (bottom).

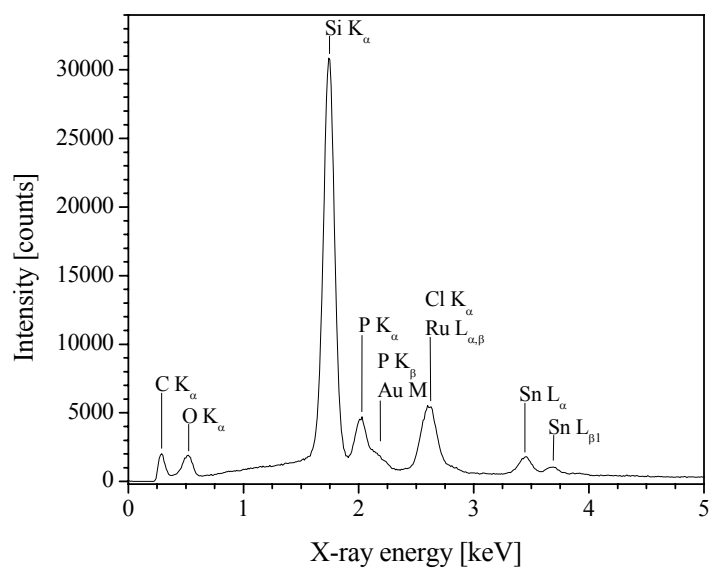


Figure 11. Typical energy-dispersive X-ray spectrum of **X15f** generated by electrons with a primary beam energy of 20 keV. Peaks are assigned to the characteristic X-ray emission lines. For the occurrence of gold and the absence of nitrogen refer to text.

3.4 Conclusion

Based on results which have been obtained in homogeneous phase the heterogenized ruthenium(II) complexes **X14a – c**, **X15a – g**, and **X16a – g**, are supposed to show high activity in the hydrogenation of unsaturated ketones. As a precondition, the reactive centers have to be accessible for the substrates. The accessibility of reactive centers is markedly improved if the polymer has excellent swelling abilities to afford the interphase. Therefore **Me-T°** was mainly used as co-condensation agent which in previous studies showed high mobility and accessibility compared to **D°-C₆-D°** which was used for reasons of comparison. On the other hand the T-silyl functionalized materials have relatively high BET values. Therefore the accessibility should be improved compared to those having D-silyl groups with less rigid pore structures. The EXAFS measurements of the neutral complexes corroborate the proposed structures from the NMR studies.

The ruthenium(II) precursor complexes were provided with T-silyl functions to increase the cross linkage of the polycondensates. Such an anchoring to the polymeric backbone suppresses the leaching problems that could arise, and increase both the surface area and the stability of the polymeric materials. The polymeric complexes which are introduced in this investigation are part of an array of interphase catalysts which have to be tested with particular screening methods to establish which of them are the best catalysts for the hydrogenation of unsaturated ketones.

Experimental Section

1.1 General Comments

All experiments were carried out under an atmosphere of dry argon by use of standard Schlenk techniques. Solvents were dried with appropriate reagents, distilled, degassed, and stored under argon.

$\text{RuCl}_3 \cdot 3 \text{H}_2\text{O}$ was purchased from ChemPur, 1,8-diaminonaphthaline, $\text{ClCH}_2\text{CH}_2\text{OCH}_3$, $n\text{-BuLi}$, p -fluorobenzylamine, $\text{MeSi}(\text{OMe})_3$, and AgBF_4 were available from Fluka. 3-(Triethoxysilyl)propyl isocyanate was obtained from Aldrich. 1,2-Diaminoethane, 1,2-diaminopropane, 1,3-diaminopropane, 1,2-phenylenediamine, 2,2'-bipyridine, 1,10-phenanthroline, $(n\text{-Bu})_2\text{Sn}(\text{OAc})_2$ were purchased from Merck, and TIPF_6 was bought from Strem. The precursor $\text{RuCl}_2(\text{PPh}_3)_3$,⁸⁹ the ether-phosphine $\text{Ph}_2\text{P}(\text{CH}_2)_2\text{OMe}$,⁹⁰ the (ether-phosphine)ruthenium (II) complex **2**,⁹¹ and the co-condensation agent $\text{D}^\circ\text{-C}_6\text{-D}^\circ$ ⁷¹ were synthesized according to the literature. Elemental analyses were performed with an Elementar Vario EL analyzer. Mass spectra were acquired on a Finnigan MAT 711A modified by AMD (8 kV, 303K) and reported as mass/charge (m/z). ESI-FTICR-MS measurements were carried out with a passively shielded 4.7 Tesla APEXTMII-ESI/MALDI-FTICR mass spectrometer (Bruker Daltonik GmbH, Bremen, Germany). IR data were obtained on a Bruker IFS 48 FT-IR spectrometer.

High resolution $^{31}\text{P}\{^1\text{H}\}$ and $^{13}\text{C}\{^1\text{H}\}$ NMR spectra were recorded on a Bruker DRX 250 spectrometer at 298 K. Frequencies and standards are as follows: $^{31}\text{P}\{^1\text{H}\}$ NMR 101.25 MHz, and $^{13}\text{C}\{^1\text{H}\}$ NMR 62.90 MHz. ^{13}C chemical shifts were measured relative to deuterated solvent peaks, which are reported relative to TMS. ^{31}P chemical shifts were

measured relative to 85% H₃PO₄ ($\delta = 0$). The assignment of the ¹³C NMR data is based on the 135 DEPT experiment and the comparison with the appropriate starting compound.

CP/MAS solid-state NMR spectra were recorded on Bruker DSX 200 (4.7 T) and Bruker ASX 300 (7.05 T) multinuclear spectrometers equipped with wide-bore magnets. Magic angle spinning was applied at 4 kHz (²⁹Si) and 10 kHz (¹³C, ³¹P) using (4 mm ZrO₂ rotors). Frequencies and standards: ³¹P, 81.961 MHz (4.7 T), 121.442 MHz (7.05 T) [85% H₃PO₄, NH₄H₂PO₄ ($\delta = 0.8$) as second standard]; ¹³C, 50.228 MHz (4.7 T), 75.432 MHz (7.05 T) [TMS, carbonyl resonance of glycine ($\delta = 176.05$) as second standard]; ²⁹Si, 39.73 MHz (4.7 T), 59.595 MHz (7.05 T, (Q8M8 as second standard).

The EXAFS measurements were performed at the ruthenium K-edge (22118 eV) at the beam line X1.1 of the Hamburger Synchrotronstrahlungslabor (HASYLAB) at DESY Hamburg, under ambient conditions, energy 4.5 GeV, and initial beam current 120 mA. For harmonic rejection, the second crystal of the Si(311) double crystal monochromator was tilted to 30 %. Data were collected in transmission mode with the ion chambers flushed with argon. The energy was calibrated with a ruthenium metal foil of 20 μ m thickness. The samples were prepared of a mixture of the samples and polyethylene.

Data were analyzed with a program package, specially developed for the requirements of amorphous samples.⁹² The program AUTOBK of the University of Washington⁹² was used for the removal of the background, and the program EXCURV92⁹³ for the evaluation of the XAFS function. The resulting EXAFS function was weighted with k Data⁹⁴ analysis in k space was performed according to the curved-wave multiple-scattering formalism of the program EXCURV92. The mean free path of the scattered electrons was calculated from the imaginary part of the potential (VPI was set to -4.00), the amplitude reduction factor AFAC was fixed at 0.8, and an overall energy shift ΔE_0 was introduced to best fit the data. In the fitting procedure the coordination numbers were at first fixed to the known values for the

ligands around the ruthenium atom in all investigated complexes, and after a first iteration of the bond distances and “Debye Waller“ factors varied.

Scanning electron microscopy was performed on a XL 30 scanning electron microscope by *Philips* equipped with an DX-4 energy dispersive X-ray detection system by *EDAX*. This consists of a liquid nitrogen cooled lithium-drifted silicon detector with an active area of 10 mm² and the eDXi 2.11 software package. The detector resolution is 149 eV at MnK_α (5.984 keV) and the sample-detector distance is 50 mm at a take-off angle of 35° in the present system. The sample powder was placed on a commercial specimen stub covered with an adhesive tab and subsequently provided with a sputtered 20 nm gold layer to ensure conductivity. The primary beam energy was 20 keV during all investigations. A probe current of 192 pA was applied for recording electron micrographs, whereas X-ray emission spectra were acquired under spot illumination applying a probe current of 569 pA for 400 live seconds. Under these conditions, count rates of 2000-3000 counts per second at dead times of approximately 33% are achieved with the present compounds. Measurements were repeated several times at various specimen positions to ensure reproducibility. Quantification of X-ray spectra was carried out employing the ZAF correction procedure after subtraction of the Bremsstrahlung background.⁹⁵⁻⁹⁷ The surface area were determined by analyzing the N₂ adsorption isotherm according to the BET method using Micromeritics Gemini.

1.2 Preparation of the Complexes **3a – g**, **4a – g**, **5a – g**

1.2.1 General Procedure for the Preparation of the Neutral Complexes **3a – g**

The corresponding dinitrogen ligand **3a – g** (10% excess) was dissolved in 25 ml of dichloromethane and added dropwise to a stirred solution of **2** in 25 ml of dichloromethane. After the reaction mixture had been stirred for another 45 min at room temperature, the

volume of the solution was concentrated to about 5 ml under reduced pressure. Addition of 80 ml of *n*-hexane caused the precipitation of a solid, which was filtered off (P3), washed three times with 25 ml portions of *n*-hexane, and dried under vacuum.

Complex 3d. Complex **2** (300 mg, 0.454 mmol) was treated with **d** (54 mg, 0.50 mmol) to give **3d**: yield 206 mg (59%) of a pale yellow powder. FD-MS: m/z 768.7 (M^+), 660.5 ($M^+ - C_6H_4(NH_2)_2$). *Anal.* Calcd for $C_{36}H_{42}Cl_2N_2O_2P_2Ru$: C, 56.25; H, 5.51; N, 3.64; Cl, 9.22. Found: C, 55.64; H, 5.97; N, 3.82; Cl, 8.94. 1H NMR ($CDCl_3$): δ = 2.2-2.4 (m, 4H, PCH_2), 2.9 (m, 6H, OCH_3), 2.9-3.0 (m, 4H, CH_2O), 4.5 (s, 4H, NH_2), 6.8-7.0 (m, 4H, C_6H_4), 7.1-7.7 (m, 20H, C_6H_5). $^{31}P\{^1H\}$ NMR ($CDCl_3$): δ = 40.7 (s). $^{13}C\{^1H\}$ NMR ($CDCl_3$): δ = 25.2 (m, PCH_2), 58.0 (s, OCH_3), 69.1 (m, CH_2O), 127.3 (s, C3, C6), 127.8 (s, C4, C5), 128.4 (m, *m*- C_6H_5), 129.4 (s, *p*- C_6H_5), 132.8 (m, *o*- C_6H_5), 134.2 (m, *i*- C_6H_5), 140.1 (s, C1, C2). $^{31}P\{^1H\}$ NMR ($CDCl_3$) for the C_1 isomer: δ = 37.6 (d, $^2J_{PP}$ = 34.9 Hz), 47.5 (d, $^2J_{PP}$ = 34.9 Hz).

1.2.2 General Procedure for the Preparation of the Monocationic Complexes **4a – g**

Use of $TiPF_6$. $TiPF_6$ (5% excess) was added to a solution of the neutral complexes **3a – g** in 25 ml of dichloromethane and stirred for 24 h. After filtration through silica the solution was concentrated to about 5 ml under reduced pressure. The corresponding cationic complex was precipitated by addition of 100 ml of diethyl ether, filtered off (P3), washed three times with 25 ml portions of diethylether, and dried under vacuum.

Use of $AgBF_4$. A solution of $AgBF_4$ (5% excess) in 25 ml of dichloromethane was added to a solution of the neutral complexes **3a – g** in 25 ml of dichloromethane and stirred for 4 h. After filtration through silica the solution was concentrated to a small volume. Adding 100 ml of

diethyl ether caused the precipitation of a solid, which was filtered off (P3), washed three times with 25 ml portions of diethyl ether, and dried under vacuum.

Complex 4d. Compound **3d** (300 mg, 0.390 mmol) was treated with AgBF_4 (79 mg, 0.410 mmol) to give **4d**: yield 337 mg (92%) of a dark brown powder which was contaminated with traces of **5d**. FAB-MS: m/z 731.1 ($\text{M}^+ - \text{BF}_4$). *Anal.* Calcd for $\text{C}_{36}\text{H}_{42}\text{BClF}_4\text{N}_2\text{O}_2\text{P}_2\text{Ru}$: C, 52.73; H, 5.16; N, 3.42 %. Due to the presence of **5d**, complex **4d** does not analyze well. ^1H NMR (CD_2Cl_2): $\delta = 2.1 - 4.6$ (m, 12H, CH_2P , CH_2O , NH_2), 3.1 (s, 3H, OCH_3), 3.9 (s, 3H, OCH_3), 6.4-7.8 (m, 24H, C_6H_5 , $\text{C}_6\text{H}_4(\text{NH}_2)_2$). $^{31}\text{P}\{^1\text{H}\}$ NMR (CD_2Cl_2): $\delta = 42.7$ (d, $^2J_{\text{PP}} = 32.6$ Hz, $\eta^2\text{-P}^{\wedge}\text{O}$), 56.1 (d, $^2J_{\text{PP}} = 32.6$ Hz, $\eta^1\text{-P}\sim\text{O}$). $^{13}\text{C}\{^1\text{H}\}$ NMR (CD_2Cl_2): $\delta = 24.5$ (d, $^1J_{\text{PC}} = 30.3$ Hz, PCH_2), 29.7 (d, $^1J_{\text{PC}} = 24.3$ Hz, PCH_2), 53.6, 62.5 (2s, OCH_3), 63.8, 74.0 (2s, CH_2O), 120.3-135.3 (C_6H_5 , $\text{C}_6\text{H}_4(\text{NH}_2)_2$).

1.2.3 General Procedure for the Preparation of the Dicationic Complexes 5a – c, e – g

A solution of the neutral complex **3a – c, e – g** in 25 ml of dichloromethane was added to AgBF_4 , AgSbF_6 , or TIPF_6 (300% excess) and stirred for 4 h. After filtration through silica the solvent was reduced to 5 ml under reduced pressure. The corresponding dicationic complex was precipitated by addition of 100 ml of diethyl ether, filtered off (P3), and washed three times with 25 ml portions of diethylether.

Complex 5d. Complex **5d** could not be isolated. It was observed as traces in the $^{31}\text{P}\{^1\text{H}\}$ NMR spectrum of **4d**. $^{31}\text{P}\{^1\text{H}\}$ NMR (CD_2Cl_2): $\delta = 69.0$ (d, $^2J_{\text{PP}} = 35.8$ Hz, $\eta^2\text{-P}^{\wedge}\text{O}$), 54.3 (d, $^2J_{\text{PP}} = 35.8$ Hz, $\eta^2\text{-P}^{\wedge}\text{O}$).

Note: for the detailed data of the rest of the homogeneous complexes see reference 42

1.3 Preparation of the T-Silyl Functionalized Complexes 10(T°), 11a(T°) – g, 12a(T°) – g, and 13a(T°)

1.3.1 Preparation of the T-Silyl Functionalized Ether-Phosphine Ligand 9(T°)

1.3.1.1 Preparation of Compound 6

Phenylphosphinic acid (180.0 g, 1.32 mol) was heated in a simple distillation apparatus equipped with an air cooling condenser. By controlling the internal temperature, the acid melts at about 82 °C and by gradual heating it started to decompose at 220 °C. The temperature should not exceed 260 °C. The crude product was dried with Na₂SO₄ to eliminate water which was formed together with benzene as a by-product. The phosphine **6** is distilled to yield 50 g (38 %) of a colorless air sensitive oil. B.p. 433 K. ³¹P{¹H} NMR (CDCl₃): δ = -120.0 (s). ¹H NMR (CDCl₃): δ = 4.22 (d, ¹J_{PH} = 201 Hz, PH₂), 7.40 – 7.75 (5H, C₆H₅).

1.3.1.2 Preparation of Compound 7

A solution of *n*-BuLi in *n*-hexane (60.28 ml of a 1.6 M solution) was added dropwise to a solution of phenylphosphine (10.0 g, 90.8 mmol) in THF (100 ml). The yellow solution consisting of C₆H₅PHLi was stirred 30 min at ambient temperature. Then a solution of ClCH₂CH₂OCH₃ (8.7 g, 91.85 mmol) in THF (50 ml) was added dropwise within 10 min. Subsequently the solution was stirred for another 30 min under reflux to complete the reaction and then it was cooled to 20 °C. To the colorless mixture a degassed aqueous solution saturated with NH₄Cl (250 ml) was added and the organic layer was separated. The solution was dried with Na₂SO₄ and separated from the solid residue. After evaporation of the volatile materials under vacuum the crude product was distilled to yield 10.82 g (70 %) of **7** as a colorless air sensitive oil. B.p. 333 K (5 mbar). ³¹P{¹H} NMR (CDCl₃): δ = - 61.6 (s). ¹H

NMR (CDCl₃): δ = 1.89 (m, 2H, PCH₂), 3.09 (s, 3H, OCH₃), 3.27 (m, 2H, PCH₂CH₂), 4.03 (d, $^1J_{\text{PH}} = 205$ Hz, PH), 7.04 – 7.38 (5H, C₆H₅). $^{13}\text{C}\{^1\text{H}\}$ NMR (CDCl₃): δ = 23.1 (d, $^1J_{\text{PC}} = 14.2$ Hz, PCH₂), 57.7 (s, OCH₃), 70.5 (d, $^2J_{\text{PC}} = 7.1$ Hz, PCH₂CH₂).

1.3.1.3 Preparation of Compound 8

Small pieces of metallic potassium (1.16 g, 29.8 mmol) were added to a solution of PhP(H)CH₂CH₂OCH₃ (**7**) (5 g, 29.8 mmol) in 1,1'-dimethoxyethane (DME) (50 ml). The reaction started immediately evolving molecular hydrogen and the corresponding potassium phosphide was formed. After the potassium had been consumed the red solution of C₆H₅PK(CH₂CH₂OCH₃) was added dropwise within 3 h to a solution of *p*-fluorobenzylamine (3.9 g, 31.24 mmol) in DME (150 ml). The color of the solution changed gradually to deep green. The reaction mixture was stirred for 6 h at ambient temperature, then another 6 h at 50 °C followed by reflux for 24 h. The solvent was evaporated under reduced pressure and the yellowish residue was washed with water (100 ml). The crude product was dried and isolated by distillation under vacuum to produce 5.3 g (65 %) of **2**. B.p. 471 K (10⁻³ mbar). MS (EI): m/z 273.2 [M⁺]. $^{31}\text{P}\{^1\text{H}\}$ NMR (CDCl₃): δ = -22.2 (s). ^1H NMR (CDCl₃): δ = 1.27 (s, 2H9), 2.26 (t, $^2J_{\text{HH}} = 7.5$ Hz, 2H3), 3.17 (s, 3H1), 3.42 (m, 2H2), 3.71 (s, 2H8), 7.10 – 7.23 (m, H5 and H6), 7.25 – 7.65 (m, H11, H12, and H13). $^{13}\text{C}\{^1\text{H}\}$ NMR (CDCl₃): δ = 29.2 (d, $^1J_{\text{PC}} = 12.8$ Hz, C3), 46.6 (s, C8), 58.9 (s, C1), 70.2 (d, $^2J_{\text{PC}} = 23.6$ Hz, C2), 127.6 (d, $^4J_{\text{PC}} = 7.4$ Hz, C6), 128.8 (m, C12 and C13), 136.6 (d, $^1J_{\text{PC}} = 12.3$ Hz, C4), 138.9 (d, $^1J_{\text{PC}} = 12.8$ Hz, C10), 132.7 (C5 and C11), 146.9 (s, C7). IR (KBr, cm⁻¹): $\nu(\text{NH}_2)$ 3378, $\nu_{\text{as}}(\text{C}_2\text{O})$ 1109.

1.3.1.4 Preparation of the Ligand 9(T⁰)

To a solution of compound **8** (5.0 g, 18.29 mmol) in dichloromethane (250 ml) a solution of 3-(triethoxysilyl)propyl isocyanate (4.5 g, 18.29 mmol) in CH₂Cl₂ (20 ml) was added dropwise. The reaction mixture was stirred at room temperature for 24 h. The solvent

was evaporated to dryness to give 9.5 g (100 %) of **8**. M.p. 117 °C. MS (EI): m/z 520 [M^+]. *Anal.* Calc. for $C_{26}H_{41}N_2O_5PSi$ (520.67): C, 59.98; H, 7.94; N, 5.38. Found: C, 59.76; H, 7.65; N, 5.36%. $^{31}P\{^1H\}$ NMR ($CDCl_3$): $\delta = -22.1$ (s). 1H NMR ($CDCl_3$): $\delta = 0.64$ (m, 2H14), 1.22 (t, $^3J_{HH} = 7.0$ Hz, 9H16), 1.61 (m, 2H13), 2.37 (t, $^3J_{HH} = 7.6$ Hz, 2H3), 3.17 (m, 2H12), 3.21 (s, 3H1), 3.50 (q, $^3J_{HH} = 7.6$ Hz, 2H2), 3.86 (q, $^3J_{HH} = 7.0$ Hz, 6H15), 4.34 (d, $^3J_{HH} = 5.9$ Hz, 2H8), 4.94 (t, $^3J_{HH} = 6.1$ Hz, 1H11), 5.14 (t, $^3J_{HH} = 5.9$ Hz, 1H9), 7.20 – 7.50 (m, C_6H_4 , C_6H_5). $^{13}C\{^1H\}$ NMR ($CDCl_3$): $\delta = 7.7$ (s, C14), 18.4 (s, C16), 23.8 (s, C13), 28.9 (d, $^1J_{PC} = 12.8$ Hz, C3), 43.0 (s, C12), 44.1 (s, C8), 53.8 (s, C15), 58.8 (s, C1), 69.9 (d, $^2J_{PC} = 23.6$ Hz, C2), 127.6 (d, $^3J_{PC} = 6.7$ Hz, C6), 128.7 (d, $^3J_{PC} = 6.7$ Hz, C19), 128.8 (s, C20), 132.7 (d, $^2J_{PC} = 16.8$ Hz, C5), 133.0 (d, $^2J_{PC} = 17.5$ Hz, C18), 137.0 (d, $^1J_{PC} = 12.1$ Hz, C4), 138.4 (d, $^1J_{PC} = 12.1$ Hz, C17), 140.5 (s, C7), 158.5 (s, C10). IR (KBr, cm^{-1}): $\nu(NH)$ 3329, $\nu(C=O)$ 1597, $\nu_{as}(C_2O)$ 1111, $\nu(SiO)$ 1077.

1.3.2 Preparation of the Complex **10(T⁰)**

A solution of **9(T⁰)** (3.3 g, 6.29 mmol) in dichloromethane (15 ml) was added to a solution of $RuCl_2(PPh_3)_3$ (3.0 g, 3.15 mmol) in the same solvent (15 ml). The reaction mixture was stirred for 3 h, then the product was precipitated from the solvent by adding dropwise diethyl ether (100 ml). This procedure was repeated two times and the solvent was removed by decanting. The pink-colored precipitate was collected by filtration (P3) and washed three times with diethyl ether (50 ml). Then the product was dried under vacuum to yield 3.6 g (95 %) of **10(T⁰)**. MS (FAB, NBA, 50 °C): m/z 1213 [M^+]. *Anal.* Calc. for $C_{26}H_{41}N_2O_5PSi$ (1213.32): C, 51.48; H, 6.81; N, 4.62. Found: C, 51.49; H, 6.74; N, 4.48%. $^{31}P\{^1H\}$ NMR ($CDCl_3$): $\delta = -68.6$ (s). 1H NMR ($CDCl_3$): $\delta = 0.56$ (m, 4H14), 1.3 (t, $^3J_{HH} = 6.9$ Hz, 18H16), 1.53 (m, 4H13), 2.82 (m, 4H3), 3.09 (m, 4H12), 3.65 – 3.85 (m, 6H1 + 12H15), 3.9 – 4.44 (m, 4H2 + 4H8), 5.51 (m, 2H11), 5.61 (t, $^3J_{HH} = 5.8$ Hz, 2H9), 6.78 – 7.30

(m, C₆H₄, C₆H₅). ¹³C{¹H} NMR (CDCl₃): δ = 7.8 (s, C14), 18.5 (s, C16), 23.9 (s, C13), 31.4 (m, C3), 43.1 (s, C12), 43.5 (s, C8), 58.6 (s, C15), 62.4 (s, C1), 72.6 (s, C2), 133.0 (m, C18), 142.1 (s, C7), 159.2 (s, C10), 125 – 160 (C₆H₅, C₆H₄). IR (KBr, cm⁻¹): ν (NH) 3352, ν (C=O) 1558.

1.3.3 General Procedure for the Preparation of the Neutral Complexes 11a(T⁰) – g(T⁰)

To a stirred solution of **8** in 25 ml of dichloromethane was added dropwise the corresponding diamine **a** – **g** (5% excess) dissolved in 25 ml of dichloromethane. The solution was stirred for 45 min at room temperature and concentrated to about 5 ml under reduced pressure. Addition of 80 ml of diethyl ether caused a precipitation of a solid which was filtered off (P3), washed three times with 25 ml of diethyl ether and dried under vacuum.

1.3.3.1 Preparation of 11a(T⁰)

10(T⁰) (300 mg, 0.247 mmol) was reacted with the diamine **a** (17.4 μl, 0.289 mmol) to give 290 mg (92%) of **11a(T⁰)** as a yellow powder. FT-ICR-MS: *m/z* 1237.5 [M⁺ – Cl]. *Anal.* Calc. for C₅₄H₉₀C₁₂N₆O₁₀P₂RuSi₂ (1273.42): C, 50.93; H, 7.12; N, 6.60. Found: C, 50.91; H, 7.12; N, 6.50%. ³¹P{¹H} NMR (CDCl₃): δ = 38.7 (s). ¹H NMR (CDCl₃): δ = 0.58 (m, 4H14), 1.3 (t, ³J_{HH} = 6.9 Hz, 18H16), 1.56 (m, 4H13), 2.3 (m, 4H3), 2.6 – 2.9 (br, 8H, CH₂NH₂), 3.00 (s, 6H1), 3.0 – 3.2 (m, 4H12 + 4H2), 3.73 (q, ³J_{HH} = 6.9 Hz, 12H15), 4.1 – 4.4 (br, 4H8), 5.5 (br, 2H11), 5.83 (br, 2H9), 6.9 – 7.6 (m, 18H, C₆H₄, C₆H₅). ¹³C{¹H} NMR (CDCl₃): δ = 7.8 (s, C14), 18.4 (s, C16), 23.9 (s, C13), 25.9 (m, C3), 43.0 (s, C12), 43.5 and 43.5 (2s, C8 and CH₂NH₂), 58.5 (s, C15), 58.2 (s, C1), 69.2 (s, C2), 133.0 (m, C18), 141.1 (s, C7), 159.0 (s, C10), 125 – 160 (C₆H₅, C₆H₄). IR (KBr, cm⁻¹): ν (NH) 3339, ν (C=O) 1558.

1.3.3.2 Preparation of **11b**(T⁰)

10(T⁰) (300 mg, 0.247 mmol) was reacted with the diamine **b** (21.7 μ l, 0.292 mmol) to give 172 mg (54%) of **11b**(T⁰) as a yellow powder. FT-ICR-MS: m/z 1251.5 [$M^+ - Cl$]. *Anal.* Calc. for C₅₄H₉₀C₁₂N₆O₁₀P₂RuSi₂ (1287.45): C, 51.31; H, 7.20; N, 6.53. Found: C, 51.08; H, 6.91; N, 6.13%. ³¹P{¹H} NMR (CD₂Cl₂): δ = 40.0 (s). ¹H NMR (CDCl₃): δ = 0.58 (m, 4H14), (t, ³J_{HH} = 7.0 Hz, 18H16), 1.56 (m, 4H13), 2.4 (m, 4H3), 2.75 – 2.97 (br m, 10H, CH₂CH₂CH₂(NH₂)₂), 3.05 (s, 6H1), 3.06 – 3.32 (m, 4H12 + 4H2), 3.8 (q, ³J_{HH} = 7.0 Hz, 12H15), 4.1 – 4.6 (br, 4H8), 5.3 (br, 2H9), 5.9 (br, 2H11), 6.9 – 7.6 (m, 18H, C₆H₄, C₆H₅). ¹³C{¹H} NMR (CDCl₃): δ = 8.1 (s, C14), 18.7 (s, C16), 24.4 (s, C13), 26.5 (m, C3), 29.9 (s, NH₂CH₂CH₂), 39.7 (s, NH₂CH₂CH₂), 43.4 (s, C12), 43.6 (s, C8), 58.2 (s, C1), 58.5 (s, C15), 69.6 (s, C2), 133.0 (m, C18), 141.7 (s, C7), 159.6 (s, C10), 125 – 160 (C₆H₅, C₆H₄). IR (KBr, cm⁻¹): ν (NH) 3320, ν (C=O) 1569.

1.3.3.3 Preparation of **11c**(T⁰)

10(T⁰) (300 mg, 0.247 mmol) was reacted with the diamine **c** (22.2 μ l, 0.292 mmol) to give 127 mg (40%) of **11c**(T⁰) as a yellow powder. FT-ICR-MS: m/z 1251.5 [$M^+ - Cl$]. *Anal.* Calc. for C₅₄H₉₀C₁₂N₆O₁₀P₂RuSi₂ (1287.45): C, 51.31; H, 7.20; N, 6.53. Found: C, 51.06; H, 7.06; N, 6.77%. ³¹P{¹H} NMR (CD₂Cl₂): δ = 39.8 (s). ¹H NMR (CDCl₃): δ = 0.60 (m, 4H14), 1.0 (m, 3H, CHCH₃), 1.17 (t, ³J_{HH} = 6.9 Hz, 18H16), 1.58 (m, 4H13), 2.8 (s, 1H, CHCH₃), 3.05 (s, 6H1), 2.2 – 3.0 (br, CH₂NH₂ (4H) + 4H3), 3.0 – 3.3 (m, 4H12 + 4H2), 3.8 (q, ³J_{HH} = 6.9 Hz, 12H15), 4.3 (br, 4H8), 6.0 (br, 2H9), 6.4 (br, 2H11), 6.9 – 7.6 (m, 18H, C₆H₄, C₆H₅). ¹³C{¹H} NMR (CDCl₃): δ = 7.8 (s, C14), 18.3 (s, C16), 20.1 (s, NH₂CHCH₃), 24.0 (s, C13), 26.2 (m, C3), 43.0 (s, C12), 43.2 (s, C8), 49.5 (s, NH₂CH₂), 49.5 (s, NH₂CH), 58.0 (s, C1),

58.4 (s, C15), 69.2 (s, C2), 133.0 (m, C18), 141.4 (s, C7), 159.4 (s, C10), 125 – 160 (C₆H₅, C₆H₄). IR (KBr, cm⁻¹): $\nu(\text{NH})$ 3339, $\nu(\text{C}=\text{O})$ 1556.

1.3.3.4 Preparation of **11d(T⁰)**

10(T⁰) (300 mg, 0.247 mmol) was reacted with the diamine **d** (28.1 mg, 0.260 mmol) to give 314 mg (96%) of **11d(T⁰)** as a brown powder. FT-ICR-MS: m/z 1286.5 [$\text{M}^+ - \text{Cl}$]. *Anal.* Calc. for C₅₄H₉₀C₁₂N₆O₁₀P₂RuSi₂ (1321.46): C, 52.72; H, 6.86; N, 6.36. Found: C, 52.88; H, 6.77; N, 6.63%. ³¹P{¹H} NMR (CD₂Cl₂): δ = 40.9 (s). ¹H NMR (CDCl₃): δ = 0.64 (m, 4H14), 1.20 (t, ³J_{HH} = 7.0 Hz, 18H16), 1.61 (m, 4H13), 2.47 (m, 4H3), 3.11 (s, 6H1), 3.16 (m, 4H12), 3.31 (m, 4H2), 3.80 (q, ³J_{HH} = 7.0 Hz, 12H15), 4.3 (br, 4H8), 4.5 (br, 4H, C₆H₄(NH₂)₂), 6.0 (br, 2H11) 6.4 (br, 2H9), 6.87 – 7.0 (m, 4H, C₆H₄), 7.0 – 7.6 (m, 18H, C₆H₄, C₆H₅), ¹³C{¹H} NMR (CDCl₃): δ = 8.0 (s, C14), 18.6 (s, C16), 24.3 (s, C13), 26.6 (m, C3), 43.3 (s, C12), 43.5 (s, C8), 58.4 (s, C1), 58.7 (s, C15), 69.5 (s, C2), 116.5 (s, C2–amine), 120.0 (s, C3–amine) 131.9 (m, C2–amine), 133.8 (m, C18), 141.0 (s, C7), 159.6 (s, C10), 125 – 160 (C₆H₅, C₆H₄, and C–amine). IR (KBr, cm⁻¹): $\nu(\text{NH})$ 3308, $\nu(\text{C}=\text{O})$ 1556.

1.3.3.5 Preparation of **11e(T⁰)**

10(T⁰) (300 mg, 0.247 mmol) was reacted with the diamine **e** (41.1 mg, 0.260 mmol) to give 309 mg (91%) of **11e(T⁰)** as a brown powder. FT-ICR-MS: m/z 1335.5 [$\text{M}^+ - \text{Cl}$]. *Anal.* Calc. for C₅₄H₉₀C₁₂N₆O₁₀P₂RuSi₂ (1371.52): C, 54.30; H, 6.76; N, 6.13. Found: C, 54.03; H, 6.35; N, 6.08%. ³¹P{¹H} NMR (CD₂Cl₂): δ = 44.0 (s). ¹H NMR (CD₂Cl₂): δ = 0.51 (m, 4H14), 1.08 (t, ³J_{HH} = 7.0 Hz, 18H16), 1.49 (m, 4H13), 2.25 (m, 4H3), 2.84 (s, 6H1), 2.9 – 3.34 (m, 4H12 + 4H2), 3.69 (q, ³J_{HH} = 7.0 Hz, 2H15), 4.0 – 5.5 (br, 4H8, NH₂ (4H)), 6.0 (br, 2H11), 6.4 (br, 2H9), 6.2 – 7.0 (m, 6H–amine), 7.0 – 7.6 (m, 18H, C₆H₄, C₆H₅). ¹³C{¹H} NMR (CDCl₃): δ = 8.2 (s, C14), 18.7 (s, C16), 24.4 (s, C13), 26.0 (m, C3), 43.3 (br, C12 +

C8), 58.3 (s, C1), 58.7 (s, C15), 69.6 (s, C2), 111.6 (s, C2–amine), 119.5 (s, C4–amine) 121.4 (s, C3–amine), 136.9 (s, C1–amine), 133.8 (m, C18), 141.0 (s, C7), 159.8 (s, C10), 125 – 160 (C₆H₅, C₆H₄, and C–amine). IR (KBr, cm⁻¹): ν(NH) 3307, ν(C=O) 1561.

1.3.3.6 Preparation of **11f**(T⁰)

10(T⁰) (300 mg, 0.247 mmol) was reacted with the diamine **f** (40.5 mg, 0.259 mmol) to give 193 mg (57%) of **11f**(T⁰) as a brown powder. FT-ICR-MS: *m/z* 1334.5 [M⁺ – Cl]. *Anal.* Calc. for C₅₄H₉₀C₁₂N₆O₁₀P₂RuSi₂ (1369.51): C, 54.37; H, 6.62; N, 6.14. Found: C, 53.98; H, 6.35; N, 5.98%. ³¹P{¹H} NMR (CD₂Cl₂): δ = 27.3 (s). ¹H NMR (CD₂Cl₂): δ = 0.48 (m, 4H14), 1.07 (t, ³J_{HH} = 7.0 Hz, 18H16), 1.44 (m, 4H13), 2.67 (m, 4H3), 2.95 (s, 6H1), 2.9 – 3.3 (m, 4H12 + 4H2), 3.68 (q, ³J_{HH} = 7.0 Hz, 12H15), 4.0 – 4.4 (br, 4H8), 5.7 (br, 2H11) 6.0 (br, 2H9), 7.0 – 7.8 (m, 18H, C₆H₄, C₆H₅), 7.8 – 8.7 (m, 6H, (2H1 + 2H3 + 2H4, amine)), ¹³C{¹H} NMR (CD₂Cl₂): δ = 8.0 (s, C14), 18.6 (s, C16), 24.3 (s, C13), 26.4 (m, C3), 43.3, 43.4 (2s, C12 + C8), 58.3 (s, C1), 58.7 (s, C15), 69.6 (s, C2), 121.2 (s, C2–amine), 122.5 (s, C4–amine), 137.3 (s, C4–amine), 149.5 (s, C1–amine), 158.8 (s, C5–amine), 136.9 (s, C1–amine), 133.8 (m, C18), 141.0 (s, C7), 159.4 (s, C10), 125 – 160 (C₆H₅, C₆H₄, and C–amine). IR (KBr, cm⁻¹): ν(NH) 3345, ν(C=O) 1560.

1.3.3.7 Preparation of **11g**(T⁰)

10(T⁰) (300 mg, 0.247 mmol) was reacted with the diamine **g** (46.7 mg, 0.259 mmol) to give 285 mg (83%) of **11g**(T⁰) as a red powder. FT-ICR-MS: *m/z* 1357.5 [M⁺ – Cl]. *Anal.* Calc. for C₅₄H₉₀C₁₂N₆O₁₀P₂RuSi₂ (1393.52): C, 55.16; H, 6.51; N, 6.03. Found: C, 54.82; H, 6.39; N, 6.01%. ³¹P{¹H} NMR (CD₂Cl₂): δ = 27.3 (s). ¹H NMR (CD₂Cl₂): δ = 0.47 (m, 4H14), 1.2 (t, ³J_{HH} = 6.9 Hz, 18H16) 1.4 (m, 4H13), 2.5 – 3.8 (m, 4H3 + 6H1 + 4H12 + 4H2), 2.97 (s, 6H1), 3.8 (q, ³J_{HH} = 6.9 Hz, 12H15), 3.8 – 4.4 (br, 4H8), 5.8 (br, 2H11), 6.2 (br, 2H9), 6.7 – 8.4 (m, 24H, C₆H₄, C₆H₅ + (2H2 + 2H3 + 2H4, amine)), 8.9 (m, (2H1, amine)), ¹³C{¹H}

NMR (CD₂Cl₂): δ = 8.1 (s, C14), 18.7 (s, C16), 24.4 (s, C13), 26.6 (m, C3), 43.3 (br, C12 + C8), 58.4 (s, C1), 58.7 (s, C15), 69.6 (s, C2), 123.4 (s, C2–amine), 126.5 (s, C4–amine), 134.7 (s, C3–amine), 149.5 (s, C1–amine), 158.8 (s, C6–amine), 133.8 (m, C18), 141.0 (s, C7), 159.4 (s, C10), 125 – 160 (C₆H₅, C₆H₄, and C–amine). IR (KBr, cm⁻¹): ν (NH) 3350, ν (C=O) 1555.

1.3.4 General Procedure for the Preparation of the Cationic Complexes **12a(T^o)** – **g(T^o)**

AgBF₄ or TIPF₆ (5% excess) was added to a solution of the neutral complexes in 25 ml of dichloromethane and stirred for 4 h. After filtration through silica gel the solution was concentrated to about 5 ml under reduced pressure. The cationic complex was precipitated by addition of 100 ml of diethyl ether, filtered off (P3) and washed three times with 25 ml of diethyl ether and dried under vacuum.

1.3.4.1 Preparation of **12a(T^o)**

11a(T^o) (300 mg, 0.247 mmol) was reacted with AgBF₄ (48 mg, 0.247 mmol) to give 237 mg (76%) of **12a(T^o)** as a yellow powder. FT-ICR-MS: m/z 1237.5 [M^+ – BF₄]. *Anal.* Calc. for C₅₄H₉₀BClF₄N₆O₁₀P₂RuSi₂ (1324.77): C, 48.96; H, 6.85; N, 6.34. Found: C, 48.52; H, 6.48; N, 6.25%. ³¹P{¹H} NMR (CDCl₃): δ = diastereomers a and b: (90%) 56.5 (d, ²J_{PP} = 37 Hz, η^2 -P[^]O), 56.6 (d, ²J_{PP} = 36 Hz, η^2 -P[^]O), 47.2 (d, ²J_{PP} = 36 Hz, η^1 -P~O), 47.0 (d, ²J_{PP} = 37 Hz, η^1 -P~O), diastereomer c: (10%) 57.4 (d, ²J_{PP} = 39 Hz, η^2 -P[^]O), 50.7 (d, ²J_{PP} = 39 Hz, η^1 -P~O). ¹H NMR (CDCl₃): δ = 0.54 (m, 4H14), 1.1 (m, 18H16), 1.52 (m, 4H13), 2.3 – 3.2 (br m, 4H12 + 4H2 + CH₂NH₂ (8H)), 3.08 (s, 3H1), 3.5 (s, 3H1), 3.7 (m, 12H15), 3.9 – 4.5 (br, 4H8), 6.1 – 6.4 (br, 2H11 + 2H9), 6.9 – 7.6 (m, 18H, C₆H₄, C₆H₅). ¹³C{¹H} NMR (CD₂Cl₂): δ = 7.8 (s, C14), 18.4 (s, C16), 23.9 (s, C13), 31.1 (m, C3), 43.0, 43.5, and 43.46 (m, C12, C8, and CH₂NH₂), 58.6 (s, C15), 58.2 (s, C1), 68.5 (s, C2), 69.3 (s, C2), 133.0 (m,

C18), 141.0 (s, C7), 158.0 (s, C10), 125 – 160 (C₆H₅, C₆H₄). IR (KBr, cm⁻¹): ν (NH) 3340, ν (C=O) 1558. For this and the following complexes the ¹H and ¹³C NMR data for only one diastereoisomer is given.

1.3.4.2 Preparation of 12b(T⁰)

11b(T⁰) (300 mg, 0.233 mmol) was reacted with AgBF₄ (48 mg, 0.247 mmol) to give 202 mg (65%) of **12b(T⁰)** as a yellow powder. FT-ICR-MS: m/z 1251.5 [$M^+ - BF_4$]. *Anal.* Calc. for C₅₅H₉₂BClF₄N₆O₁₀P₂RuSi₂ (1338.8): C, 49.34; H, 6.93; N, 6.28. Found: C, 49.14; H, 6.90; N, 6.10%. ³¹P{¹H} NMR (CD₂Cl₂): δ = 2 diastereomers, 53.5 (d, ²J_{PP} = 36 Hz, η^2 -P[^]O), 52.9 (d, ²J_{PP} = 37 Hz, η^2 -P[^]O), 45.7 (d, ²J_{PP} = 36 Hz, η^1 -P~O), 45.1 (d, ²J_{PP} = 37 Hz, η^1 -P~O). ¹H NMR (CDCl₃): δ = 0.57 (m, 4H14), (m, 18H16), 1.5 (m, 4H13), 2.1 (br m, 2H3), 2.3 – 3.3 (br, 2H3 + 4H12 + 4H2 + CH₂CH₂CH₂(NH₂)₂ (10H)), 3.05 (s, 3H1), 3.7 (br, 3H1 + 12H15), 4.0 – 4.6 (br, 4H8), 5.3 (br, 2H9), 6.3 (br, 2H11), 6.7 – 8.2 (m, 18H, C₆H₄, C₆H₅). ¹³C{¹H} NMR (CDCl₃): δ = 8.0 (s, C14), 18.6 (s, C16), 24.3 (s, C13), 26.3 (m, C3), 28.5 (s, NH₂CH₂CH₂), 30.6 (m, C3), 40.6 (s, NH₂CH₂CH₂), 42.9 (s, C12), 43.3 (s, C8), 58.4 (s, C1), 58.6 (s, C15), 60.9 (s, C1), 68.3 (s, C2), 73.9 (s, C2), 133.0 (m, C18), 141.0 (s, C7), 159.2 (s, C10), 125 – 160 (C₆H₅, C₆H₄). IR (KBr, cm⁻¹): ν (NH) 3313, ν (C=O) 1576.

1.3.4.3 Preparation of 12c(T⁰)

11c(T⁰) (300 mg, 0.233 mmol) was reacted with AgBF₄ (48 mg, 0.247 mmol) to give 218 mg (70%) of **12c(T⁰)** as a yellow powder. FT-ICR-MS: m/z 1251.5 [$M^+ - BF_4$]. *Anal.* Calc. for C₅₅H₉₂BClF₄N₆O₁₀P₂RuSi₂ (1338.8): C, 49.34; H, 6.93; N, 6.28. Found: C, 49.10; H, 6.80; N, 6.20%. ³¹P{¹H} NMR (CD₂Cl₂): δ = 58.0 (d, ²J_{PP} = 36 Hz, η^2 -P[^]O), 56.3 (d, ²J_{PP} = 37 Hz, η^2 -P[^]O), 56.1 (d, ²J_{PP} = 37 Hz, η^2 -P[^]O), 46.0 (m, η^1 -P~O). ¹H NMR (CD₂Cl₂): δ = 0.51 (m, 4H14), 0.64 (br, 3H, CHCH₃), 1.18 (m, 18H16), 1.48 (m, 4H13), 2.8 – 3.0 (br,

$CHCH_3 + CH_2(NH_2)_2$ (6H) + 3H1 + 4H3 + 4H12 + 4H2), 3.6 (br m, 3H1 + 12H15), 4.2 (br s, 4H8), 6.2 (br m, 2H9 + 2H11), 6.8 – 8.3 (m, 18H, C₆H₄, C₆H₅). ¹³C{¹H} NMR (CD₂Cl₂): δ = 8.0 (s, C14), 18.6 (m, C16), 19.7 (s, NH₂CHCH₃), 24.3 (s, C13), 30.2 (m, C3), 32.1 (m, C3), 43.3 (s, C12), 43.6 (s, C8), 51.2 (s, NH₂CH₂), 53.6 (s, NH₂CH), 58.2 (s, C1), 58.7 (s, C15), 60.6 (d, ³J_{PC} = 22.4 Hz, C2), 69.2 (s, C2), 133.0 (m, C18), 140.4 (s, C7), 158.3 (s, C10), 125 – 160 (C₆H₅, C₆H₄). IR (KBr, cm⁻¹): ν(NH) 3333, ν(C=O) 1572.

1.3.4.4 Preparation of 12d(T⁰)

11d(T⁰) (300 mg, 0.227 mmol) was reacted with AgBF₄ (47 mg, 0.241 mmol) to give 249 mg (80%) of **12d(T⁰)** as a brown powder. FT-ICR-MS: *m/z* 1286.5 [M⁺ – BF₄]. *Anal.* Calc. for C₅₈H₉₀BClF₄N₆O₁₀P₂RuSi₂ (1372.8): C, 50.74; H, 6.61; N, 6.12. Found: C, 50.34; H, 6.53; N, 6.01%. ³¹P{¹H} NMR (CDCl₃): δ = 38.6 (m, η²-P[∘]O), 35.0 (d, ²J_{PP} = 30 Hz, η¹-P[∘]O), 34.8 (d, ²J_{PP} = 31 Hz, η¹-P[∘]O). ¹H NMR (CDCl₃): δ = 0.53 (m, 4H14), 1.13 (m, 18H16), 1.5 (m, 4H13), 2.6 – 3.2 (br m, 4H3 + 3H1 + 4H12 + 4H2), 3.5 (m, 3H1), 3.7 (m, 12H15), 4.3 (br, 4H8), 6.1 – 6.8 (br, C₆H₄(NH₂)₂ (4H) + 2H11 + 2H9), 6.8 – 8.0 (br, 22H, C₆H₄ (amine), C₆H₄, C₆H₅). ¹³C{¹H} NMR (CDCl₃): δ = 8.1(s, C14), 18.7 (s, C16), 23.8 (s, C13), 24.3 (m, C3), 43.6 (br, C8 + C12), 58.4 (s, C1), 58.8 (s, C15), 61.5 (s, C1), 59.5 (s, C2), 68.1 (s, C2), 123 – 136 (C₆H₅, C₆H₄, C₆H₄(NH₂)₂), 159.5 (s, C10), 125 – 160 (C₆H₅, C₆H₄, and C-amine). IR (KBr, cm⁻¹): ν(NH) 3336, ν(C=O) 1558.

1.3.4.5 Preparation of 12e(T⁰)

11e(T⁰) (300 mg, 0.219 mmol) was reacted with AgBF₄ (45 mg, 0.231 mmol) of to give 242 mg (78%) of **12e(T⁰)** as a brown powder. FT-ICR-MS: *m/z* 1335.5 [M⁺ – BF₄]. *Anal.* Calc. for C₆₂H₉₂BClF₄N₆O₁₀P₂RuSi₂ (1422.9): C, 52.34; H, 6.52; N, 5.91. Found: C, 51.96; H, 6.50; N, 5.93%. ³¹P{¹H} NMR (CD₂Cl₂): δ = 61.5 (m, η²-P[∘]O), 51.1 (m, η¹-P[∘]O), 49.1 (m,

$\eta^1\text{-P}\sim\text{O}$). ^1H NMR (CD_2Cl_2): $\delta = 0.44$ (m, 4H14), 1.08 (m, 18H16), 1.36 (m, 4H13), 2.3 – 3.0 (br, 4H3 + 3H1 + 4H12 + 4H2), 3.69 (m, 15H15 + 3H1), 3.85 – 4.4 (br, 4H8), 6.0 (br, 2H11), 6.4 (br, 2H9), 6.1 – 6.8 (br, $\text{C}_{10}\text{H}_6(\text{NH}_2)_2$ (4H) + 2H11 + 2H9), 7.0 – 7.6 (m, $\text{C}_{10}\text{H}_6(\text{NH}_2)_2$ (6H) + C_6H_4 (8H) + C_6H_5 (10H)). $^{13}\text{C}\{^1\text{H}\}$ NMR (CDCl_3): $\delta = 8.0$ (s, C14), 18.6 (s, C16), 24.1 (s, C13), 26.7 (m, C3), 30.9 (m, C3), 43.3 (br, C12 + C8), 58.3 (s, C1), 58.8 (s, C15), 62.6 (s, C1), 69.6 (s, C2), 72.3 (s, C2), 120 – 138 (C_6H_5 , C_6H_4 , $\text{C}_{10}\text{H}_6(\text{NH}_2)_2$), 159.17 (s, C10), 125 – 160 (C_6H_5 , C_6H_4 , and C-amine). IR (KBr, cm^{-1}): $\nu(\text{NH})$ 3351, $\nu(\text{C}=\text{O})$ 1569.

1.3.4.6 Preparation of **12f**(T^0)

11f(T^0) (300 mg, 0.219 mmol) was reacted with TIPF_6 (81 mg, 0.232 mmol) to give 232 mg (63%) of **12f**(T^0) as a brown powder. FT-ICR-MS: m/z 1334.5 [$\text{M}^+ - \text{PF}_6$]. *Anal.* Calc. for $\text{C}_{62}\text{H}_{90}\text{ClF}_6\text{N}_6\text{O}_{10}\text{P}_3\text{RuSi}_2$ (1479.02): C, 50.35; H, 6.13; N, 5.68. Found: C, 49.93; H, 5.82; N, 5.25%. $^{31}\text{P}\{^1\text{H}\}$ NMR (CD_2Cl_2): $\delta =$ diastereomer a: (16%) 45.1 (d, $^2J_{\text{PP}} = 33$ Hz, $\eta^2\text{-P}^\wedge\text{O}$), 39.7 (d, $^2J_{\text{PP}} = 33$ Hz, $\eta^1\text{-P}\sim\text{O}$), diastereomer b: (84%) 44.8 (d, $^2J_{\text{PP}} = 33$ Hz, $\eta^2\text{-P}^\wedge\text{O}$), 40.5 (d, $^2J_{\text{PP}} = 33$ Hz, $\eta^1\text{-P}\sim\text{O}$). ^1H NMR (CD_2Cl_2): $\delta = 0.58$ (m, 4H14), 1.07 (m, 18H16), 1.44 (m, 4H13), 2.3 – 3.4 (m, 4H3 + 3H1 + 4H12 + 4H2), 3.68 (m, 12H15 + 3H1), 3.75 (m, 15H15 + 3H1), 4.0 – 4.5 (br, 4H8), 5.5 – 6.6 (br, 2H11 + 2H9), 6.6 – 7.9 (m, 18H, C_6H_4 , C_6H_5), 7.9 – 8.7 (m, 2H1 + 2H3 + 2H4, amine). $^{13}\text{C}\{^1\text{H}\}$ NMR (CD_2Cl_2): $\delta = 8.0$ (s, C14), 18.6 (s, C16), 24.2 (s, C13), 28.0 (d, $^1J_{\text{PC}} = 29$ Hz, C3), 32.4 (m, C3), 44.3, 44.6 (2s, C12 + C8), 59.3 (s, C1), 59.7 (s, C15), 62.4 (s, C1), 69.2 (s, C2), 75.0 (s, C2), 120 – 157 (C_6H_5 , C_6H_4 , $\text{C}_{10}\text{H}_{11}\text{N}_2$), 152.2 (s, C1-amine) 158.8 (s, C5-amine), 140.0 (s, C7), 159.2 (s, C10), 125 – 160 (C_6H_5 , C_6H_4 , and C-amine). IR (KBr, cm^{-1}): $\nu(\text{NH})$ 3418, $\nu(\text{C}=\text{O})$ 1568.

1.3.4.7 Preparation of **12g**(T^0)

11g(T^0) (300 mg, 0.215 mmol) was reacted with TIPF_6 (80 mg, 0.229 mmol) to give 224 mg (61%) of **12g**(T^0) as a red powder. FT-ICR-MS: m/z 1357.5 [$\text{M}^+ - \text{PF}_6$]. *Anal.* Calc.

for $C_{64}H_{90}ClF_6N_6O_{10}P_3RuSi_2$ (1503.0): C, 51.14; H, 6.04; N, 5.59. Found: C, 50.82; H, 5.84; N, 5.28%. $^{31}P\{^1H\}$ NMR (CD_2Cl_2): δ = diastereomer a: (12%) 45.7 (d, $^2J_{PP} = 34$ Hz, $\eta^2-P^{\wedge}O$), 39.9 (d, $^2J_{PP} = 34$ Hz, $\eta^1-P^{\sim}O$), diastereomer b: (88%) 44.5 (d, $^2J_{PP} = 34$ Hz, $\eta^2-P^{\wedge}O$), 41.1 (d, $^2J_{PP} = 34$ Hz, $\eta^1-P^{\sim}O$), 1H NMR (CD_2Cl_2): δ = 0.52 (m, 4H14), 1.1 (m, 18H16), 1.5 (m, 4H13), 2.3 – 3.2 (br m, 4H3 + 3H1 + 4H12 + 4H2), 3.7 (m, 12H15 + 3H1), 3.8 – 4.6 (m, 4H8), 6.2 (m, 2H11), 6.4 (m, 2H9), 6.7 – 8.4 (m, , C_6H_4 (8H) + C_6H_5 (10H) + 2H2 + 2H3 + 2H4, amine) 8.6 (m, 2H1, amine). $^{13}C\{^1H\}$ NMR (CD_2Cl_2): δ = 7.9 (s, C14), 18.6 (s, C16), 24.3 (s, C13), 29.3 (d, $^1J_{PC} = 25.0$ Hz, C3), 31.1 (d, $^1J_{PC} = 29.0$ Hz, C3), 43.4 (s, C12), 43.2 (s, C8), 58.2 (s, C1), 58.7 (s, C15), 61.4 (s, C1), 68.0 (m, C2), 73.9 (s, C2), 126.5 (s, C4–amine), 134.7 (s, C3–amine), 149.6 (s, C1–amine), 159.2 (s, C6–amine), 133.8 (m, C18), 141.0 (s, C7), 159.7 (s, C10), 125 – 160 (C_6H_5 , C_6H_4 , and C–amine). IR (KBr, cm^{-1}): $\nu(NH)$ 3412, $\nu(C=O)$ 1557.

1.3.5 Preparation of the Dicationic Complex **13a(T^o)**

11a(T^o) (300 mg, 0.247 mmol) was added to $TiPF_6$ (1.235 g, 3.54 mmol) in 25 ml of dichloromethane and the mixture was refluxed for 24 h. After filtration through silica gel the solvent was reduced under vacuum to 5 ml. The dicationic complex was precipitated by addition of 100 ml of diethyl ether, filtered off (P3) and washed three times with 25 ml of diethyl ether. FT-ICR-MS: m/z 601 [$M^{2+} - 2PF_6$]. $^{31}P\{^1H\}$ NMR (CD_2Cl_2): dicationic complex **13a(T^o)** (75%), δ = 50.5 (d, $^2J_{PP} = 36$ Hz, $\eta^2-P^{\wedge}O$), 50.7 (d, $^2J_{PP} = 35$ Hz, $\eta^2-P^{\wedge}O$), 51.5 (d, $^2J_{PP} = 35$ Hz, $\eta^2-P^{\wedge}O$), 64.1 (d, $^2J_{PP} = 36$ Hz, $\eta^2-P^{\wedge}O$), 65.0 (d, $^2J_{PP} = 36$ Hz, $\eta^2-P^{\wedge}O$), 65.1 (d, $^2J_{PP} = 35$ Hz, $\eta^2-P^{\wedge}O$), **11a(T^o)**: (25%) 38.2 (s).

1.4 Preparation of the Heterogenized Complexes **X14a – g**, **X15a – g**, **X16a – g**, and **X17a – g**

1.4.1 General Procedure for Sol–Gel Processing

To a solution of **11a(T°) – g(T°)** in 5 ml of MeOH and 15 ml of THF the corresponding amount of the co-condensation agent **D°–C₆–D°** or **Me–T°**, H₂O, and 100 µl of (*n*-Bu)₂Sn(OAc)₂ were added. After 3 d stirring at room temperature, the precipitated gel was washed with each 10 ml of toluene and diethyl ether, and 15 ml of petroleum ether (40 – 70). Finally the xerogels were grinded and dried under vacuum for 24 h.

1.4.1.1 Preparation of **X14a**

11aT° (300 mg, 0.235 mmol) and **D°–C₆–D°** (692 mg, 2.35 mmol) were sol–gel processed with water (600 µl, 33.3 mmol) to give 420 mg (87 %) of **X14a** as a pale yellow powder *Anal.* Calc. for C₂₀₂H₄₂₀Cl₂N₆O₂₂P₂RuSi₄₂: C, 47.58; H, 8.30; N 1.65. Found: C, 43.54; H 7.99; N, 0.95 %. ³¹P CP/MAS NMR: δ = 37.6. ¹³C CP/MAS NMR: δ = –0.4 (SiCH₃), 17.6, 22.8, 33.4 (CH₂ of co-condensation agent and spacer), 49.5 (SiOCH₃), 128.7, 139.0 (br, C–phenyl). ²⁹Si CP/MAS NMR: δ = –2.4 (D°), –12.8 (D¹), –22.5 (D²), –58.1(T²), –67.2 (T³). IR (KBr, cm^{–1}): ν(C=O) 1559, 1663. N₂ surface area: 2.31 m² g^{–1}.

1.4.1.2 Preparation of **X14b**

11bT° (300 mg, 0.233 mmol) and **D°–C₆–D°** (686 mg, 2.33 mmol) were sol–gel processed with water (600 µl, 33.3 mmol) to give 438 mg (90 %) of **X14b** as a pale yellow powder *Anal.* Cal. for C₂₀₃H₄₂₂Cl₂N₆O₂₂P₂RuSi₄₂: C, 47.69; H, 8.32; N, 1.64. Found: C, 44.45; H, 7.83; N, 0.98 %. ³¹P CP/MAS NMR: δ = 39.7. ¹³C CP/MAS NMR: δ = –0.3 (SiCH₃), 17.6, 23.1, 33.1 (CH₂ of co-condensation agent and spacer), 43.0 (C_{8,12}, see

Scheme 5), 49.5 (SiOCH₃), 58.0 (OCH₃), 69.3 (CH₂O), 158.6 (C=O), 128.7 (br, C-phenyl). ²⁹Si CP/MAS NMR: $\delta = -2.3$ (D^o), -13.1 (D¹), -22.6 (D²), -58.2 (T²), -68.1 (T³). IR (KBr, cm⁻¹): ν (C=O) 1556, 1659. N₂ surface area: 3.09 m² g⁻¹.

1.4.1.3 Preparation of X14c

11cT^o (300 mg, 0.233 mmol) and **D^o-C₆-D^o** (686 mg, 2.33 mmol) were sol-gel processed with water (600 μ l, 33.3 mmol) to give 450 mg (93 %) of **X14c** as a pale yellow powder. *Anal.* Cal. for C₂₀₃H₄₂₂Cl₂N₆O₂₂P₂RuSi₄₂: C, 47.69; H, 8.32; N, 1.64. Found: C, 43.35; H, 8.14; N, 0.98 %. ³¹P CP/MAS NMR: $\delta = 38.1$. ¹³C CP/MAS NMR: $\delta = -5.8$ ((H₃CO)₂SiCH₃), -0.3 (SiCH₃), 17.6, 23.1, 33.1 (CH₂ of co-condensation agent and spacer), 42.7 (C_{8,12}), 49.5 (SiOCH₃), 57.7 (OCH₃), 69.3 (CH₂O), 159.0 (C=O), 128.7 (br, C-phenyl). ²⁹Si CP/MAS NMR: $\delta = -1.9$ (D^o), -14.2 (D¹), -22.5 (D²), -58.5 (T²), -67.7 (T³). IR (KBr, cm⁻¹): ν (C=O) 1569, 1653.

1.4.1.4 Preparation of X15a

11aT^o (300 mg, 0.235 mmol) and **Me-T^o** (320 mg, 2.35 mmol) were sol-gel processed with water (300 μ l, 16.6 mmol) to give 333 mg (82 %) of **X15a** as a pale yellow powder. *Anal.* Cal. for C₅₂H₉₀Cl₂N₆O₂₂P₂RuSi₁₂: C, 36.26; H, 5.27; N, 4.88. Found: C, 34.67; H, 4.94; N, 4.00 %. ³¹P CP/MAS NMR: $\delta = 37.2$. ¹³C CP/MAS NMR: $\delta = -3.8$ (SiCH₃), 12.9 (C₁₄), 26.2 (C_{3,13}), 43.0 (C-amine, C_{8,12}), 57.1 (OCH₃), 68.7 (CH₂O), 128.4 (br, C-phenyl), 158.5 (C=O). ²⁹Si CP/MAS NMR: $\delta = -58.0$ (T²), -65.2 (T³). IR (KBr, cm⁻¹): ν (C=O) 1567, 1650.

1.4.1.5 Preparation of X15b

11bT^o (300 mg, 0.233 mmol) and **Me-T^o** (317 mg, 2.33 mmol) were sol-gel processed with water (300 μ l, 16.6 mmol) to give 321 mg (79 %) of **X15b** as a pale yellow powder. *Anal.* Cal. for C₅₃H₉₂Cl₂N₆O₂₂P₂RuSi₁₂: C, 36.66; H, 5.34; N, 4.84. Found: C, 35.49; H, 5.58; N, 4.16 %. ³¹P CP/MAS NMR: δ = 42.2. ¹³C CP/MAS NMR: δ = -4.1 (SiCH₃), 12.9 (C14), 26.4 (C3,13), 42.1 (C-amine, C8,12), 56.9 (OCH₃), 68.6 (CH₂O), 128.4 (br, C-phenyl), 158.8 (C=O). ²⁹Si CP/MAS NMR: δ = -58.0 (T²), -65.2 (T³). IR (KBr, cm⁻¹): ν (C=O) 1567, 1651. N₂ surface area: 5.94 m² g⁻¹.

1.4.1.6 Preparation of X15c

11cT^o (300 mg, 0.233 mmol) and **Me-T^o** (317 mg, 2.33 mmol) were sol-gel processed with water (300 μ l, 16.6 mmol) to give 353 mg (87 %) of **X15c** as a pale yellow powder. *Anal.* Cal. for C₅₃H₉₂Cl₂N₆O₂₂P₂RuSi₁₂: C, 36.66; H, 5.34; N, 4.84. Found: C, 34.00; H, 4.99; N, 3.78 %. ³¹P CP/MAS NMR: δ = 38.3. ¹³C CP/MAS NMR: δ = -4.1 (SiCH₃), 12.9 (C14), 21.5 (CH-amine), 26.2 (C3,13), 42.8 (C8,12), 57.4 (OCH₃), 68.7 (CH₂O), 128.4 (br, C-phenyl), 159.4 (C=O). ²⁹Si CP/MAS NMR: δ = -58.0 (T²), -65.2 (T³). IR (KBr, cm⁻¹): ν (C=O) 1559, 1653.

1.4.1.7 Preparation of X15d

11dT^o (300 mg, 0.227 mmol) and **Me-T^o** (309 mg, 2.27 mmol) were sol-gel processed with water (300 μ l, 16.6 mmol) to give 339 mg (84 %) of **X15d** as a brown powder. *Anal.* Cal. for C₅₆H₉₀Cl₂N₆O₂₂P₂RuSi₁₂: C, 37.99; H, 5.12; N, 4.75. Found: C, 36.55; H, 4.26; N, 3.83 %. ³¹P CP/MAS NMR: δ = 44.1. ¹³C CP/MAS NMR: δ = -3.9 (SiCH₃), 12.9 (C14), 26.4 (C3,13), 43.0 (C8,12), 57.2 (OCH₃), 68.4 (CH₂O), 128.5, 140.5 (br, C-phenyl), 158.8 (C=O). ²⁹Si CP/MAS NMR: δ = -58.0 (T²), -65.2 (T³). IR (KBr, cm⁻¹): ν (C=O) 1558, 1653.

1.4.1.8 Preparation of X15e

11eT^o (300 mg, 0.219 mmol) and **Me-T^o** (298 mg, 2.19 mmol) were sol-gel processed with water (300 μ l, 16.6 mmol) to give 290 mg (73 %) of **X15e** as a brown powder. *Anal.* Cal. for C₆₀H₉₂Cl₂N₆O₂₂P₂RuSi₁₂: C, 39.59; H, 5.09; N, 4.62. Found: C, 37.56; H, 5.38; N, 3.50 %. ³¹P CP/MAS NMR: δ = 43.9. ¹³C CP/MAS NMR: δ = -3.8 (SiCH₃), 13.2 (C14), 26.4 (C3,13), 42.9 (C8,12), 57.7 (OCH₃), 68.5 (CH₂O), 128.5 (br, C-phenyl), 159.2 (C=O). ²⁹Si CP/MAS NMR: δ = -58.0 (T²), -65.3 (T³). IR (KBr, cm⁻¹): ν (C=O) 1570, 1653.

1.4.1.9 Preparation of X15f

11fT^o (300 mg, 0.219 mmol) and **Me-T^o** (298 mg, 2.19 mmol) were sol-gel processed with water (300 μ l, 16.6 mmol) to give 346 mg (87 %) of **X15f** as a brown powder. *Anal.* Cal. for C₆₁H₉₃Cl₂N₆O₂₂P₂RuSi₁₂: C, 40.56; H, 5.46; N, 4.51. Found: C, 42.11; H, 4.26; N, 3.84 %. ³¹P CP/MAS NMR: δ = 29.2. ¹³C CP/MAS NMR: δ = -3.8 (SiCH₃), 13.1 (C14), 26.6 (C3,13), 42.6 (C8,12), 57.3 (OCH₃), 68.0 (CH₂O), 128.0 (br, C-phenyl), 158.4 (C=O). ²⁹Si CP/MAS NMR: δ = -58.0 (T²), -65.3 (T³). IR (KBr, cm⁻¹): ν (C=O) 1558, 1653.

1.4.1.10 Preparation of X15g

11gT^o (300 mg, 0.215 mmol) and **Me-T^o** (292 mg, 2.15 mmol) were sol-gel processed with water (300 μ l, 16.6 mmol) to give 297 mg (75 %) of **X15g** as a red powder. *Anal.* Cal. for C₆₃H₉₃Cl₂N₆O₂₂P₂RuSi₁₂: C, 40.74; H, 5.05; N, 4.52. Found: C, 39.13; H, 4.04; N, 3.40 %. ³¹P CP/MAS NMR: δ = 29.3. ¹³C CP/MAS NMR: δ = -3.8 (SiCH₃), 12.8 (C14), 26.5 (C3,13), 42.5 (C8,12), 57.3 (OCH₃), 68.9 (CH₂O), 128.9 (br, C-phenyl), 149.1 (br, C-amine), 158.1 (C=O). ²⁹Si CP/MAS NMR: δ = -58.0 (T²), -65.3 (T³). IR (KBr, cm⁻¹): ν (C=O) 1558, 1653.

1.4.1.11 Preparation of X16a

11aT^o (300mg, 0.235 mmol) and **Me-T^o** (640 mg, 4.70 mmol) were sol-gel processed with water (600 μ l, 16.6 mmol) to give 451 mg (80 %) of **X16a** as a pale yellow powder. *Anal.* Cal. for C₆₂H₁₂₀Cl₂N₆O₃₇P₂RuSi₂₂: C, 31.11; H, 5.05; N, 3.51. Found: C, 33.38; H, 4.59; N, 2.57 %. ³¹P CP/MAS NMR: δ = 36.7. ¹³C CP/MAS NMR: δ = -4.1 (SiCH₃), 13.1 (C14), 25.9 (C3,13), 42.7 (C-amine, C8,12), 57.4 (OCH₃), 67.7 (CH₂O), 128.4, 140.0 (br, C-phenyl), 159.3 (C=O). ²⁹Si CP/MAS NMR: δ = -58.0 (T²), -65.7 (T³). IR (KBr, cm⁻¹): ν (C=O) 1570, 1651.

1.4.1.12 Preparation of X16b

11bT^o (300 mg, 0.233 mmol) and **Me-T^o** (635 mg, 4.66 mmol) were sol-gel processed with water (600 μ l, 16.6 mmol) to give 454 mg (81 %) of **X16b** as a pale yellow powder. *Anal.* Cal. for C₆₃H₁₂₂Cl₂N₆O₃₇P₂RuSi₂₂: C, 31.43; H, 5.11; N, 3.49. Found: C, 33.30; H, 4.33; N, 2.79 %. ³¹P CP/MAS NMR: δ = 43.6. ¹³C CP/MAS NMR: δ = -3.6 (SiCH₃), 13.4 (C14), 26.8 (C3,13), 43.1 (C-amine, C8,12), 57.7 (OCH₃), 68.6 (CH₂O), 128.4, 140.0 (br, C-phenyl), 159.4 (C=O). ²⁹Si CP/MAS NMR: δ = -58.0 (T²), -64.8 (T³). IR (KBr, cm⁻¹): ν (C=O) 1570, 1656. N₂ surface area: 4.36 m² g⁻¹.

1.4.1.13 Preparation of X16c

11cT^o (300mg, 0.233 mmol) and **Me-T^o** (635 g, 4.66 mmol) were sol-gel processed with water (600 μ l, 16.6 mmol) to give 476 mg (85 %) of **X16c** as a pale yellow powder. *Anal.* Cal. for C₆₃H₁₂₂Cl₂N₆O₃₇P₂RuSi₂₂: C, 31.43; H, 5.11; N, 3.49. Found: C, 29.71; H, 4.56; N, 2.75 %. ³¹P CP/MAS NMR: δ = 36.3. ¹³C CP/MAS NMR: δ = -3.9 (SiCH₃), 13.2 (C14), 21.5 (CH-amine), 26.4 (C3,13), 43.1 (C8,12), 57.2 (OCH₃), 68.2 (CH₂O), 128.0 (br, C-

phenyl), 158.9 (C=O). ^{29}Si CP/MAS NMR: $\delta = -58.0$ (T^2), -65.2 (T^3). IR (KBr, cm^{-1}): $\nu(\text{C}=\text{O})$ 1569, 1653.

1.4.1.14 Preparation of X16d

11dT $^\circ$ (300 mg, 0.227 mmol) and **Me-T $^\circ$** (618 mg, 4.54 mmol) were sol-gel processed with water (600 μl , 16.6 mmol) to give 478 mg (86 %) of **X16d** as a brown powder. *Anal.* Cal. for $\text{C}_{66}\text{H}_{120}\text{Cl}_2\text{N}_6\text{O}_{37}\text{P}_2\text{RuSi}_{22}$: C, 31.47; H, 4.95; N, 3.44. Found: C, 28.99; H, 4.58; N, 2.69 %. ^{31}P CP/MAS NMR: $\delta = 44.2$. ^{13}C CP/MAS NMR: $\delta = -3.9$ (SiCH_3), 13.3 (C14), 26.3, 22.5 (C3,13), 42.7 (C8,12), 57.4 (OCH_3), 67.9 (CH_2O), 128.1, 140.0 (br, C-phenyl), 159.0 (C=O). ^{29}Si CP/MAS NMR: $\delta = -58.0$ (T^2), -65.2 (T^3). IR (KBr, cm^{-1}): $\nu(\text{C}=\text{O})$ 1572, 1656.

1.4.1.15 Preparation of X16e

11eT $^\circ$ (300 mg, 0.219 mmol) and **Me-T $^\circ$** (597 mg, 4.38 mmol) were sol-gel processed with water (600 μl , 16.6 mmol) to give 473 mg (87 %) of **X16e** as a brown powder. *Anal.* Cal. for $\text{C}_{70}\text{H}_{122}\text{Cl}_2\text{N}_6\text{O}_{37}\text{P}_2\text{RuSi}_{22}$: C, 33.74; H, 4.94; N, 3.37. Found: C, 31.99; H, 3.98; N, 2.30 %. ^{31}P CP/MAS NMR: $\delta = 42.6$. ^{13}C CP/MAS NMR: $\delta = -3.8$ (SiCH_3), 13.2 (C14), 26.4, 22.5 (C3,13), 43.1 (C8,12), 57.3 (OCH_3), 68.4 (CH_2O), 128.4 (br, C-phenyl), 159.2 (C=O). ^{29}Si CP/MAS NMR: $\delta = -58.0$ (T^2), -65.1 (T^3). IR (KBr, cm^{-1}): $\nu(\text{C}=\text{O})$ 1571, 1651.

1.4.1.16 Preparation of X16f

11fT $^\circ$ (300 mg, 0.219 mmol) and **Me-T $^\circ$** (597 mg, 4.38 mmol) were sol-gel processed with water (600 μl , 16.6 mmol) to give 485 mg (89 %) of **X16f** as a brown powder. *Anal.* Cal. for $\text{C}_{71}\text{H}_{123}\text{Cl}_2\text{N}_6\text{O}_{37}\text{P}_2\text{RuSi}_{22}$: C, 34.05; H, 4.95; N, 3.36. Found: C, 30.51; H, 4.20; N, 2.87 %. ^{31}P CP/MAS NMR: $\delta = 29.4$. ^{13}C CP/MAS NMR: $\delta = -3.7$ (SiCH_3), 13.2 (C14),

22.5, 26.4 (C3,13), 42.7 (C8,12), 57.5 (OCH₃), 67.9 (CH₂O), 128.5 (br, C-phenyl), 158.8 (C=O). ²⁹Si CP/MAS NMR: $\delta = -58.0$ (T²), -65.0 (T³). IR (KBr, cm⁻¹): ν (C=O) 1570, 1653.

1.4.1.17 Preparation of X16g

11gT^o (300 mg, 0.215 mmol) and **Me-T^o** (586 mg, 4.30 mmol) were sol-gel processed with water (600 μ l, 16.6 mmol) to give 420 mg (78 %) of **X16g** as a red powder. *Anal.* Cal. for C₇₃H₁₂₃Cl₂N₆O₃₇P₂RuSi₂₂: C, 34.67; H, 4.90; N, 3.32. Found: C, 34.18; H, 4.22; N, 2.45 %. ³¹P CP/MAS NMR: $\delta = 28.8$. ¹³C CP/MAS NMR: $\delta = -3.8$ (SiCH₃), 13.3 (C14), 22.5, 26.6 (C3,13), 42.7 (C8,12), 57.5 (OCH₃), 68.0 (CH₂O), 129.1 (br, C-phenyl), 149.0 (br, C-amine), 158.7 (C=O). ²⁹Si CP/MAS NMR: $\delta = -58.0$ (T²), -65.3 (T³). IR (KBr, cm⁻¹): ν (C=O) 1570, 1653.

1.4.1.18 Preparation of X17a

12aT^o (300 mg, 0.226 mmol) and **Me-T^o** (617 mg, 4.53 mmol) were sol-gel processed with water (600 μ l, 16.6 mmol) to give 470 mg (85 %) of **X17a** as a pale yellow powder. *Anal.* Cal. for C₆₂H₁₂₀BClF₄N₆O₃₇P₂RuSi₂₂: C, 30.46; H, 4.95; N, 3.44. Found: C, 28.40; H, 4.12; N, 2.31 %. ³¹P CP/MAS NMR: $\delta = 52.6$ (η^2 -P^oO), 44.9 (η^1 -P~O). ¹³C CP/MAS NMR: $\delta = -3.9$ (SiCH₃), 13.2 (C14), 26.6 (C3,13), 43.2 (C-amine, C8,12), 57.7 (OCH₃), 68.6, 71.0 (CH₂O), 129.2, 142.5 (br, C-phenyl), 159.0 (C=O). ²⁹Si CP/MAS NMR: $\delta = -58.0$ (T²), -65.2 (T³). IR (KBr, cm⁻¹): ν (C=O) 1556, 1652.

1.4.1.19 Preparation of X17b

12bT^o (300 mg, 0.224 mmol) and **Me-T^o** (611 mg, 4.48 mmol) were sol-gel processed with water (600 μ l, 16.6 mmol) to give 446 mg (81 %) of **X17b** as a pale yellow powder. *Anal.* Cal. for C₆₃H₁₂₂BClF₄N₆O₃₇P₂RuSi₂₂: C, 30.77; H, 5.00; N, 3.42. Found: C,

27.91; H, 3.94; N, 2.18 %. ^{31}P CP/MAS NMR: $\delta = 50.0$ ($\eta^2\text{-P}^{\circ}\text{O}$), 43.3 ($\eta^1\text{-P}\sim\text{O}$). ^{13}C CP/MAS NMR: $\delta = -3.7$ (SiCH_3), 13.1 (C14), 26.7 (C3,13), 42.6 (C-amine, C8,12), 49.3 (SiOCH_3), 57.5 (OCH_3), 68.2 (CH_2O), 129.6, 142.0 (br, C-phenyl), 159.2 (C=O). ^{29}Si CP/MAS NMR: $\delta = -58.0$ (T^2), -65.4 (T^3). IR (KBr, cm^{-1}): $\nu(\text{C}=\text{O})$ 1555, 1653.

1.4.1.20 Preparation of X17c

12cT^o (300 mg, 0.224 mmol) and **Me-T^o** (611 mg, 4.48 mmol) were sol-gel processed with water (600 μl , 16.6 mmol) to give 469 mg (85 %) of **X17c** as a pale yellow powder. *Anal.* Cal. for $\text{C}_{63}\text{H}_{122}\text{BClF}_4\text{N}_6\text{O}_{37}\text{P}_2\text{RuSi}_{22}$: C, 30.77, H, 5.00, N, 3.42. Found: C 28.81, H 4.49, N 3.01 %. ^{31}P CP/MAS NMR: $\delta = 53.7$ ($\eta^2\text{-P}^{\circ}\text{O}$), 45.2 ($\eta^1\text{-P}\sim\text{O}$). ^{13}C CP/MAS NMR: $\delta = -3.9$ (SiCH_3), 13.2, 11.1 (C14), 20.5 (CH-amine), 26.8 (C3,13), 43.0 (C8,12), 49.7 (s, NH_2CH_2), 57.8 (OCH_3), 68.6 and 73.2 (CH_2O), 128.0 (br, C-phenyl), 158.9 (C=O). ^{29}Si CP/MAS NMR: $\delta = -58.0$ (T^2), -65.5 (T^3). IR (KBr, cm^{-1}): $\nu(\text{C}=\text{O})$ 1556, 1656.

1.4.1.21 Preparation of X17d

12dT^o (300 mg, 0.219 mmol) and **Me-T^o** (595 mg, 4.37 mmol) were sol-gel processed with water (600 μl , 16.6 mmol) to give 480 mg (88 %) of **X17d** as a brown powder. *Anal.* Cal. for $\text{C}_{66}\text{H}_{120}\text{BClF}_4\text{N}_6\text{O}_{37}\text{P}_2\text{RuSi}_{22}$: C, 31.80; H, 4.85; N, 3.37. Found: C, 31.22; H, 2.95; N, 2.09 %. ^{31}P CP/MAS NMR: $\delta = 46.4$ ($\eta^2\text{-P}^{\circ}\text{O}$), 37.5 ($\eta^1\text{-P}\sim\text{O}$). ^{13}C CP/MAS NMR: $\delta = -3.8$ (SiCH_3), 13.3 (C14), 26.7, 22.5 (C3,13), 43.1 (C8,12), 57.5 (OCH_3), 67.8 (CH_2O), 128.4, 140.0 (br, C-phenyl), 159.0 (C=O). ^{29}Si CP/MAS NMR: $\delta = -58.0$ (T^2), -65.6 (T^3). IR (KBr, cm^{-1}): $\nu(\text{C}=\text{O})$ 1556, 1650.

1.4.1.22 Preparation of X17e

12eT^o (300 mg, 0.211 mmol) and **Me-T^o** (575 mg, 4.22 mmol) were sol-gel processed with water (600 μ l, 16.6 mmol) to give 418 mg (78 %) of **X17e** as a brown powder. *Anal.* Cal. for C₇₁H₁₂₆BClF₄N₆O₃₇P₂RuSi₂₂: C, 33.32; H, 4.96; N, 3.28. Found: C, 27.35; H, 3.88; N, 2.40 %. ³¹P CP/MAS NMR: δ = 62.6 (η^2 -P^oO), 49.5 (η^1 -P~O). ¹³C CP/MAS NMR: δ = -3.8 (SiCH₃), 11.1, 13.2 (C14), 27.0, 22.5 (C3,13), 41.7 (C8,12), 57.3, 63.0 (OCH₃), 68.5, 72.0 (CH₂O), 128.5 (br, C-phenyl), 159.0 (C=O). ²⁹Si CP/MAS NMR: δ = -58.0 (T²), -65.8 (T³). IR (KBr, cm⁻¹): ν (C=O) 1558, 1653.

1.4.1.23 Preparation of X17f

12fT^o (300 mg, 0.203 mmol) and **Me-T^o** (553 mg, 4.06 mmol) were sol-gel processed with water (600 μ l, 16.6 mmol) to give 474 mg (90 %) of **X17f** as a brown powder. *Anal.* Cal. for C₇₀H₁₂₀BClF₄N₆O₃₇P₂RuSi₂₂: C, 33.09; H, 4.76; N, 3.31. Found: C, 30.61; H, 3.93; N, 2.50 %. ³¹P CP/MAS NMR: δ = 40.7 (br, η^2 -P^oO, η^1 -P~O). ¹³C CP/MAS NMR: δ = -3.7 (SiCH₃), 13.4 (C14), 26.8 (C3,13), 42.8 (C8,12), 49.2 (SiOCH₃), 57.7 (OCH₃), 68.0 (CH₂O), 128.7, 140.0 (br, C-phenyl), 158.4 (C=O). ²⁹Si CP/MAS NMR: δ = -58.0 (T²), -65.5 (T³). IR (KBr, cm⁻¹): ν (C=O) 1556, 1652.

1.4.1.24 Preparation of X17g

12gT^o (300 mg, 0.200 mmol) and **Me-T^o** (544 mg, 3.99 mmol) were sol-gel processed with water (600 μ l, 16.6 mmol) to give 425 mg (81 %) of **X17g** as a red powder. *Anal.* Cal. for C₇₂H₁₂₁BClF₄N₆O₃₇P₂RuSi₂₂: C, 33.70; H, 4.75; N, 3.28. Found: C 32.62; H 3.91; N 2.74 %. ³¹P CP/MAS NMR: δ = 41.3 (η^2 -P^oO), 33.7 (η^1 -P~O). ¹³C CP/MAS NMR: δ = -3.9 (SiCH₃), 13.2 (C14), 24.3 (C3,13), 42.6 (C8,12), 57.2 (OCH₃), 68.1 (CH₂O),

129.1 (br, C-phenyl), 158.7 (C=O). ^{29}Si CP/MAS NMR: $\delta = -58.0$ (T^2), -65.7 (T^3). IR (KBr, cm^{-1}): $\nu(\text{C=O})$ 1556, 1649.

References

- [1] G. Jung, *Combinatorial Chemistry: Synthesis, Analysis, Screening*, Wiley, Weinheim, 1999.
- [2] S. Pierfausto, *Chim. Ind.*, **1998**, 80, 1183.
- [3] S. Richard, *Drug Discovery Today*, **1996**, 1, 248.
- [4] U. Grether, H. Waldmann, *Angew. Chem., Int. Ed.* **2000**, 39, 1629.
- [5] H. E. Tuinstra, C. H. Cummins, *Adv. Mater.* **2000**, 12, 1819.
- [6] K. C. Menke, *J. Autom. Methods. Manage. Chem.* **2000**, 22, 143
- [7] W. F. Maier, *Angew. Chem., Int. Ed.* **1999**, 38, 1216.
- [8] T. Bein, *Angew. Chem., Int. Ed.* **1999**, 38, 323.
- [9] J. M. Newsam, F. Schuth, *Biotechnol. Bioeng.* **1999**, 61, 203.
- [10] G. Mayer, A. Schober, J. M. Kohler, *Reviews in Molecular Biotechnology*, **2001**, 82, 137.
- [11] R. Sally, *Drug Discovery Today*, **2002**, 7, 133.
- [12] J. C. Wijkmans, R. P. Beckett, *Drug Discovery Today*, **2002**, 7, 126.
- [13] J. A. Flygare, D. P. Sutherline, S. D. Brown, *Methods Mol. Biol.* **2001**, 176, 353.
- [14] J. K. Borchardi, *Modern Drug Discovery*, **2001**, 4, 38.
- [15] R. Schlögl, *Angew. Chem., Int. Ed.* **1998**, 37, 2333.
- [16] A. Holzwarth, H. Schmidt, W. F. Maier, *Angew. Chem., Int. Ed.* **1998**, 37, 2644.
- [17] K. D. Shimizu, M. L. Snapper, A. H. Hoveyda, *Chem. Eur. J.* **1998**, 4, 1885.
- [18] K. W. Kuntz, M. L. Snapper, A. H. Hoveyda, *Current Opinion in Chemical Biology*, **1999**, 3, 313.
- [19] R. Schlögl, *Angew. Chem., Int. Ed.* **1998**, 37, 2333.
- [20] d. G. Powers, D. L. Coffen, *Drug discovery Today*, **1999**, 4, 377.
- [21] G. A. Truran, S. K. Aiken, R. T. Fleming, J. P. Webb, H. J. Markgraf, *J. Chem Educ.*, **2002**, 79, 85.

- [22] D. Charmot, P. Mansky, O. Kolosov, D. Benoit, G. Klarner, M. Jayaraman, M. Piotti, H. Chang, V. Nava-Salgado, *Polymer Preprints*, **2001**, 42, 627.
- [23] M. C. Pirrung, *Chem. Rev.* **1997**, 97, 473.
- [24] F. D. Hess, R. J. Anderson, J. D. Reagan, *Weed Sci.* **2001**, 49, 249.
- [25] J. P. Kiplinger, R. O. Cole, S. Robinson, E. J. Roskamp, R. S. Ware, H. J. O'connell, A. Brailsford, J. Batt, *Rapid Commun. Mass Spectrom.* **1998**, 12, 658.
- [26] J. F. Cargill, R. R. Maiefski, *Lab. Rob. Autom.* **1996**, 8, 139.
- [27] C. J. Andres, R. T. Swann, K. Grant-Young, S. V. D'Anderea, M. S. Deshpande, *Comb. Chem. High Throughput Screening*, **1999**, 2, 29.
- [28] P. A. Ramsland, *Comb. Chem. High Throughput Screening*, **2001**, 4, 5.
- [29] C. J. Manly, *J. Autom. Methods Manage. Chem.*, **2001**, 23, 191.
- [30] A. Hagemeyer, B. Jandeleit, Y. Liu, M. Damodara, H. W. Turner, A. F. Volpe, *Appl. Catal., A: General*, **2001**, 221, 23.
- [31] J. Long, J. Hu, X. Shen, B. Ji, K. Ding, *J. Am. Chem. Soc.* **2002**, 124, 10.
- [32] G. T. Copeland, S. J. J. Miller, *J. Am. Chem. Soc.* **1999**, 121, 4306.
- [33] M. T. Reetz, M. H. Becker, H. W. Klein, D. Stockigt, *Angew. Chem., Int. Ed.* **1999**, 38, 1758.
- [34] S. Senkan, K. Krantz, S. Ozturk, V. Zengin, I. Onal, *Angew. Chem., Int. Ed.* **1999**, 38, 2794.
- [35] O. Lavastre, J. P. Morken, *Angew. Chem., Int. Ed.* **1999**, 38, 3163.
- [36] R. H. Crabtree, *Chem. Commun.* **1999**, 1611.
- [37] B. Jandeleit, D. J. Schaefer, T. S. Powers, H. W. Turner, W. H. Weinberg, *Angew. Chem., Int. Ed.* **1999**, 38, 2495.
- [38] R. Schlögl, *Angew. Chem., Int. Ed.* **1998**, 37, 2333.
- [39] A. Holzwarth, H. Schmidt, W. F. Maier, *Angew. Chem., Int. Ed.* **1998**, 37, 2644.
- [40] K. D. Shimizu, M. L. Snapper, A. H. Hoveyda, *Chem. Eur. J.* **1998**, 4, 1885.

- [41] B. Cornils W. A. Herrmann, *Applied Homogeneous Catalysis with Organometallic Compounds-A Comprehensive*, Wiley-VCH: Weinheim, Germany, 1996.
- [42] C. Nachtigal, S. Al-Gharabli, K. Eichele, E. Lindner, H. A. Mayer, *Organometallics*, **2002**, 21, 105.
- [43] R. Noyori, T. Ohkuma, *Angew. Chem., Int. Ed.* **2001**, 40, 40.
- [44] M. D. Tudor, J. J. Becker, P. S. White, M. R. Gagne, *Organometallics*, **2000**, 19, 4376.
- [45] M. J. Burk, W. Hems, D. Herzberg, C. Malan, A. Canotti-Gerosa, *Org. Lett.* **2000**, 2, 4173.
- [46] P. Braunstein, C. Graiff, F. Naud, A. Pfaltz, A. Tiripicchio, *Inorg. Chem.* **2000**, 39, 4468.
- [47] W. C. Chan, C. P. Lau, Y. Z. Chen, Y. Q. Fang, S. M. Ng, G. C. Jia, *Organometallics*, **1997**, 16, 34.
- [48] H. I. Beerens, P. Wijkens, J. T. B. H. Jastrzebski, F. Verpoort, L. Verdonck, van G. Koten, *J. Organomet. Chem.* **2000**, 603, 244.
- [49] H. Yang, M. Alvarez-Gressier, N. Lugan, R. Mathieu, *Organometallics*, **1997**, 16, 1401.
- [50] Y. Arikawa, M. Ueoka, K. Matoba, Y. Nishibayashi, M. Hidai, S. Uemura, *J. Organomet. Chem.* **1999**, 572, 163.
- [51] H. L. Kwong, W. S. Lee, T. S. Lai, W. T. Wong, *Inorg. Chem. Commun.* **1999**, 2, 66.
- [52] R. O. Rosete, D. J. Cole-Hamilton, G. Wilkinson, *J. Chem. Soc., Dalton Trans.* **1979**, 1618.
- [53] H. Doucet, T. Ohkuma, K. Murata, T. Yokozawa, M. Kozawa, E. Katayama, A. F. England, T. Ikariya, R. Noyori, *Angew. Chem., Int. Ed.* **1998**, 37, 1703.
- [54] K. Mikami, T. Korenaga, M. Terada, T. Ohkuma, T. Pham, R. Noyori, *Angew. Chem., Int. Ed.* **1999**, 38, 495.
- [55] K. Abdur-Rashid, A. J. Lough, R. H. Morris, *Organometallics*, **2001**, 20, 1047.
- [56] K. Abdur-Rashid, A. J. Lough, R. H. Morris, *Organometallics*, **2000**, 19, 2655.
- [57] T. Ohkuma, H. Ooka, T. Ikariya, R. Noyori, *J. Am. Chem. Soc.* **1995**, 117, 10417.

- [58] J. X. Gao, P. P. Xu, X. D. Yi, C. B. Yang, H. Zhang, S. H. Cheng, H. L. Wan, K. R. Tsai, T. Ikariya, *J. Mol. Catal. A*, **1999**, 147, 105.
- [59] M. Yamakawa, H. Ito, R. Noyori, *J. Am. Chem. Soc.* **2001**, 122, 1466.
- [60] E. Lindner, I. Warad, H. A. Mayer, unpublished results.
- [61] E. Lindner, T. Schneller, F. Auer, H. A. Mayer, *Angew. Chem., Int. Ed.* **1999**, 38, 2154
- [62] O. Lavastre, J. P. Morken, *Angew. Chem., Int. Ed.* **1999**, 38, 3163.
- [63] E. Lindner, M. Kemmler, T. Schneller, H. A. Mayer, *Inorg. Chem.* **1995**, 34, 5489.
- [64] E. Lindner, R. Schreiber, T. Schneller, P. Wegner, H. A. Mayer, W. Goepel, C. Ziegler, *Inorg. Chem.* **1996**, 34, 5489.
- [65] U. Deschler, P. Kleinschmit, P. Panster, *Angew. Chem., Int. Ed. Eng.* **1986**, 25, 237.
- [66] E. Lindner, S. Al-Gharabli, H. A. Mayer, *Inorg. Chim. Acta*, **2002**, in press.
- [67] E. Lindner, S. Pautz, R. Fawzi, M. Steimann, *J. Organomet. Chem.* **1998**, 555, 247
- [68] A. Bader, E. Lindner, *Coord. Chem. Rev.* **1991**, 108, 27.
- [69] J. C. Brinker, W. G. Scherer, *Sol Gel Science*, Academic Press, London, 1990.
- [70] L. L. Hench, K. J. West, *Chem. Rev.* **1990**, 90, 33.
- [71] E. Lindner, T. Schneller, H. A. Mayer, H. Bertagnolli, T. S. Ertel, W. Hörner, *Chem. Mater.* **1997**, 9, 1524.
- [72] H. Egelhaaf, E. Holder, P. Herman, H. A. Mayer, D. Oelkrug, E. Lindner, *J. Mater. Chem.* **2001**, 11, 2445.
- [73] P. E. Garrou, *Chem. Rev.* **1981**, 81, 229.
- [74] A. Michaelis, *Liebigs Ann. Chem.* **1876**, 181, 305.
- [75] A. Bader, Diploma Thesis, University of Tübingen, 1988.
- [76] M. Lischewski, K. Issleib, H. Tille, *J. Organomet. Chem.* **1973**, 54, 195.
- [77] E. Lindner, R. Fawzi, H. A. Mayer, K. Eichele, W. Hiller, *Organometallics*, **1992**, 11, 1033.

- [78] L. Quin, F. Verkade, Phosphorus-31 NMR Spectral Properties in Compound Characterization and Structural Analysis, VCH Publishers, New York, (1994) 215.
- [79] E. Lindner, A. Baumann, P. Wegner, H. A. Mayer, U. Reinöhl, A. Weber, T. S. Ertel, H. Bertagnolli, *J. Mater. Chem.* **2000**, 10, 1655.
- [80] E. Lindner, F. Auer, A. Baumann, P. Wegner, H. A. Mayer, H. Bertagnolli, U. Reinöhl, T. S. Ertel, A. Weber, *J. Mol. Cat. A* **2000**, 157, 97.
- [81] E. Lindner, W. Wielandt, A. Baumann, H. A. Mayer, U. Reinöhl, A. Weber, T. S. Ertel, H. Bertagnolli, *Chem. Mater.* **1999**, 11, 1833.
- [82] E. Lindner, T. Shneller, F. Auer, P. Wegner, H. A. Mayer, *Chem. Eur. J.* **1997**, 11, 1833.
- [83] G. E. Maciel, D. W. Sindorf, *J. Am. Chem. Soc.* **1980**, 102, 7607.
- [84] C. A. Fyfe, *Solid State NMR for Chemists*, 1984.
- [85] E. A. Stern, *Phys. Rev. B* **1974**, 10, 3027.
- [86] F. W. Lytle, D. E. Sayers, E. A. Stern, *Phys. Rev. B* **1975**, 11, 4825.
- [87] L. Reimer, *Scanning Electron Microscopy*, Springer-Verlag, New York, 1998.
- [88] E. Lindner, S. Brugger, S. Steinbrecher, E. Plies, M. Seiler, H. Bertagnolli, P. Wegner, H. A. Mayer, *Inorg. Chim. Acta*, **2002**, 327, 54.
- [89] T. A. Stephenson, G. Wilkinson, *J. Inorg. Nucl. Chem.* **1966**, 28, 945.
- [90] E. Lindner, S. Meyer, P. Wegner, B. Karle, A. Sickinger, B. Steger, *J. Organomet. Chem.* **1987**, 335, 59.
- [91] E. Lindner, U. Schober, R. Fawzi, W. Hiller, U. Englert, P. Wegner, *Chem. Ber.* **1987**, 120, 1621.
- [92] T. S. Ertel, H. Bertagnolli, S. Hückmann, U. Kolb, D. Peter, *Appl. Spectrosc.* **1992**, 46, 690.
- [93] M. Newville, P. Livins, Y. Yakobi, J. J. Rehr, E. A. Stern, *Phys. Rev. B*, **1993**, 47, 14126.
- [94] J. S. Gurman, N. Binsted, I. Ross, *J. Phys. C*, **1986**, 19, 1845.
- [95] V. D. Scott, G. Love, *X-Ray Spectrom.* **1992**, 21, 27.

[96] J. Wernisch, *X-Ray Spectrom.* **1985**, 14, 109.

[97] C. Poehn, J. Wernisch, W. Hanke, *X-Ray Spectrom.* **1985**, 14,120.

Summary

The strong competition in the chemical industry put an enormous pressure on research and development with the consequence that conventional methods are not able to provide suitable solutions in that short time. Therefore, the combinatorial process which involves the design and synthesis of libraries of structurally diverse compounds in a reasonable time at efficient exploring time become of increasing interest. In catalysis research, these new methods have been introduced only gradually. An intermediate step between combinatorial chemistry and traditional synthesis is parallel synthesis with commonly one compound per well, coupled to automated screens. Recently this technique was transferred to homogeneous and heterogeneous catalysis. On the other hand, the anchoring of reactive centers, in particular catalytically active transition metal complexes, to polymeric matrices receives considerable attention. The driving force is the careful handling with expensive chemicals and the application of environmentally friendly processes. The outstanding behaviour of such materials is traced both to the combination of the advantages of homogeneous (defined reactive centers, high activity and selectivity) and heterogeneous catalysis (easy separation and recycling possibilities of the reactive centers). However, the leaching of the active material and the limited accessibility of the reactive centers due to the reduction of the mobility of the polymeric matrices combined with a decreased selectivity thwarted the commercial use of heterogenized catalysts. However, interphase systems are able to overcome or even prevent such problems. This concept provides a material imitating a homogeneous phase by the penetration of a stationary phase (e.g functional polymer) and a mobile phase (solvent, solid or gaseous reactant) on a molecular level. This affords a better accessibility to the reactive centers without essential leaching of the active material. In this context the sol-gel process is considered as an exciting prospect for the preparation of suitable polymeric frameworks under mild conditions. Simultaneous co-condensation of T-silyl functionalized

metal complexes or ligands with various alkoxysilanes or organosilanes provides materials in which the reactive centers are nearly homogeneously distributed across a chemical and thermal inert carrier matrix.

The objective of the present work is the synthesis of an array of novel neutral and cationic diamine-bis(ether-phosphine)ruthenium(II) complexes in homogeneous and heterogeneous phase acting as examples for parallel testing of catalysts in interphases.

In the first part of this work, a matrix of neutral diamine-bis(ether-phosphine)ruthenium(II) complexes were synthesized by treatment of the precursor complex $\text{RuCl}_2(\eta^2\text{-Ph}_2\text{PCH}_2\text{CH}_2\text{OCH}_3)_2$ with various chelating diamines like 1,2-diaminoethane, 1,2-diaminopropane, 1,3-diaminopropane, 1,2-phenylenediamine, 1,8-diaminonaphthalene, 2,2'-bipyridine, 1,10-phenanthroline. Due to the remarkable effect of the co-ligand on the catalytic activity of such complexes, this group of aliphatic and aromatic diamines was selected to vary the electronic and steric character of the metal center. This route was found to be the most straightforward and efficient way to generate these complexes. Moreover, this method is generally applicable to numerous comparable examples and thus is promising for later use in parallel synthesis. In solution, all complexes prefer the *trans*-chloro-*cis*-phosphine arrangement, as deduced by NMR spectroscopy. X-ray studies showed that in the solid state three possible isomers of the octahedral $\text{Cl}_2\text{Ru}(\text{ether-phosphine})_2(\text{diamine})$ complexes are present. The reaction of the complexes $\text{RuCl}_2(\eta^1\text{-Ph}_2\text{PCH}_2\text{CH}_2\text{OCH}_3)_2(\text{diamine})$ with one equivalent of AgSbF_6 , AgBF_4 , or TIPF_6 led to the abstraction of one chloride by simultaneously coordinating one ether-oxygen atom to ruthenium with formation of the monocationic compounds $[\text{RuCl}(\eta^1\text{-Ph}_2\text{PCH}_2\text{CH}_2\text{OCH}_3)(\eta^2\text{-Ph}_2\text{PCH}_2\text{CH}_2\text{OCH}_3)(\text{diamine})]^+$. If a large excess of silver or thallium salt is used, the dichloro complexes are converted to the dications $[\text{Ru}(\eta^2\text{-Ph}_2\text{PCH}_2\text{CH}_2\text{OCH}_3)_2(\text{diamine})]^{2+}$. In the case of 1,2-phenylenediamine as

coligand, the corresponding dication is only observed in traces. NMR spectroscopic investigations and X-ray structural analyses confirm the η^1 and η^2 coordination of the ether-phosphine ligands in the corresponding mono- and dicationic ruthenium(II) complexes.

Compounds of this type are potential candidates for the application for parallel methods. This presumption is based on the fact that diaminediphosphineruthenium(II) complexes with classical phosphine ligands were already successfully employed in the catalytic hydrogenation of unsaturated ketones with high diastereo- and enantioselectivity.

To merge parallel synthesis and interphase chemistry, the ether-phosphine ligand $\text{Ph}_2\text{PCH}_2\text{CH}_2\text{OCH}_3$ in the second part of the work was modified by providing an adequate spacer carrying a triethoxysilyl group (T-silyl) at the periphery of the ligand system. The hemilabile, triethoxysilyl functionalized ether-phosphine ligand was obtained by reaction of $\text{PhP(H)CH}_2\text{CH}_2\text{OCH}_3$ with 4-fluorobenzylamine in 1,1'-dimethoxyethane in the presence of potassium and subsequent treatment of the resulting coupling product with $(\text{EtO})_3\text{Si}(\text{CH}_2)_3\text{NCO}$ in dichloromethane. The modified ligand $\text{C}_6\text{H}_5\text{P}(\text{CH}_2\text{CH}_2\text{OCH}_3)\text{C}_6\text{H}_4\text{CH}_2\text{NHC(O)NHCH}_2\text{CH}_2\text{CH}_2\text{Si(OEt)}_3$ was used in the synthesis of a matrix of T-silyl functionalized neutral ruthenium(II) complexes $\text{Cl}_2\text{Ru}(\text{P}\sim\text{O})_2(\text{diamine})$ by addition of the same series of aliphatic and aromatic diamines as already mentioned to the bis(chelated) precursor complex $\text{Cl}_2\text{Ru}(\text{P}\sim\text{O})_2$. Since the weak ruthenium-oxygen bonds are easily cleaved during the reaction with the amines, the employment of ether-phosphines controls the reaction kinetically and avoids the formation of by-products. The corresponding monocationic ruthenium(II) complexes $[\text{ClRu}(\text{P}^\wedge\text{O})(\text{P}\sim\text{O})(\text{diamine})][\text{BF}_4]$ were available by chloride abstraction from the neutral precursors one with AgBF_4 or TIPF_6 in dichloromethane. Only in the case of $\text{Cl}_2\text{Ru}(\text{P}\sim\text{O})_2(\text{ethylenediamine})$ it was possible to partially abstract both chlorides to give the dicationic complex $[\text{Ru}(\text{P}^\wedge\text{O})_2(\text{ethylenediamine})][\text{PF}_6]_2$ in low yields.

In the third part of this work, the T-silyl functionalized diamine-bis(ether-phosphine)ruthenium(II) complexes were sol-gel processed in the presence of different amounts of co-condensation agents. Fluorescence spectroscopic studies of inorganic-organic hybrid polymers have demonstrated that materials provided with $\text{CH}_3\text{Si}(\text{OMe})_3$ (**Me-Tⁿ**) as a copolymer have the best swelling abilities in different solvents. Therefore in this investigation **Me-Tⁿ** has been selected as one of the co-condensation agents. To compare the results as a second co-condensation agent $(\text{MeO})_2\text{SiMe}-(\text{CH}_2)_6-\text{MeSi}(\text{OMe})_2$ (**D^o-C₆-D^o**) has been employed.

Three kinds of stationary phases were obtained: xerogels **I** were synthesized by co-condensation of the T-silyl functionalized neutral ruthenium(II) complexes with **D^o-C₆-D^o**; while xerogels **II** were formed by co-condensation of the same complexes with two different amounts of **Me-T^o** ($T : T' = 1 : 5$ and $1 : 10$, respectively), the cationic xerogels **III** were generated by sol-gel processing of the modified ruthenium(II) complexes $[\text{ClRu}(\text{P}^{\wedge}\text{O})(\text{P}\sim\text{O})(\text{diamine})][\text{BF}_4]$ with **Me-T^o** in a 1 : 10 ratio

The presence of an ether oxygen atom in the cationic species is responsible for the stabilization of a vacant coordination site at the ruthenium center. The resulting hybrid polymers symbolize a new array of complexes with variable mobilities, which represent potential interphase catalysts for the hydrogenation of conjugated ketones. Due to cross-linking effects the solubility of the polymeric materials is rather limited. Therefore multinuclear CP/MAS solid-state NMR spectroscopy as well as EXAFS, EDX, SEM and BET methods were used as powerful techniques for the characterization of polymers.

All ^{31}P resonances in the ^{31}P CP/MAS NMR spectra of the neutral polymeric materials are found in the expected ranges and are broadened due to the chemical shift dispersion. In the charged polycondensates, diastereomers are present exerting an additional influence on the line width of the ^{31}P resonances.

EXAFS measurements of the neutral complexes corroborated the proposed structures from NMR studies.

The ruthenium(II) precursor complexes were provided with T-silyl functions to increase the crosslinkage of the polycondensates during the sol-gel process. Such an anchoring of the reactive centers to the polymeric backbone suppresses leaching problems that could arise. The polymeric complexes which are introduced in this investigation are part of an array of interphase catalysts which have to be tested with particular screening methods to establish which of them are the best catalysts for the hydrogenation of unsaturated ketones.

Meine akademische Ausbildung verdanke ich:

K. Abu Dari – A. Abu Shamleh – M. H. Abu Zarga – G. Aharonian – K. Albert – M. Al-Hourani – H. Al-Salahat – S. Al-Taweel – M. Ashram – H. Bertagnolli – M. M. El-Abadelah – A. El-Alali – G. A. Derwish – T. Fanni – M. Fayad – Q. Ibraheem – Q. Jaradat – G. Jung – E. Lindner – A. Mahasneh – H. A. Mayer – K. Momani – E. Plies – A. H. Qasem – S. S. Sabri – B. Speiser – J. Strähle – M. Sway – W. Voelter – K.-P. Zeller

Lebenslauf

Persönliche Daten

Name: Samer Ibrahim Abed-Rabbo Al-Gharabli

Geburtstag/-ort: 12. Feb. 1974 in Jordan

Eltern: Ibrahim Abed-Rabbo Al-Gharabli

Subhieh Mahmoud Al-Gharabli

Staatsangehörigkeit: Jordanisch

Schulbildung:

1980-1988 Grundschule / Saudia Arabia

1989-1990 Gymnasium Jordanien

Juli. 1991 Abitur in Amman-Jordanien

Hochschulbildung

09. 1991 - 06. 1995 B.Sc. Studium an der Mu'tah Universität in Karak-Jordanien

16.06.1995 B.Sc. Titel

09.1995 – 31.08.1998 M.Sc. Studium an der "University of Jordan" in Amman-Jordanien

April 1998 M.Sc. Examen mit dem Thema "Synthesis, Characterization and Chelation Properties of som Oxime Containing Polymers" bei Prof. Dr. K. Ibraheem und Dr. M. Mubarak am Institut für Chemie der "University of Jordan" Amman-Jordanien

31. 08. 1998 Zeugnis der M.Sc. Prüfung in Chemie

7. 1999 - 04. 2002 Dissertation unter Leitung von Herrn Prof. Dr. E. Lindner am Institut für Anorganische Chemie mit dem Thema: Synthese neuartiger neutraler und kationischer Diamin-bis(ether-phosphan)ruthenium(II)-Komplexe in homogener und heterogener Phase als Werkzeug für paralleles Katalysator-Screening

Beschäftigung

09.1995 – 05.1998	"Teaching Assistent" an der "University of Jordan"- Amman/ Jordanien
06.1998 – 06.1999	Wissenschaftlicher Angestellter an der "University the Hashemite" Zarqa/ Jordanien
7.1999 – 10.1999	Wissenschaftliche Hilfskraft, Institut für Anorganische Chemie, Universität Tübingen
11.1999 – 04.2002	Wissenschaftlicher Angestellter, Institut für Anorganische Chemie, Universität Tübingen (Planstelle)
11. 1999 – 04. 2002	Assistent im Anorganisch-chemischen Praktikum für Fortgeschrittene, Teil II
07.2000 – 04. 2002	Mitglied im Graduiertenkolleg "Chemie in Interphasen"